THEORETICAL STUDIES ON METALLACYCLES, BORAZINES AND NOVEL THREE MEMBERED RINGS

A Thesis

Submitted for the Degree of

DOCTOR OF PHILOSOPHY

By

Ashwini Kumar Phukan

School of Chemistry

University of Hyderabad

Hyderabad 500 046

INDIA

April 2004

Dedicated to

My Beloved

Grand Parents

CONTENTS

CHAPTER 2: Theoretical Study of Structure, Bonding, Stability and Aromaticity of Complexes of Titanocene and Zirconocene

CHAPTER 3: Aromaticity and Reactivity of Benzenoid Aromatics and their B-N Analogues

CHAPTER 4: Electronic Structure and Stability of Tricoordinate Pyramidal Boron

STATEMENT

I do hereby declare that the work embodied in this thesis is the result of investigations carried out by me in the **School of Chemistry, University of Hyderabad, Hyderabad, India,** under the supervision of **Prof. Eluvathingal D. Jemmis**.

In keeping with the general practice of reporting scientific observations, due acknowledgements have been made whenever the work described is based on the findings of other investigators.

Ashwini Kr. Phukan

Ashwini Kumar Phukan

CERIFICATE

Certified that the work embodied in the thesis entitled "**Theoretical Studies on Metallacycles, Borazines and Novel Three Membered Rings**" has been carried out by **Ashwini Kumar Phukan** under my supervision and the same has not been submitted elsewhere for any degree.

E D Jemmis

Eluvathingal D. Jemmis
Thesis Supervisor

E D Jemmis 30-04-04

Dean
School of Chemistry

Dean
School of Chemistry
University of Hyderabad
Hyderabad-500 046, India

Acknowledgements

It's a rare privilege to have a supervisor like Prof. E. D. Jemmis. I thank him for his constant guidance and encouragement.

I thank the Dean and the faculty members of the School of Chemistry. Special thanks are due to Profs. M. Durgaprasad, T. P. Radhakrishnan, K. C. Kumara Swamy and late Bhaskar G. Maiya.

I take this opportunity to thank my collaborators, Prof. Uwe Rosenthal and Dr. Haijun Jiao. The financial assistance from the Council of Scientific and Industrial Research (CSIR), New Delhi is gratefully acknowledged.

I thank the non-teaching staff of the School of Chemistry, University of Hyderabad for their cooperation. I am also thankful to all the staff of the Computer Center and specially, Mr. Vinod Kumar for providing the computational facilities.

This thesis would not have been completed without the encouragement and blessings from my Guru, Prof. P. K. Gogoi of Dibrugarh University. I also thank all my teachers at the Chemistry Department of Dibrugarh University.

I am very fortunate to have helpful seniors like Dr. B. Kiran, Dr. M. Manoharn and Dr. Pankaz K. Sharma. In the initial days, Pankaz helped me in learning the basics of computational chemistry. Kiran was always there to give me the necessary insight and suggestions whenever I faced any difficulty with the analysis of the results. I also thank Mano for his love and affection.

I am blessed with polite, helpful and obedient juniors like Anoop, Parameswaran, Bishu, Prasad, Jayasree, Pancharatna and Usha. If Bishu brought fresh life to the lab, then Usha brought homely atmosphere to it. I thank all of them for their help with the thesis work.

I thank all my friends at the School of Chemistry and the NRS Hostel for making a lively atmosphere for research.

Words are not enough to express the love and support provided by my parents and grand mother. They always stood by me at several critical moments. I owe a lot to them. I also thank my in-laws for their support during the most crucial phase of this thesis work. I am indebted to all my family friends and well wishers for their concern. The smiling face of my little son, Arunabh, helped me in handling some of the tense moments.

Finally, I thank my wife, Mousumi for her care, support and encouragement.

Ashwini

CHAPTER 1

A Brief Introduction to Computational Chemsitry

[1.0] GENERAL INTRODUCTION :

Computational chemistry has evolved as a useful supplement to experiments in studying problems in chemistry. Theoretical methods have the inherent advantage over experiments in that it can study any model systems, which are otherwise difficult to investigate by experimental means. From the theoretical perspective, both classical mechanics and quantum chemistry provides a useful basis for the understanding of structure, dynamics and reactivity of molecules. The availability of several state-of-the art quantum chemical packages, which can carry out computations on reasonably large molecules has added momentum to this effort. Many a time, the results obtained from such computations match with those obtained from sophisticated experimental techniques. In this chapter, we give a brief introduction to the major methods of electronic structure theory followed by a brief overview of the remaining chapters.

[1.1] Theoretical Methods

There are two major computational methods for the study of structure and reactivity of molecules, viz., molecular mechanics and electronic structure theory. A brief description of these methods are given below.

[1.1.1] Molecular Mechanics

Molecular Mechanics (MM) or Empirical Force Field (EPF) method[1] uses the fundamental laws of classical mechanics. In MM method, a molecule is described by "ball and spring" model. The basic idea behind this method is the observation that molecules tend to be composed of units, which are structurally similar in different molecules. There are various MM methods and each of them is characterized by their own force field. A typical force field consists of the following :

i) a set of equations which describes the change in the potential energy of a molecule with respect to its constituent atoms.

ii) a series of atom types which defines the characteristics of an element. The atom type depends on the atomic number and the type of hybridization it is involved in.

iii) a set of parameters which fit the equations and atom types to experimental data. In a MM method, calculations are performed on the basis of interactions between the nuclei.

The energy of a molecule is given by

$$E_{FF} = E_{str} + E_{bend} + E_{tors} + E_{vdw} + E_{es} \qquad (1.1)$$

where E_{str} is the potential energy for stretching a bond between two atoms, E_{bend} is the amount of energy required for bending an angle, E_{tors} is the torsional energy for rotation

around a bond, E_{vdw} is the van der Waals energy describing the nonbonded interactions between atoms, E_{es} is the energy arising out of electrostatic interactions between polar bonds. Some illustrative examples to estimate these individual contributors are given below.

The stretch energy is considered as a quadratic function of the displacement of each bond length l_i from its equilibrium length $l_{i,0}$.

$$E_{str} = \frac{1}{2}\sum_i k_{s,i}(l_i - l_{i,0})^2 \qquad (1.2)$$

where $k_{s,i}$ is the force constant for the stretching bond i.

The bending energy is given by,

$$E_{bend} = \frac{1}{2}\sum_i k_{\theta,i}(\theta_i - \theta_{i,0})^2 \qquad (1.3)$$

where θ_i, $\theta_{i,0}$ and $k_{\theta,i}$ are the angle, the equilibrium angle and the bending force constant for the bond angle i.

The torsional energy is written as,

$$E_{tors}(\omega) = \sum_{n=1} V_n \cos(n\omega) \qquad (1.4)$$

where V_n is the barrier height and ω is the torsional angle.

The energy of van der Waals interaction is written as the sum of interactions between pairs of non-bonded atoms and is preferably given by the Lennard-Jones potential.[2]

$$E_{vdw} = \frac{a}{R^{12}} - \frac{b}{R^6} \qquad (1.5)$$

where a and b are constants and R is the interatomic distance.

The electrostatic energy, E_{es} arises from internal distribution of the electrons and is given by the Coulomb potential.

$$E_{es} = \sum_{\alpha} \sum_{\beta>\alpha} \frac{q_\alpha q_\beta}{R_{\alpha\beta}} \qquad (1.6)$$

where q_α and q_β are the point charges located at the nuclei α and β and $R_{\alpha\beta}$ is the distance between the nuclei. Different force fields differ in the details of these terms.

Even though the MM calculations are quite fast and inexpensive, they can not be used for solving problems where electronic effects play a major role and where transferability is minimum.

[1.1.2] Electronic Structure Methods

Electronic structure methods use the laws of quantum mechanics to study molecules and their properties. The well known Schrödinger equation, the time independent form of which can be expressed in the most succinct form as,

$$\mathbf{H\Psi=E\Psi} \qquad (1.7)$$

Forms the basis for most ground state properties. There are three major classes of electronic structure methods, viz., semi-empirical and *ab-initio* molecular orbital methods,[3, 4] and density functional methods.[5]

[1.1.2.2] *Ab-initio* Molecular Orbital Theory

Ab initio molecular orbital methods[4] do not use any experimental parameters. It is solely based on the fundamental laws of quantum mechanics, and a few physical constants such as the Planck's constant, the speed of light and the mass and charge of electrons and nuclei. This theory is primarily concerned with predicting the atomic and molecular properties. Even though the *ab-initio* methods are computationally quite

expensive as compared to the semi-empirical methods, the results obtained from *ab-initio* calculations are highly accurate. *Ab initio* methods use the following mathematical approximations for solving the Schrödinger equation.

i) Born-Oppenheimer Approximation[6]

For a system of nuclei (α, β, …) and electrons (i, j, …), the Hamiltonian is given by,

$$H(r, R) = -\sum_{\alpha} \frac{h^2}{8\pi^2 M_\alpha} \nabla_\alpha^2 - \sum_{i=1} \frac{h^2}{8\pi^2 m_i} \nabla_i^2 + V(r, R) \qquad (1.8)$$

where r and R are the electronic and nuclear coordinates.

The potential energy V(r, R) consists of nuclear-electron attraction, electron-electron repulsion and nuclear-nuclear repulsion. It is given by,

$$V(r, R) = \sum_{\alpha} \sum_{i} \frac{Z_\alpha e^2}{r_{i\alpha}} + \sum_{i<j} \frac{e^2}{r_{ij}} + \sum_{\alpha<\beta} \frac{Z_\alpha Z_\beta e^2}{R_{\alpha\beta}} \qquad (1.9)$$

In eqn. (1.8), the first term denotes the nuclear kinetic energy operator T_N and the combination of the second and third term represents the electronic Hamiltonian operator, H_e. Separation of the nuclear kinetic energy terms from the Hamiltonian gives,

$$H(r, R) = T_N(R) + H_e(r, R) \qquad (1.10)$$

The electronic operator, $H_e(r, R)$ describes the motion of electrons in a fixed nuclear framework. Since the nuclei are much heavier than the electrons, it can be assumed that the movement of nuclei is much slower than the electrons. Therefore, one can assume a configuration with fixed positions for the nuclei and solve the electronic equation,

$$H_e(r, R)\Psi_e(r, R) = E(R)\Psi_e(r, R) \qquad (1.11)$$

where E(R) and $\Psi_e(r, R)$ denote the energy and the electronic wave function for a particular fixed nuclear framework respectively.

While the electronic wave function Ψ_e depends on r and R, the nuclear wave function Ψ_N depends only on R. Hence, the complete wave function can be written as

$$\Psi(r, R) = \Psi_e(r, R)\, \Psi_N(R) \tag{1.12}$$

Combining eqns. (1.10) and (1.12) one gets,

$$H(r, R)\, \Psi(r, R) = [T_N(R) + H_e(r, R)]\, \Psi_e(r, R)\Psi_N(R) \tag{1.13}$$

The solution of eqn. (1.13) leads to the following two separate equations,

$$-\sum_i \frac{h^2}{8\pi^2 m_i}\nabla_i^2 \Psi_e(r, R) + V(r, R)\Psi_e(r, R) = E(R)\Psi_e(r, R) \tag{1.14}$$

and

$$-\sum_\alpha \frac{h^2}{8\pi^2 M_\alpha}\nabla_\alpha^2 \Psi_N(R) + E(R)\Psi_N(R) = E\Psi_N(R) \tag{1.15}$$

or

$$H_e\Psi_e(r, R) = E(R)\Psi_e(r, R) \tag{1.16}$$

and

$$[T_N + E(R)]\Psi_N(R) = E\Psi_N(R)$$

$$\text{or} \qquad H_N\Psi_N(R) = E\Psi_N(R) \tag{1.17}$$

Eqns. (1.16) and (1.17) represent the elec nic and nuclear Schrödinger equations respectively. This method of separating the electronic and nuclear terms is known as Born-Oppenheimer approximation.

ii) Variational Theorem:

Most quantum chemistry calculations are based on the variational method which allows one to obtain an approximation for the ground state energy of a system. According to this theorem, the expectation value of energy E for any trial wave function ψ, will be greater than or equal to the energy for the exact wave function E^0. Thus,

$$E = \frac{\int \psi^* H \psi \delta\tau}{\int \psi^* \psi \delta\tau} \geq E^0 \qquad (1.18)$$

A standard variational calculation involves the following steps:

(a) choose a trial wave function ψ having variable parameters

(b) write down the Hamiltonian operator H for the system

(c) minimize eqn. (1.18) for E with respect to variation in the parameters.

The trial wave function ψ must satisfy the following conditions : it should be single valued, continuous, finite, and normalized. It is clear from eqn. (1.18) that the lower the value of the variational integral, the better the approximation one obtains for E^0. However, in practice, in order to the variational integral, one incorporates several parameters into the trial function ψ, and then varies these parameters.

iii) LCAO-MO Approximation

In order to solve the Schrödinger equation of a molecule having several atoms, one has to consider a trial function for Ψ. This can be done by using a linear combination of several atomic orbitals called as basis functions.

If $\phi_1, \phi_2, \phi_3 \ldots\ldots \phi_n$ are the atomic orbitals, then

$$\psi = \sum_{i=1}^{n} C_i \varphi_i \qquad (1.19)$$

The expectation value of the energy can be calculated from the variation theorem,

$$E = \frac{< \sum_{i=1}^{n} C_i \varphi_i \; | H | \sum_{i=1}^{n} C_i \varphi_i >}{< \sum_{i=1}^{n} C_i \varphi_i \; | \sum_{i=1}^{n} C_i \varphi_i >} = f(C_1, C_2, C_3, \ldots\ldots\ldots\ldots, C_n) \qquad (1.20)$$

Minimization of the energy with respect to C_1, C_2, C_3, ……., C_n gives the stationary values of E. Thus,

$$\partial E(C_1, C_2, \ldots\ldots C_n) = \frac{\partial E}{\partial C_1}\partial C_1 + \frac{\partial E}{\partial C_2}\partial C_2 + \ldots\ldots\ldots\ldots + \frac{\partial E}{\partial C_n}\partial C_n = 0 \qquad (1.21)$$

The solution of the above equation results in the approximate values of E_i and Ψ_i. It follows from eqn. (1.20) that

$$E = \frac{\sum_{i}^{n} C_i^2 H_{ii} + 2\sum_{i>j}^{n} C_i C_j H_{ij}}{\sum_{i}^{n} C_i^2 S_{ii} + 2\sum_{i>j}^{n} C_i C_j S_{ij}} \qquad (1.22)$$

where $H_{ii} = \langle \phi_i | H | \phi_i \rangle$

$H_{ij} = \langle \phi_i | H | \phi_j \rangle$

$S_{ii} = \langle \phi_i | \phi_i \rangle$

$S_{ij} = \langle \phi_i | \phi_j \rangle$

Rearrangement of equation (1.22) gives,

$$\sum_{i}^{n} C_i^2 H_{ii} + 2\sum_{i>j}^{n} C_i C_j H_{ij} = E\,[\sum_{i}^{n} C_i^2 S_{ii} + 2\sum_{i>j}^{n} C_i C_j S_{ij}\,] \qquad (1.23)$$

Now, if one considers all other coefficients as fixed and differentiates eqn. (1.23) with respect to C_i, then the above eqn. (1.23) becomes

$$2C_iH_{ii} + 2\sum_{j\neq 1} C_iH_{ij} = E[2C_iS_{ii} + 2\sum_{j\neq i}^{n} C_jS_{ij}] \qquad (1.24)$$

Applying the condition of stationarity to eqn. (1.24), one can write,

$$2C_i(H_{ii} - ES_{ii}) + 2\sum_{j\neq 1} C_j(H_{ij} - ES_{ij}) = 0$$

Since, the C_i and C_j are independent of each other, therefore for an arbitrary C_i,

$$\sum_{j=1}^{n} C_j(H_{ij} - ES_{ij}) = 0 \qquad (1.25)$$

Thus, if one systematically minimizes eqn. (1.24) with respect to the coefficients C_1, C_2, ...Cn, the following sets of secular equations are obtained.

$$\left.\begin{aligned} &C_1(H_{11} - ES_{11}) + C_2(H_{12} - ES_{12}) + \ldots\ldots\ldots\ldots\ldots\ldots = 0 \\ &C_1(H_{21} - ES_{21}) + C_2(H_{22} - ES_{22}) + \ldots\ldots\ldots\ldots\ldots\ldots = 0 \\ &C_1(H_{n1} - ES_{n1}) + C_2(H_{n2} - ES_{n2}) + \ldots\ldots\ldots\ldots\ldots + C_n(H_{nn} - ES_{nn}) = 0 \end{aligned}\right\} \qquad (1.26)$$

All these n equations are linear and homogeneous and are to be solved simultaneously. They can have a non-trivial solution only if the corresponding secular determinant vanishes. That is,

$$H_{ij} - ES_{ij} = \begin{vmatrix} H_{11} - ES_{11} & H_{12} - ES_{12} & H_{1n} - ES_{1n} \\ H_{21} - ES_{21} & H_{22} - ES_{22} & H_{2n} - ES_{2n} \\ H_{n1} - ES_{n1} & H_{n2} - ES_{n2} & H_{nn} - ES_{nn} \end{vmatrix} = 0 \qquad (1.27)$$

Since this is an n^{th} order determinant, it will have n roots, viz., E_1, E_2, ... E_n and thus a set of n wavefunctions Ψ_1, Ψ_2, ...Ψ_n respectively. Thus, by applying the LCAO-MO method, one can generate several molecular orbitals for each molecule.

iii) Hartree-Fock Approximation

The Hartree-Fock theory[7] is a milestone in the development of theoretical chemistry and is a powerful method for the calculation of ground state energy of many electron atoms. One starts with this theory for more accurate approximations including that of electron correlation.

Considering an infinitely heavy nucleus (Born-Oppenheimer approximation), the Hamiltonian operator for an n-electron atom can be written as,

$$H = -\frac{h^2}{8\pi^2 m_e}\sum_{i=1}^{n}\nabla_i^2 - \sum_{i=1}^{n}\frac{Ze^2}{r_i} + \sum_{i=1}^{n-1}\sum_{j=i+1}^{n}\frac{e^2}{r_{ij}} \qquad (1.28)$$

The solution of Schrödinger equation for an atom or molecule is made difficult by the presence of inter-electronic repulsion term e^2/r_{ij} in the Hamiltonian of equation (1.28). Neglecting the inter-electronic repulsion terms, one obtains a zeroth-order wave function. This in turn helps to separate the total Schrödinger equation into n one-elctron hydrogen like equations. Thus, the zeroth-order wave function can be written as a product of n hydrogen like orbitals, i.e.,

$$\Psi^{(0)} = u_1(r_1,\theta_1,\varphi_1)u_2(r_2,\theta_2,\varphi_2).....u_n(r_n,\theta_n,\varphi_n) \qquad (1.29)$$

where the hydrogen like orbitals are

$$u = R_{nl}(r)Y_l^m(\theta,\varphi) \qquad (1.30)$$

Even though it is qualitatively advantageous to use the approximate wave function represented by equation (1.29), the wave function is devoid of any quantitative accuracy. However, the accuracy of the wave function can be improved by considering different effective numbers for different orbitals, which will take care of screening of

electrons. The wave function thus obtained is far from accurate. In order to further improve the quality of the wave function, a variational function like $\psi^{(0)}$ (eqn. 1.29) is considered which is independent of any restriction. This leads to the following wave function for variation,

$$\Phi = v_1(r_1,\theta_1,\varphi_1)v_2(r_2,\theta_2,\varphi_2).....v_n(r_n,\theta_n,\varphi_n) \qquad (1.31)$$

And then try to determine the functions v_1, v_2, ...v_n that minimizes the following variational integral,

$$\int \frac{\phi^* H \phi d\tau}{\phi^* \phi d\tau} \qquad (1.32)$$

Computationally, it is very difficult to find the best possible approximate wave function. Therefore one considers a set of orbitals, which are product of a radial factor and a spherical harmonic:

$$v_i = w_i(r_i)Y_{l_i}^{m_i}(\theta_i,\varphi_i) \qquad (1.33)$$

This procedure is known as the Hartree-Fock self-consistent field (SCF) method. According to Hartree, one guesses a wave function, which is a product of several hydrogen like orbitals with effective atomic numbers. It is given by,

$$\Phi_0 = a_1(r_1,\theta_1,\varphi_1)a_2(r_2,\theta_2,\varphi_2).....a_n(r_n,\theta_n,\varphi_n) \qquad (1.34)$$

where each a_i is a normalized function of r with a probability density of $|a_i|^2$ and is multiplied by a spherical harmonic.

Averaging the instantaneous interactions between any one electron and all the other electrons of the system, one obtains a situation where the electrons behave like point charges. Thus, the potential energy of interaction between two arbitrary point charges q_1 and q_2 is given by,

$$V_{12} = \frac{q_1 q_2}{4\pi\varepsilon_0 r_{12}} \tag{1.35}$$

Now, if q_2 is smeared out into a continuous charge distribution having a charge density of ρ_2 and the infinitesimal charge in the volume element is $\rho_2 d\tau_2$, then the sum of the interactions between q_1 and the infinitesimal charge element gives,

$$V_{12} = \frac{q_1}{4\pi\varepsilon_0} \int \frac{\rho_2}{r_{12}} d\tau_2 \tag{1.36}$$

The total sum of all the interactions of electron 1 with other electrons in the system results in,

$$V_{12} + V_{13} + \ldots\ldots\ldots\ldots\ldots + V_{1n} = \sum_{j=2}^{n} e^2 \int \frac{|a_j|^2}{r_{1j}} d\tau_j \tag{1.37}$$

The potential energy of interaction between electron 1 and the other electrons, and that between electron 1 and nucleus is,

$$V_1(r_1, \theta_1, \varphi_1) = \sum_{j=2}^{n} e^2 \int \frac{|a_j|^2}{r_{1j}} d\tau_j - \frac{Ze^2}{r_1} \tag{1.38}$$

Another more accurate approximation known as the central-field approximation is made by considering that the effective potential acting on an electron in an atom can be adequately approximated by a function of r only. Thus, by using $V_1(r_1)$ as the potential energy, the one-electron Schrödinger equation can be written as,

$$\left[-\frac{h^2}{8\pi^2 m_e} \nabla_1^2 + V_1(r_1) \right] \varphi_1(1) = \varepsilon_1 \varphi(1) \tag{1.39}$$

The solution of the above equation gives an improved orbital for electron 1 with the orbital energy of ε_1. Equation (1.39) is the famous Hartree-Fock equation. It has the general form of $F\phi_i = \varepsilon_i \phi_i$ where ϕ_i is the i^{th} spin-orbital, F is the effective Hartree-Fock

Hamiltonian called as the Fock (or Hartree-Fock) operator and the eigenvalue ε_i is the energy of spin-orbital i.

iv) Basis Sets

A basis set is a mathematical representation of the molecular orbitals of a molecular system. The accuracy of the results obtained from *ab initio* MO or DFT methods depend on the kind of basis sets used. A smaller basis set can not give a proper representation to the molecular orbitals. On the other hand, a larger basis set can approximate the orbitals more accurately by imposing fewer restrictions on the locations of the electrons in space.

In general, electronic structure calculations are based on Slater type orbitals (STO) and Gaussian type orbitals (GTO). A Slater type orbital[8] is defined as,

$$\chi_{n,l,m}(r,\theta,\varphi) = Nr^{n-l}e^{-\zeta r}Y_l^m(\theta,\varphi) \qquad (1.40)$$

where N is a normalization constant, Y_l^m the spherical harmonic, r, θ, and ϕ are the polar coordinate with respect to the nucleus, n the principal quantum number and ζ, the orbital exponent.

However, the Slater functions lead to two, three or four center two-electron repulsion integrals, the evaluation of which is computationally very demanding. To get rid of this problem, Gaussian type orbitals are introduced. It has the general form[9]

$$g = Nx^i y^j z^k e^{-\alpha r^2} \qquad (1.41)$$

where α is a constant determining the radial extent of the function (define N, x, y, z, i, j, k…). These gaussians are called primitive gaussians.

Standard basis sets for electronic structure calculations use linear combination of gaussian functions to form orbitals. In general, linear combinations of gaussian primitives are used as basis functions, given by the following relationship:

$$\Psi_i = \sum_i c_{\mu i} g_i \qquad (1.42)$$

where ψ_i is called a contracted gaussian type function and the g_i's are called gaussian primitives. In general, the gaussian type orbitals are obtained by least square fit of STOs. These are called STO-nG basis sets where n is the number of gaussian primitives used to fit a STO. Pople and co-workers have introduced another notation like n-ijG or n-ijkG where n and ij (or ijk) are the number of primitives for contractions in the inner and valence shells respectively. ij and ijk denotes the quality of the basis sets, the former describes double zeta and the latter describes triple zeta quality of the basis sets.

A *minimal basis set* contain only one basis function for each atomic orbital of a particular atom with one coefficient assigned to it. The STO-nG is a minimal basis set.

A better MO wave function can be obtained by replacing an AO with an extended basis set, which consists of more than one function characterized by its own coefficient. If every MO of a minimal basis set is replaced by two functions having different orbital exponents (ζ), then the basis set is a *double-zeta basis set* (DZ). Dunning-Huzinaga (D95) and cc-pCVDZ are examples of such a basis set. Similarly, a triple zeta basis set is obtained by using three basis functions per AO. An example of such a basis set is cc-pCVTZ.

Another type of basis set, known as the *split-valence basis set*, can be formed by using two basis functions for the valence AOs and a single function for each inner

shell orbital. The basis sets 6-31G and 6-311G are examples of split-valence double and triple zeta basis sets respectively. Even though split-valence basis sets change the size of the orbitals, it lacks the ability to distort the shape of the orbitals. This was overcome by the addition of orbitals with higher angular momentum than what is necessary to describe the ground state of an atom. The basis set thus obtained is called a *polarized basis set.* A polarized basis set is indicated by putting a 'star' after the basis set or by putting the higher angular momentum orbitals within parenthesis. For example, 6-31G** or 6-31G(d, p) indicates that d-functions and p-functions are added as polarization on heavy atoms and H-atom respectively of the standard 6-31G basis sets. In general, one adds d-functions to heavy atoms, f-functions to transition metal elements and p-functions to H-atom to account for polarization. It may be noted that the d-type functions that are added to a particular basis set to get a polarized basis set are a single set of uncontracted gaussian primitives. There are two types of d-functions, viz., pure and cartesian as given below.

Cartesian : d_x^2, d_y^2, d_z^2, d_{xy}, d_{yz}, d_{zx}

Pure : $d_{x^2-y^2}$, d_z^2, d_{xy}, d_{yz}, d_{zx}.

Similarly, f-polarization function can be of 10-cartesian types, which are formed by the linear combination of a set of seven pure f orbitals.

However, the above mentioned basis sets failed to adequately describe the molecules containing lone pairs, anions or systems with low ionization potential or systems in excited states. This was overcome by the addition of diffuse functions, which are larger in size than the standard valence size functions. These gaussians have very small exponents and decay slowly with increasing distance from the nucleus. Diffuse functions allow orbitals to occupy a larger region of space. They are indicated

by a '+' sign. For example, a 6-31+G(d) basis set indicates that diffuse functions are added to the heavy atoms.

In electron correlation methods much larger basis sets are needed to describe the interactions between electrons. Such a basis set, known as high angular momentum basis sets, can be generated by the addition of multiple polarization functions both on heavy atoms (d and f functions) and hydrogen atoms (d and p functions). For example, if the basis set is 6-311G(3df, 2df, p), it contains 3d functions and 1f function on heavy atoms of the second and higher rows, 2d functions and 1f function on first row heavy atoms and 1p function on H-atoms.

Computations involving heavier atoms (third and higher rows of the periodic table) are relatively troublesome than those involving first and second row atoms. The chief source of this problem is an increase in the number of two-electron integrals and the relativistic effects. These dilemmas are encompassed by the use of pseudopotentials. Since the core (inner shell) orbitals are not affected by the changes in chemical bonding, one can treat them as an averaged potential. The valence electrons are described by basis functions.

There are two types of pseudopotentials : *ab initio* model potential (AIMP)[10] and effective core potential (ECP)[11]. The construction of an ECP for a particular atom involves the following steps:

i) Generation of a good quality all-electron wave function for the atom by a Hartree-Fock calculation.

ii) Substitution of the valence electrons by a set of nodeless pseudo-orbitals. These pseudo-orbitals are designed in such a way that they do not interfere with the core orbitals, but behave correctly in the outer part.

iv) Replacement of the core electrons by a suitable potential which accounts for the relativistic effect.

iv) Fitting of this potential to a set of gaussian functions.

The ECP has the general form,

$$ECP(r) = \sum_{i=1}^{k} c_i r^{n_i} e^{-\alpha_i r^2} \qquad (1.43)$$

where k is the number of terms in the expansion, c_i is a coefficient characteristic of each term, r is the distance from nucleus with a power of n_i for the i^{th} term, and α_i is an exponent for i^{th} term. The use of ECP is found to be computationally very efficient, particularly for transition metals, because it reduces the number of basis functions. One needs to consider the basis functions for only the valence electrons. ECP also makes room for the incorporation of relativistic effects. An extensive use of ECPs provided by Hay and Wadt[12] for Ti and Zr was made in Chapter 2 of this thesis.

[1.1.2.1] Semi-empirical Methods

These methods[3] use a modified version of the molecular Hamiltonian to solve an approximate form of the Schrödinger equation. They use experimentally available parameters for simplification of the calculation. Thus, the availability of appropriate parameters is very crucial for the accuracy of a computation for a given molecular system. Semi-empirical methods save lot of computational time by reducing the number of two-electron repulsion integrals necessary for the construction of Fock matrix. All semi-empirical methods should satisfy the following general conditions :

a) The methods must be simple enough so that one can apply them to relatively

large molecules without any extra computational cost.

b) The approximations introduced in a semi-empirical theory must take into consideration all the primary physical interactions (for example, electrostatic repulsion between electrons) which are crucial for the determination of equilibrium geometry of the molecules.

c) The approximate wave function should be generated without considering empirically derived information such as the covalent or ionic nature of the molecule.

d) The theory should be made simpler for easy interpretation of the results.

Semi-empirical MO theories can be divided into two types depending on the kind of Hamiltonian used: those using a Hamiltonian consisting of all one-electron terms, and those using a Hamiltonian, which includes both one and two electron terms. The Hückel and Extended Hückel (EH)[13] methods are one electron theories while the Pariser-Parr-Pople (PPP)[14], MNDO[15], AM1[16], PM3[17] are two electron methods.

The central assumption of semi-empirical method is the Zero Differential Overlap (ZDO) approximation.[3a,18] According to this approximation, if ϕ_μ and ϕ_ν are two atomic orbitals centered on either the same atom or two different atoms, then

$$\phi_\mu\phi_\nu = 0 \qquad (1.44)$$

wherever they occur. It implies that,

$$(\mu\nu|\alpha\beta) = (\mu\mu|\alpha\alpha)\delta_{\mu\nu}\delta_{\alpha\beta} \qquad (1.45)$$

where ϕ_μ , ϕ_ν, ϕ_α, and ϕ_β are centered on different atoms and the overlap integrals, and the overlap integrals,

$$S_{\mu\nu} = \int\phi_\mu\phi_\nu d\tau = \delta_{\mu\nu} \qquad (1.46)$$

The core Hamiltonian integrals are given by,

$$H^c_{\mu\nu} = \int \phi_\mu H^c \phi_\nu d\tau \tag{1.47}$$

The Hartree-Fock-Roothaan equation for a closed-shell species is,

$$\sum_\nu F_{\mu\nu} c_{\nu i} = \sum_\nu S_{\mu\nu} c_{\nu i} \varepsilon_i \tag{1.48}$$

If one invokes ZDO approximation, then equation (1.48) simplifies to

$$\sum_\nu F_{\mu\nu} c_{\nu i} = \sum_\nu \varepsilon_i c_{\mu i} \tag{1.49}$$

where the elements of the Fock matrix are given by,

$$F_{\mu\mu} = H^c_{\mu\mu} - \frac{1}{2} P_{\mu\mu} (\mu\mu \mid \mu\mu) + \sum_\alpha P_{\alpha\alpha} (\mu\mu \mid \alpha\alpha) \tag{1.50}$$

and

$$F_{\mu\nu} = H^c_{\mu\nu} - \frac{1}{2} P_{\mu\nu} (\mu\mu \mid \nu\nu) \qquad (\text{for } \mu \neq \nu) \tag{1.51}$$

In equations (1.50) and (1.51), $P_{\mu\nu}$ are known as the density matrix or Mulliken population matrix. It is given by,

$$P_{\mu\nu} = 2 \sum_i^{\text{occ. MOs}} c^*_{\mu i} c_{\nu i} \tag{1.52}$$

The two center electron-electron repulsion integrals can also be written as,

$$(\varphi^A_\mu \varphi^A_\mu \mid \varphi^B_\alpha \varphi^B_\alpha) = \gamma_{AB} \tag{1.53}$$

where φ_μ and φ_α are centered on atoms A and B respectively. At large inter-atomic distances R_{AB}, γ_{AB} is approximately equal to $1/R_{AB}$. Thus, equations (1.50) and (1.51) simplifies to,

$$F_{\mu\mu} = H^c_{\mu\mu} - \frac{1}{2} P_{\mu\mu} \gamma_{AA} + \sum_B P_{BB} \gamma_{AB} \qquad (\phi_\mu \text{ on A}) \tag{1.54}$$

and

$$F_{\mu\nu} = H^c_{\mu\nu} - \frac{1}{2} P_{\mu\nu} \gamma_{AB} \qquad (\phi_\mu \text{ on A}, \phi_\nu \text{ on B}) \tag{1.55}$$

where P_{BB} represents the total electron density associated with atom B.

The core Hamiltonian integral is,

$$H^c = -\frac{1}{2}\nabla^2 + \sum_A V_A \qquad (1.56)$$

where $V_A = -Z_A/r_A$, is the potential due to the nucleus and inner shells of atom A.

These approximations give rise to three different types of core Hamiltonian integrals:

$$H^c_{\mu\mu} = U_{\mu\mu} + \sum_{B(\neq A)} <\varphi_\mu \mid V_B \mid \varphi_\mu > \qquad (\phi_\mu \text{ on A}) \qquad (1.57)$$

$$H^c_{\mu\nu} = U_{\mu\nu} + \sum_{B(\neq A)} <\varphi_\mu \mid V_B \mid \varphi_\nu > \qquad (\text{both } \phi_\mu \text{ and } \phi_\nu \text{ on A}) \qquad (1.58)$$

$$H^c_{\mu\nu} = <\varphi_\mu \mid -\frac{1}{2}\nabla^2 + V_A + V_B \mid \varphi_\nu > + \sum_{C(\neq A,B)} <\varphi_\mu \mid V_C \mid \varphi_\nu > \qquad (1.59)$$

(ϕ_μ on A and ϕ_ν on B)

where $U = -\frac{1}{2}\nabla^2 + V_A$

If one uses these approximations, the matrix elements of the Fock Hamiltonian given by equation (1.50) rearranges to,

$$F_{\mu\mu} = U_{\mu\mu} + (P_{AA} - \frac{1}{2}P_{\mu\mu})\gamma_{AA} + \sum_{B(\neq A)} (P_{BB}\gamma_{AB} - V_{AB})$$

$$= U_{\mu\mu} + (P_{AA} - \frac{1}{2}P_{\mu\mu})\gamma_{AA} + \sum_{B(\neq A)} (P_{BB} - Z_B)\gamma_{AB} \qquad (1.60)$$

($\Theta\, V_{AB}=Z_B\gamma_{AB}$)

Extended Hückel Method: One of the simplest, chemically intuitive and computationally inexpensive one electron semi-empirical theory is Extended Hückel Theory (EHT). In this method, only the valence electrons are considered. The

Hamiltonian is the sum of one electron effective Hamiltonians which are not considered explicitely. The basis sets consists of Slater type orbitals (STO) and the MOs are given as linear combination of the AOs, i.e.,

$$\Psi = \sum_{j=1}^{n} c_{\alpha j} \varphi_j \tag{1.61}$$

Application of the variational principle to eqn. (1.61) results in the following set of secular equations:

$$\sum_{j=1}^{n} \left(H_{ij} - \varepsilon_\alpha S_{ij}\right) c_{ij} = 0 \tag{1.62}$$

where $$S_{ij} = \int \varphi_i^* \varphi_j \, d\tau \tag{1.63}$$

and $$H_{ij} = \int \varphi_i^* \, H \varphi_j \, d\tau \tag{1.64}$$

The orbital energies and the coefficients are obtained by solving the secular determinants and the total energy is given by the sum of the energies of the occupied orbitals.

In the Extended Hückel method, the diagonal elements of the Hamiltonian are considered to be equal to the valence state ionization potential (VSIP) of an electron of the isolated atom, i.e.,

$$H_{ii} = -\text{VSIP}(\varphi_i) \tag{1.65}$$

And the off-diagonal elements of the Hamiltonian are evaluated using the Wolfsberg-Helmholz relation,

$$H_{ij} = K S_{ij} \frac{(H_{ii} + H_{jj})}{2} \tag{1.66}$$

where K is an adjustable parameter.

[1.1.2.4] Electron Correlation

In the Hartree-Fock (HF) method, an average interaction was used instead of the actual electron-electron interaction to solve the Schrödinger equation. In other words, the correlation of electrons are not treated explicitly in the HF method.[19] The difference between the HF energy and the exact non-relativistic energy is called the correlation energy.[1, 20] There are three types of electron-correlation effects, viz.,

i) *in-out* or *radial* correlation where one electron is close to, and the other far from the nucleus. Such effects are taken care of by the inclusion of basis sets having higher radial exponents.

ii) *left-right* correlation, where the two electrons tend to stay near different nuclei.

iii) angular correlation, where the two electrons tend to stay on opposite sides of the nucleus. This kind of correlation is incorporated by the inclusion of higher angular momentum functions.

Any method which include electron-correlation effects should have the following characteristics: *size extensivity*[21-24] and *size consistency*.[25] The term size extensivity refers to those methods which scales linearly with the number of particles. For example, if a homogeneous system has N units, then the energy is linear in N. The size extensivity characterizes the linear size dependence of properties such as the total energy, polarizability etc. in the limit of an infinite system of finite density. On the otherhand, in some quantum mechanical methods, the energy and thus the error in energy of a particular computation vary linearly with the number of particles as the size of the system increases. These methods are called as size consistent. The question of size consistency becomes important when one compares the energies of molecules of different sizes, e.g., a monomer and a dimer. A special case in hand is that of size consistency for infinitely separable atoms. A method is said to be size consistent if the

energy of a system made up of two infinitely apart subsystems X and Y is equal to the sum of the energies of X and Y calculated separately by the same method. In general, there are two major methods for treating the effect of electron-correlation in computations, viz., Configuration Interaction (**CI**)[26] and Møller-Plesset perturbation theory.[27]

i) Configuration Interaction (CI):

In this method, the wave function is considered as a linear combination of many Slater determinats. Each of these determinants represent an individual electronic configuration and they are constructed by replacing one or more of the occupied orbitals (ϕ_i, ϕ_j.....) with virtual spin orbitals (ϕ_a, ϕ_b.....).

If, within a given determinant, a virtual orbital ϕ_a replaces an occupied orbital ϕ_i, then it is called single substitution (ψ_i^a). Similarly, in double substitution (ψ_{ij}^{ab}), two occupied orbitals are replaced by virtual orbitals and so on. In a full **CI** calculation, one considers a wave function Ψ which is a linear combination of the HF determinants and all substituted determinants. Thus, for a full CI,

$$\Psi = c_0\psi_0 + \sum_{i>0} c_i\psi_i \qquad (1.67)$$

where the 0-indexed term is the HF level, and *i* runs over all possible substitutions. The sets of coefficients *c* are solved by minimizing the energy of the resultant wavefunction. The full CI is well defined, size consistent, variational, and thus is a perfect theoretical model.

The major disadvantage of the full CI method is that it is computationally highly expensive, and hence is not suitable for large molecules. Generally, the CI

expansion is truncated at some level and only a limited set of substitution is considered. Therefore, the following methods were introduced: **CIS** that includes single excitations with the HF determinant, **CID** that includes double excitation, and **CISD** that includes both single and double excitation. However, such limited CI is not size-consistent, which can be overcome by quadratic configuration interaction (**QCI**) method.

ii) Møller-Plesset Perturbation Theory (MPPT):

This method is mainly derived from many body perturbation theory (**MBPT**) and put forward by Rayleigh and Schrodinger. It adds higher excitations to HF theory as a non-iterative correction in contrast to the CI methods. In the perturbation theory, the Hamiltonian is considered as the sum of two parts, the second being a perturbation of the first. In general, the Hamiltonian is expressed as,

$$H = H^0 + \lambda H' + \ldots\ldots\ldots\ldots \quad (1.68)$$

where H^0 is the Hamiltonian for an unperturbed system. According to this assumption, the perturbed wavefunction and energy can be expressed as a power series in H'. Thus,

$$\Psi = \Psi^{(0)} + \lambda\Psi^{(1)} + \lambda^2\Psi^{(2)} + \lambda^2\Psi^{(3)} + \ldots\ldots\ldots\ldots \quad (1.69)$$

$$E = E^{(0)} + \lambda E^{(1)} + \lambda^2 E^{(2)} + \lambda^2 E^{(3)} + \ldots\ldots\ldots\ldots\ldots \quad (1.70)$$

Substitution of equations (1.64), (1.65) and (1.66) into the Schrödinger equation gives,

$$(H^0 + \lambda H^1 + \ldots)(\Psi^{(0)} + \lambda\Psi^{(1)} + \ldots) = (E^{(0)} + \lambda E^{(1)} + \ldots)(\Psi^{(0)} + \lambda\Psi^{(1)} + \ldots) \quad (1.71)$$

After collecting terms having similar power, one gets the following equations,

$$H^0\Psi^{(0)} = E^{(0)}\Psi^{(0)} \quad (1.72)$$

$$(H' - E^{(1)})\Psi^{(0)} + (H^0 - E^{(0)})\Psi^{(1)} = 0 \quad (1.73)$$

Solution of these equations led to different orders of correction to energy. Truncation of the series (1.69) and (1.71) after second order, third order etc. results in levels such as MP1, MP2, MP3, etc. As the order of the perturbation increases, the extent of electron correlation incorporated into a calculation also increases and thus the computing time. MPn methods are size consistent even though they are not variational. The most commonly used MPn method is MP2. Some of the other well known methods for treating electron correlation are Coupled Cluster (CC) theory[28] and Multiconfiguration self-consistent field (MCSCF) methods.[29]

[1.1.2.3] Density Functional Theory (DFT)

Density Functional Theory[5] is another approach for looking at the electronic ground state. In contrast to the wave function based *ab initio* methods, the density based DFT method provides a solid foundation for the development of computational methodologies for the evaluation of structure, energetics and properties of molecules at a much lower computational cost. Of particular interest is the efficiency of DFT methods in including the effects of electron correlation. Conceptually, *ab initio* and DFT methods are complementary in the sense that while the former are constructed from single-electron orbitals, ψ_i, and many electron wave functions Ψ, the root of DFT is the electron density $\rho(r)$.

As mentioned above, the main variable in DFT is the single particle density $\rho(r)$. For an N particle system, it is defined as

$$\rho(r_1) = N \int \ldots\ldots \int dr_2 dr_3 \ldots\ldots\ldots dr_N P(r_1, r_2, \ldots\ldots\ldots, r_N) \qquad (1.74)$$

Normalization of $\rho(r)$ gives the total number of electrons, i.e.,

$$\int \rho(r)\, dr = N \qquad (1.75)$$

For a many particle system characterized by an external potential $\upsilon(r)$ (due to the nuclei) the first **Hohenberg-Kohn theorem** (HK-I)[5c] states that there is a one-to-one mapping between the potential $\upsilon(r)$, the particle density $\rho(r)$, and the ground state wave function Ψ_0,

(HK-I) $$\rho(r) \leftrightarrow \upsilon(r) \leftrightarrow \Psi_0$$

The Hamiltonian for a system of N nonrelativistic, interacting electrons in an external potential, $\upsilon(r)$ is given by,

$$H = T + V + G$$

where $T = \sum_{i=1}^{N} -\frac{1}{2}\nabla_i^2$, $\quad V = \sum_{i=1}^{N} \upsilon(r_i) = \sum_{i=1}^{N}\sum_{\alpha=1}^{A} \frac{-Z_\alpha}{|R_\alpha - r_i|}$, $\quad G = \sum_{i<j}^{N} \frac{1}{r_{ij}}$

Since $\rho(r)$ determines N, $\upsilon(r)$ and all the properties of the ground state, therefore, the total energy of a system should be a functional of $\rho(r)$. Thus, the ground state energy $E_{\upsilon(r)}[\rho(r)]$ can be expressed as a function of $\rho(r)$ as,

$$\begin{aligned} E_{\upsilon(r)}[\rho(r)] &= T[\rho(r)] + V_{ne}[\rho(r)] + V_{ee}[\rho(r)] \\ &= \int \rho(r)\upsilon(r)dr + F_{HK}[\rho(r)] \end{aligned} \qquad (1.76)$$

where $$F_{HK}[\rho(r)] = T[\rho(r)] + V_{ee}[\rho(r)] \qquad (1.77)$$

Equation (1.77) can be rewritten as

$$F_{HK}[\rho(r)] = \langle \Psi[\rho(r)] | T + V_{ee} | \Psi[\rho(r)] \rangle \qquad (1.78)$$

where Ψ is the ground state wave function associated with ρ.

The introduction of the energy variational principle as suggested by the second **Hohenberg-Kohn** theorem (HK-II)[5c] gives,

$$E_{\upsilon(r)}[\rho(r)] = F_{HK}[\rho(r)] + \int\rho(r)\upsilon(r)dr \geq E_{\upsilon(r)}[\rho_0(r)] \qquad (1.79)$$

where $E_{\upsilon(r)}[\rho_0(r)]$ and $\rho_0(r)$ are the ground state energy and density. The variationally stable energy functional for a system of noninteracting electrons and a given external potential υ_s is,

$$E_s[\rho] = \langle\Psi_s[\rho]|T + V_s|\Psi[\rho]\rangle = T_s[\rho] + \int\upsilon_s(r)\rho(r)dr \geq E_{s,0} \qquad (1.80)$$

The Hohenberg-Kohn functional, F_{HK} can be written as

$$F_{HK}[\rho(r)] = T_s[\rho(r)] + J[\rho(r)] + E_{xc}[\rho(r)] \qquad (1.81)$$

where $T_s[\rho(r)]$ is the kinetic energy functional of a non-interacting system given by,

$$T_s[\rho(r)] = \sum_i^N \langle \Psi_i | -\frac{1}{2}\nabla^2 | \Psi_i \rangle \qquad (1.82)$$

$J[\rho(r)]$ is the classical Coulombic interaction energy,

$$J[\rho(r)] = \frac{1}{2}\iint\frac{\rho(r)\rho(r')}{|r-r'|}drdr' \qquad (1.83)$$

And $E_{xc}[\rho(r)]$ is the exchange-correlation energy.

The only difference between Hartree-Fock approximation and the above theory is the presence of the exchange-correlation term, E_{xc} in the later. Combining equations (1.76), (1.81), (1.82) and (1.79), one gets

$$E_{\upsilon(r)}[\rho(r)] = \int\rho(r)\upsilon(r)dr + \sum_i^N \langle \Psi_i | -\frac{1}{2}\nabla^2 | \Psi_i \rangle + \frac{1}{2}\iint\frac{\rho(r)\rho(r')}{|r-r'|}drdr' + E_{xc}[\rho(r)] \qquad (1.84)$$

Minimization of the energy functional $E_{\upsilon(r)}[\rho(r)]$ results in the following one particle **Kohn-Sham** (**KS**) equation,

$$[-\frac{1}{2}\nabla^2 + \upsilon_{eff}(r:[\rho])]\Psi_i = \varepsilon_i\Psi_i \tag{1.85}$$

where the density $\rho(r)$ is obtained as the sum

$$\rho(r) = \sum_i^N |\Psi_i(r)|^2 \tag{1.86}$$

and the **KS** effective potential υ_{eff} is given by

$$\begin{aligned}\upsilon_{eff}(r) &= \upsilon(r) + \frac{\delta J[\rho(r)]}{\delta\rho(r)} + \frac{\delta E_{xc}[\rho(r)]}{\delta\rho(r)} \\ &= \upsilon(r) + \int\frac{\rho(r')}{|r-r'|}dr' + \upsilon_{xc}(r)\end{aligned} \tag{1.87}$$

The energy correlation functional of the above equation is defined as,

$$\upsilon_{xc} = \frac{\delta E_{xc}[\rho(r)]}{\delta\rho(r)} \tag{1.88}$$

The ground state energy is given by,

$$E = \sum_i^N \varepsilon_i - \frac{1}{2}\int\frac{\rho(r)\rho(r')}{|r-r'|}drdr' + E_{xc}[\rho(r)] - \int\upsilon_{xc}(r)\rho(r)dr \tag{1.89}$$

where ε_i and ρ are the self-consistent quantities.

The key to the success of DFT lies in the approximations made for the exchange-correlation energy, $E_{xc}[\rho]$. The local density approximation (**LDA**) is found to be one of the simplest and efficient approximation for $E_{xc}[\rho]$. It is given by,

$$E_{xc}^{LDA}[\rho(r)] = \int\rho(r)\varepsilon_{xc}[\rho(r)]dr \tag{1.90}$$

where $\varepsilon_{xc}(\rho)$ is the exchange-correlation energy per particle of a uniform electron gas of density ρ. The corresponding exchange-correlation potential represented by eqn. (1.87) becomes,

$$\upsilon_{xc}^{LDA}(r) = \frac{\delta E_{xc}^{LDA}}{\delta\rho(r)} = \varepsilon_{xc}[\rho(r)] + \rho(r)\frac{\delta E_{xc}(\rho)}{\delta\rho} \tag{1.91}$$

Also, the Kohn-Sham orbitals are now given by,

$$\left[-\frac{1}{2}\nabla^2 + \upsilon(r) + \int\frac{\rho(r')}{|r-r'|}dr' + \upsilon_{xc}^{LDA}(r)\right]\Psi_i = \varepsilon_i\Psi_i \qquad (1.92)$$

The self-consistent solution of the above equation is called as the **LDA** method.

Other widely used approximations are generalized gradient approximation (**GGA**) and hybrid (HF + density) functional. One of the most popular hybrid method is the BLYP/HF method. One such method, viz., Becke3LYP[30] is extensively used in this thesis. In this method, the exchange energy is replaced by an exchange-correlation functional from Becke and Lee-Yang-Parr approximations using the electron density from HF. This functional is sum of parallel-spin (Becke) and antiparallel-spin parts (Lee-Yang-Parr). The different parameters and molecular properties obtained from this method are comparable to those obtained from more expensive *ab initio* calculations (for example, MP2).

[1.2] Brief Overview of the Remaining Chapters

[1.2.1] Chapter 2: Theoretical Study of Structure, Bonding, Stability and Aromaticity of Complexes of Titanocene and Zirconocene

Transition metal organometallics is a challenging research area of chemistry. Even though there are many similarities in reactivity and properties between the elements of a given group in the periodic table, there are contradictions as well. This chapter considers the reactivity of two such elements, viz., Ti and Zr, which behave differently under similar reaction conditions.

In the realm of transition metal organometallic chemistry, the in situ generated metallocenes, biscyclopentadienyl titanium (Cp_2Ti) and biscyclopentadienyl zirconium (Cp_2Zr) play a key role in the stoichiometric C-C coupling and cleavage reactions of unsaturated molecules such as alkynes, olefins, acetylides and vinylides. A variety of metallacycles, both saturated and unsaturated, results from such reactions. In the first section of this chapter, theoretical calculations on various five membered metallacycles of Ti and Zr are presented. The second section discusses the stabilities of an unstable five-membered organic specie C_5H_4 and the differences brought in as a result of replacement of one CH_2 group by Cp_2Ti or Cp_2Zr. The dimerization of metallacyclocumulene to metal substituted radialenes is presented in the last section.

[1.2.1.1] Structure and Neutral Homoaromaticity of Metallacyclopentene, -pentadiene, -pentyne and –pentatriene

Theoretical analysis of the structure, bonding and aromaticity of a series of five membered metallacycles (**1-6**) are presented. Theoretical studies at the DFT level shows significant metal-π interaction in all the metallacycles except **1** and **4**. The ring

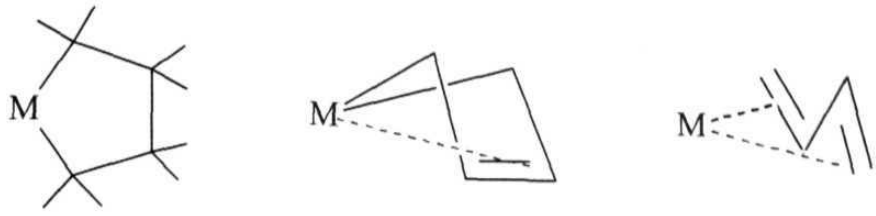

1 **2** **3**

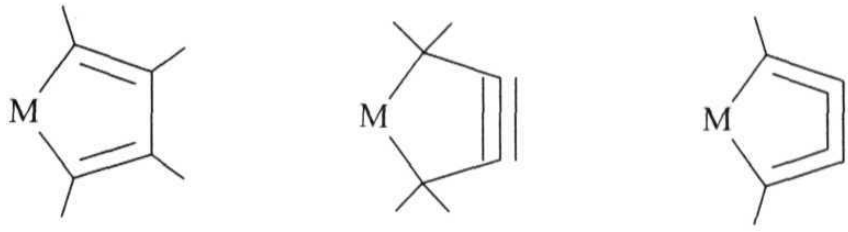

4 **5** **6**

strain in these metallacycles are evaluated from successive hydrogenation energies and compared with the parent carbocycles. Nucleus Independent Chemical Shift (**NICS**) calculations reveal that the metallacyclopentene (**2**) and metallacyclopentyne (**5**) are neutral bishomoaromatic, while the metallacyclopentatriene (**6**) is neutral in-plane aromatic.

[1.2.1.2] Dependence of the Structure and Stability of Cyclocumulenes and Cyclopropenes on the replacement of CH_2 group by Titanocene and Zirconocene

The replacement of small groups in organic structures by transition metal fragments has a dramatic impact on their stability and reactivity. The relative thermodynamic stabilities of cyclocumulene (**1**), alkynylcyclopropene (**2**), dialkynylmethane (**3**) and the isomers obtained by the replacement of the CH_2 group by Cp_2Ti and Cp_2Zr (**4**, **5**, and **6**) are presented in this section. The resulting metallacyclocumulenes (**4**), metallacyclopropenes (**5**), and metal bisacetylides (**6**) are important intermediates in the transformations of conjugated and non-conjugated alkadiynes by

Cp_2Ti and Cp_2Zr. The differences between **4** and **5** is calculated to be much smaller than that between **1** and **2**. Experimentally, the compound **5** is known only for Ti and it

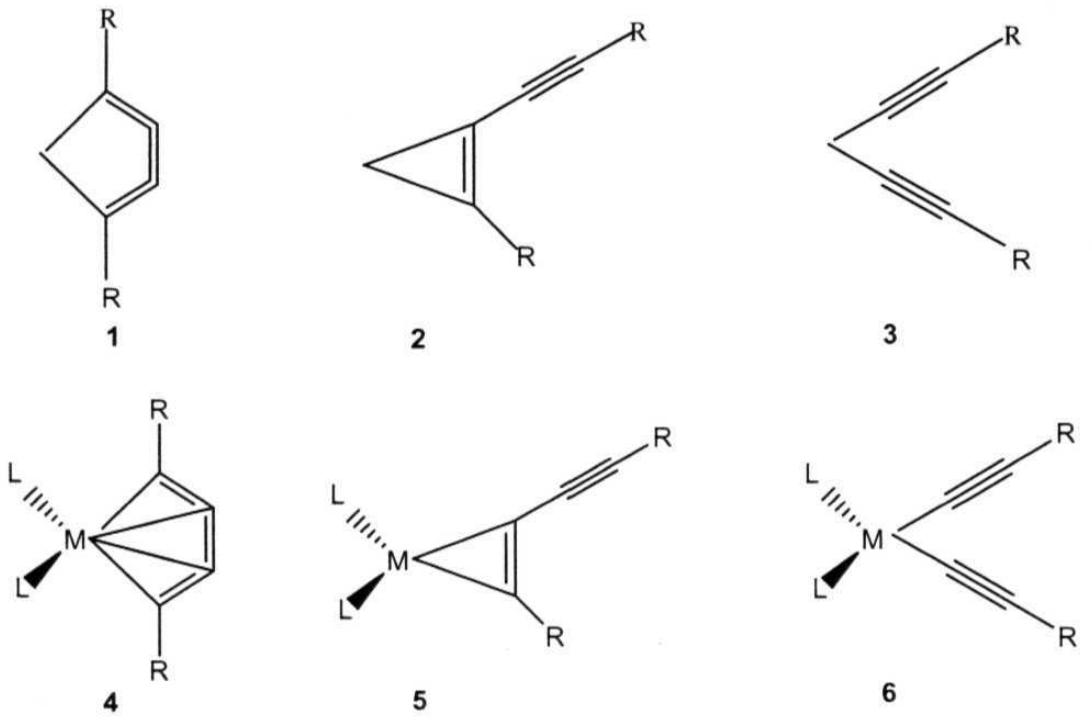

is found to exist in a dynamic equilibrium with **4**. Computational studies at the B3LYP/LANL2DZ level suggest that both **4** and **5** could be realized for Ti and Zr by using R =CN as the substituent on the carbon skeleton. A transition state connecting **4** and **5** is also characterized.

[1.2.1.3] Structure and Bonding of Metallacyclocumulenes, Radialenes, Butadiyne Complexes and Their Possible Interconversion

The Dewar-Chatt-Duncanson (DCD) model gave an elegant and simple description of the transition metal-alkene bonding in terms of π donation and metal back-donation. The properties of a complexed double bond, e.g., that of a metalla-cyclocumulene, depend on the extent of back bonding. In this section, the dimerization of metallacyclocumulenes (**1-3**) to either a radialene structure **A** or a bis(butadiyne)

geometry **B** is presented. While **1** is found to dimerize to **4**, **3** dimerizes to **9**. At the same time, neither **5** nor **8** could be realized for Zr. The conservation of orbital symmetry during the transformation of **1** → **4**, **4** → **7** and **6** → **9** are discussed. These

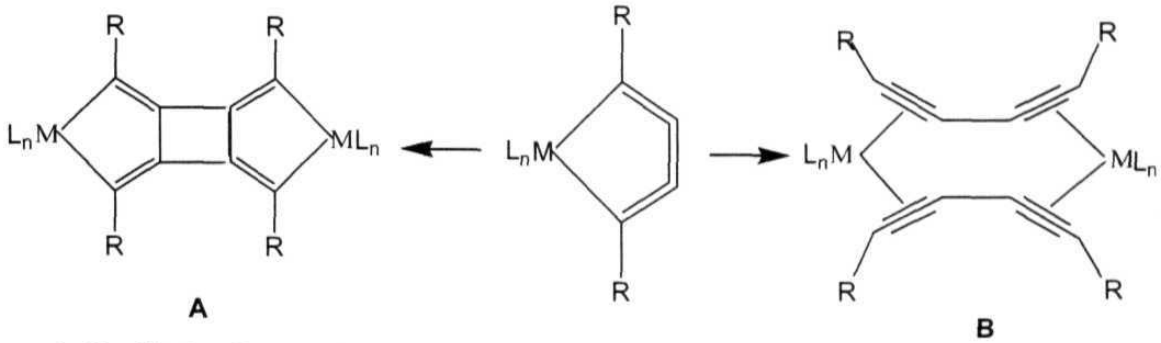

4 ; M = Ti ; L = Cp ; n=2
5 ; M = Zr ; L = Cp ; n=2
6 ; M = Ni ; L = NH_3 ; n=1

1 ; M = Ti ; L = Cp ; n=2
2 ; M = Zr ; L = Cp ; n=2
3 ; M = Ni ; L = NH_3 ; n=1

7 ; M = Ti ; L = Cp ; n=2
8 ; M = Zr ; L = Cp ; n=2
9 ; M = Ni ; L = NH_3 ; n=1

are all found to be symmetry allowed processes. The effect of substituents on the dimerization of metallacyclocumulenes is also analyzed and similar energetics are found for Ti and Zr.

[1.2.2] Chapter 3:Aromaticity of Cyclic Hydrocarbons and their B-N Analogues

Aromaticity is one of the most important concept in chemistry. The inorganic benzene, borazine, is a textbook example of six π–electron six membered ring. Compared to benzene, the cyclic delocalization of electrons in the borazine ring is reduced due to the large electronegativity difference between boron and nitrogen. Even though borazine has equal B-N bond lengths like benzene, the polarity of the BN bond causes borazine to show different reactivity pattern from that of benzene. Thus, it is natural that the chemistry of borazine is dominated by addition reactions.

The linearly annelated benzene rings, also known as the polycyclic aromatic hydrocarbons (PAHs) or acenes are important because of their role as pollutants, and in

particular, as carcinogens. Owing to their remarkable stability, these PAHs are found in substantial quantities in the interstellar space and are of substantial chemical interest. While the chemistry of benzene and its linearly annelated compounds is well developed, the corresponding B-N analogues are relatively unknown.

In the first part of this chapter, the extent of aromaticity in benzene and borazine are compared from their respective protonation and methylation energies. The aromaticity of the condensed derivatives of benzene and borazine are discussed in the next part. The B-N analogues of the hydrocarbons are obtained by replacing the carbon atoms with alternating B and N atoms.

[1.2.2.1] Parallel Aromatic Behavior of Benzene and Borazine

Even though borazine is predicted to undergo addition reactions, recent experimental evidence shows that borazine undergoes electrophilic aromatic substitution in the gas phase similar to its organic counterpart, benzene. Over the years, a number of criteria were employed to estimate the aromaticity in these molecules. Here, we attempt to judge the extent of aromaticity in benzene and borazine from their respective protonation and methylation energies.

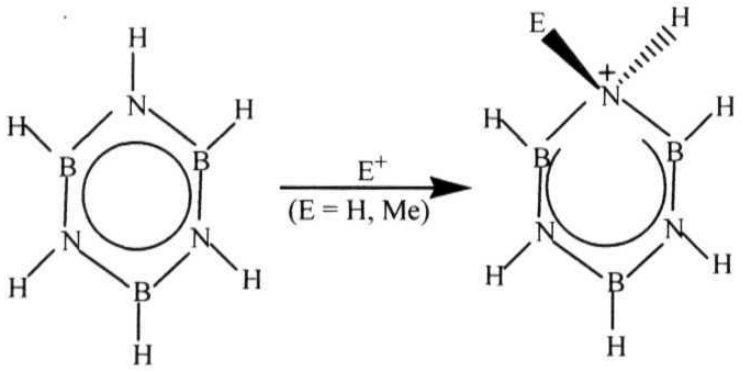

The results show that the stability of the σ- complex obtained from protonation or methylation is a good indicator of aromaticity. Even though there are quantitative

differences between hydrocarbons and the B-N analogues, the general trends show that $B_3N_3H_6$ is a stable species in the context of σ- complex. While the contribution of the σ- and π- electrons to the stability of the σ- complex can not be separated easily, this stabilization is a characteristic, in estimating aromaticity. According to this, $B_3N_3H_6$ is aromatic, though it is about half of that of benzene.

[1.2.2.2] Aromaticity of Acenes and Their B-N Analogues

The stabilization or resonance energies of the linear acenes and their BN analogues are evaluated by using the following equation:

E (*n* 1, 3-cyclohexadiene) + E (*trans*-perhydroacene) = E (acene) + E (*n* cyclohexene)

(n =3,5,7…)

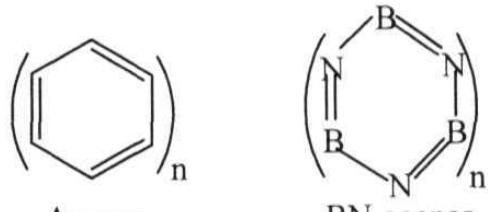

Acenes BN-acenes

n = 1-5

Even though the stabilization energy of the acenes and their BN analogues increases linearly from benzene to pentacene and borazine to BN-pentacene, the resonance energy per π electron remains constant only for the acenes. However, it increases steadily for the BN-acenes. On the other hand, nucleus independent chemical shift (**NICS**) calculations show that the aromaticity of the inner rings of the acenes is more than that of benzene, but the aromaticity of the individual rings in the BN-acenes remains constant and they are less than that of borazine.

[1.2.3] Chapter 4: Electronic Structure and Stability of Tricoordinate Pyramidal Boron

It is a common knowledge that the preferred conformation of tetracoordinate carbon is tetrahedral, and, it remained unchallenged till Hoffmann mooted the idea of a planar tetracoordinate carbon in 1970. During the last three decades, tremendous progress has been made in the theoretical understanding and synthesis of molecules with planar tetracoordinate carbon. This has opened the gate for other novel rule breaking structures. In this chapter, we discuss the electronic structure and bonding of such novel molecules having a tricoordinate pyramidal boron center by using both *ab initio* MO and density functional theory. The extent of pyramidalization and the difference in energy between the planar geometry, which is a transition state, and the pyramidal geometry, is found to be effected by the substituents on boron as well as by the nature of the heavy atom.

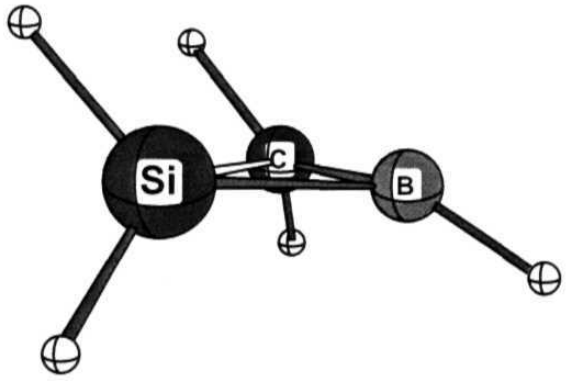

[1.3] References :

1. Bowen, J. P.; Allinger, N. L.; *Revs. In Computational Chem.* **1991**, *2*, 81.
2. Lennard-Jones, J. E. *Proc. R. Soc. London, Ser. A,* **1924**, *106*, 463.
3. (a) Pople, J. A.; Beveridge, D. L. *Approximate Molecular Orbital Theory* McGraw Hill Book Company, New York, 1970.

   (b) Chandra A.C *Introductory Quantum Chemistry*, 4th Edn., Tata McGraw Hill Publishing Company Limited, New Delhi, 1988.

   (c) Szabo, A.; Ostlund, N. S. *Modern Quantum Chemistry*, McGraw-Hill Publishing Company, New York, 1982.

   (d) Datta, S. N. *Lectures on Chemical Bonding and Quantum Chemistry*, Prism Books Pvt. Ltd., Bangalore (India) 1998.

   (e) Levine, I. N. *Quantum Chemistry*, 2nd Edn. Allyn and Bacon, Boston.

   (f) Lowe, J. P. *Quantum Chemistry*, Academic Press, New York, 1978.

   (g) McQuarrie, D. A. *Quantum Chemistry*, Oxford University Press, California, U.S.A., 1983.

   (h) Pilar, F. L. Elementary Quantum Chemistry, McGraw Hill Publishing Company, New York, 1968.

   (i) Foresman, J. B.; Frisch A Exploring Chemistry with Electronic Structure Methods. Gaussian Inc. Pittsburgh, USA.

   (j) Schaefer III, H. F. *Electronic Structure of Atoms and Molecules* Addison-Wesley, Massachusetts, USA, 1972.

   (k) Jensen, F. Introduction to Computational Chemistry John Wiley and Sons, West Sussex, England, 1999.
4. Hehre, W J.; Radom, L.; Schleyer, P. v. R.; Pople, J. A. *Ab-initio Molecular Orbital Theory* John Wiley & Sons, New York, 1986.
5. (a) Parr, R. G.; Yang, W. *Density functional Theory of Atoms and Molecules* Oxford University Press, Oxford, 1989.

   (b) Koch, W.; Holthausen, M. C. A *Chemist's Guide to Density Functional*

Theory; Wiley-VCH: Weinheim, 2000.

(c) Hohenberg, P.; Kohn, W. *Phys. Rev.* **1964**, *136B*, 864.

(d) Kohn, W.; Sham, L. J. *Phys. Rev.* **1965**, *A140*, 1133.

(e) Kohn, W.; Becke, A. D.; Parr, R. G. *J. Phys. Chem.* **1996**, *100*, 12974.

(f) Baerends, E. J.; Gritsenko, O. V. *J. Phys. Chem.* **1997**, *101*, 5383.

(g) Ghosh, S. K. *Int. J. Mol. Sci.* **2002**, *3*, 260.

(h) Geerlings, P.; De Proft, F.; Langenaeker, W. *Chem. Rev.* **2003,** *103,* 1793-1873.

6. Born, M.; Oppenheimer, J. R. *Ann. Physik* **1927**, *84*, 457.
7. (a) Hartree, D. R. *Proc. Cambridge Phil. Soc.* **1928**, *24*, 89.

   (b) Fock, V. *Z. Phys.* **1930**, *61*, 126.
8. Slater, J. C. Phys. Rev. **1930**, *36*, 57.
9. Boys, S. F. *Proc. R. Soc. (London) A*, **1950**, *200*, 542.
10. Barandiaran, Z.; Seijo, L.; Huzinaga, S. *J. Chem. Phys.* **1990**, *93*, 5843.
11. Frenking, G.; Antes, I.; Bohme, M.; Dapprich, S.; Ehlers, A. W.; Jonas, V.; Neuhaus, A.; Otto, M.; Stegmann, R.; Veldkamp, A.; Vyboishchikov, S. F. *Reviews in Computational Chemistry*; Lipkowitz, K. B., Boyd, D. B., Eds.; VCH: New York, **1996**, *8*, 63.
12. (a) Hay, P. J.; Wadt, W. R. *J. Chem. Phys.* **1985**, *82*, 270.

    (b) Wadt, W. R.; Hay, P. J. *J. Chem. Phys.* **1985**, *82*, 284.

    (c) Hay, P. J.; Wadt, W. R. *J. Chem. Phys.* **1985**, *82*, 299.
13. (a) Hoffmann, R.; Lipscomb, W. N. *J. Chem. Phys.* **1962**, *36*, 2179.

    (b) Hoffmann, R.; *J. Chem. Phys.* **1963**, *39*, 1397, **1964**, *40*, 2474, 2480, 2745.

    (c) Hoffmann, R. *Angew. Chem. Int. Ed. Engl.* **1982**, *21*, 711.
14. J. A.; Beveridge, D. L.; Dobosh, P. A. *J. Chem. Phys.* **1967**, *47*, 2026
15. Dewar, M. J. S.; Thiel, W. *J. Am. Chem. Soc.* **1977**, *99*, 4899.
16. Dewar, M. J. S.; Zoebisch, E. G.; Healy, E. F.; Stewart, J. J. P. *J. Am. Chem. Soc.* **1985**, *107*, 3902.
17. Stewart, J. J. P. *J. Comp. Chem.* **1989**, *10*, 209.

18. Pople, J. A.; Santry, D. P.; Segal, G. A. *J. Chem. Phys.* **1965**, *43*, 5129.

19. McWeeny, R. *Int. J. Quant. Chem.* **1967**, *15*, 351.

20. (a) Simons, J. *J. Phys. Chem.* **1991**, *95*, 1017.

(b) Bartlett, R. J.; Stanton, J. F. *Rev. Comput. Chem.* **1994**, *5*, 65.

21. Brueckner, K. A. *Phys. Rev.* **1955**, *97*, 1353.

22. Brueckner, K. A. *Phys. Rev.* **1955**, *100*, 36.

23. Goldstone, J. *Proc. Roy. Soc. London* **1957**, *239*, 267.

24. Bartlett, R. J.; Purvis, G. D. *Int. J. Quant. Chem.* **1978**, *14*, 561.

25. Pople, J. A.; Binkley, J. S.; Seeger, R. *Int. J. Quantum Chem., Symp.* **1976**, *10*, 1.

26. (a) Hurley, A. C. *Electron Correlation in Small Molecules* Academic Press, London, 1977.

(b) Wilson, S. *Electron Correlation in Molecules* Clarendon Press, Oxford, 1984.

(c) Raghavachari, K.; Anderson, J. B. *J. Phys. Chem.* **1996**, *100*, 12960.

27. Møller, C.; Plesset, M. S. *Phys. Rev.* **1934**, *46*, 618.

28. Hoffmann, M. R.; Schaefer, H. F. *Adv. Quantum Chem.* **1986**, *18*, 207.

29. Wahl, A. C.; Das, G. in *Methods of Electronic Structure Theory*, Schaefer, H. F. (Ed.); Plenum Press: New York, 1977, p. 51-78.

30. (a) Becke, A. D. *Phys. Rev.* **1988**, *A38*, 3098.

(b) Becke, A. D. *J. Chem. Phys.* **1993**, *98*, 5648.

(c) Lee, C.; Yang, W.; Parr, R. G. *Phys. Rev.* **1988**, *B37*, 785.

CHAPTER 2

THEORETICAL STUDY OF STRUCTURE, BONDING, STABILITY AND AROMATICITY OF COMPLEXES OF TITANOCENE AND ZIRCONOCENE

[2.0] ABSTRACT :

The reactive organometallic fragments biscyclopentadienyl titanium (Cp_2Ti) and biscyclopentadienyl zirconium (Cp_2Zr) are known to catalyze C-C coupling reactions of unsaturated molecules such as alkynes resulting in the formation of different metallacycles having unusual structures. A systematic analysis of the structure and bonding of a series of such metallacycles (**1-6**) will be discussed in the first section of this chapter (Scheme 2.1). While there is no interaction between the metal and the middle carbon atoms in metallacyclopentane (**1**) and metallacyclopentadiene (**4**), strong metal-π interaction is found in the other metallacycles. The metallacyclopentene (**2**)and metallacyclopentyne (**5**)are found to be neutral bishomoaromatic, while the metallacyclopentatriene (**6**)is neutral in-plane aromatic. The calculated NICS values and other bonding parameters support the strong cyclic delocalization of electrons in **2**, **5** and **6**.

A study of the energetics of the isomers of C_5H_4–cyclocumulene (**1**), ethynylcyclopropene (**2**), diethynylmethane (**3**), and their organometallic analogs obtained by replacing the CH_2 groups by Cp_2Ti and Cp_2Zr (**4**, **5**, **6**) forms the basis of the second section (Scheme 2.4). Computational studies at the B3LYP/LANL2DZ level shows that the transition metal fragments Cp_2Ti and Cp_2Zr has a dramatic impact on the stability of strained hydrocarbons. The calculated relative energies confirm the experimental observation that the metallacyclopropene (**5**) is more favorable for the Ti complex.

The last section of this chapter discusses the dimerization of metallacyclocumulenes (**1**, **2** and **3**) to metal substituted radialenes (**4**, **5** and **6**) (Scheme 2.7). These

are compared with the dimerization of ethylene to cyclobutane and cumulene to radialene (Scheme 2.8). A possible mechanism for the formation of bis(butadiyne) complex of Ni (**9**) is also presented. Correlation diagrams constructed for the conversion of the radialene type structure to that of the bis(butadiyne) complex show that it is allowed for both Ti and Ni.

[2.1] Structure and Neutral Homoaromaticity of Metallacyclopentene, -pentadiene, -pentyne and –pentatriene

[2.1.1] Introduction :

In the realm of transition metal organometallic chemistry, the in situ generated metallocenes, bis-cyclopentadienyl titanium (Cp_2Ti) and biscyclopentadienyl zirconium (Cp_2Zr) with d^2 valence electron count, play a key role.[1] In their many different forms, these metallocenes are extensively used as catalysts in olefin polymerization which is an important research area in catalytic chemistry.[2] Their importance arises from the extraordinary control that they have over the properties of the resulting polyolefins such as stereoregularity and stereoselectivity. Cp_2Ti and Cp_2Zr are also used in the synthesis of several precursors for the study of organometallic chemical vapor deposition (OMCVD) of ceramic thin films.[3] They play an important role in the stoichiometric C-C coupling and cleavage reactions of unsaturated molecules such as alkynes, olefins, acetylides and vinylides.[4] A variety of metallacycles, both saturated and unsaturated, results from such reactions, and some of these are represented in Scheme 2.1 in the order of increasing number of formal π bonds.[5-10] The five-

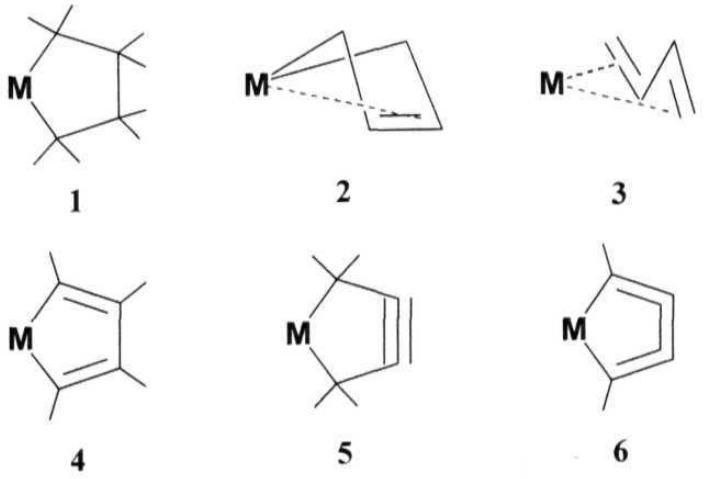

1 2 3

4 5 6

Scheme 2.1. Representative metallacycles (**1-6**), **M = Ti, Zr**

membered metallacycles occupy a special place in the chemistry of transition metal organometallics as they are involved in important reactions such as the synthesis of carbocyclic and heterocyclic compounds and their unusual ability to stabilize highly reactive organic entities.[4] The experimental approaches towards the realization of **1-6** are given in Scheme 2.2. The saturated metallacyclopentane (**1**) can be generated by

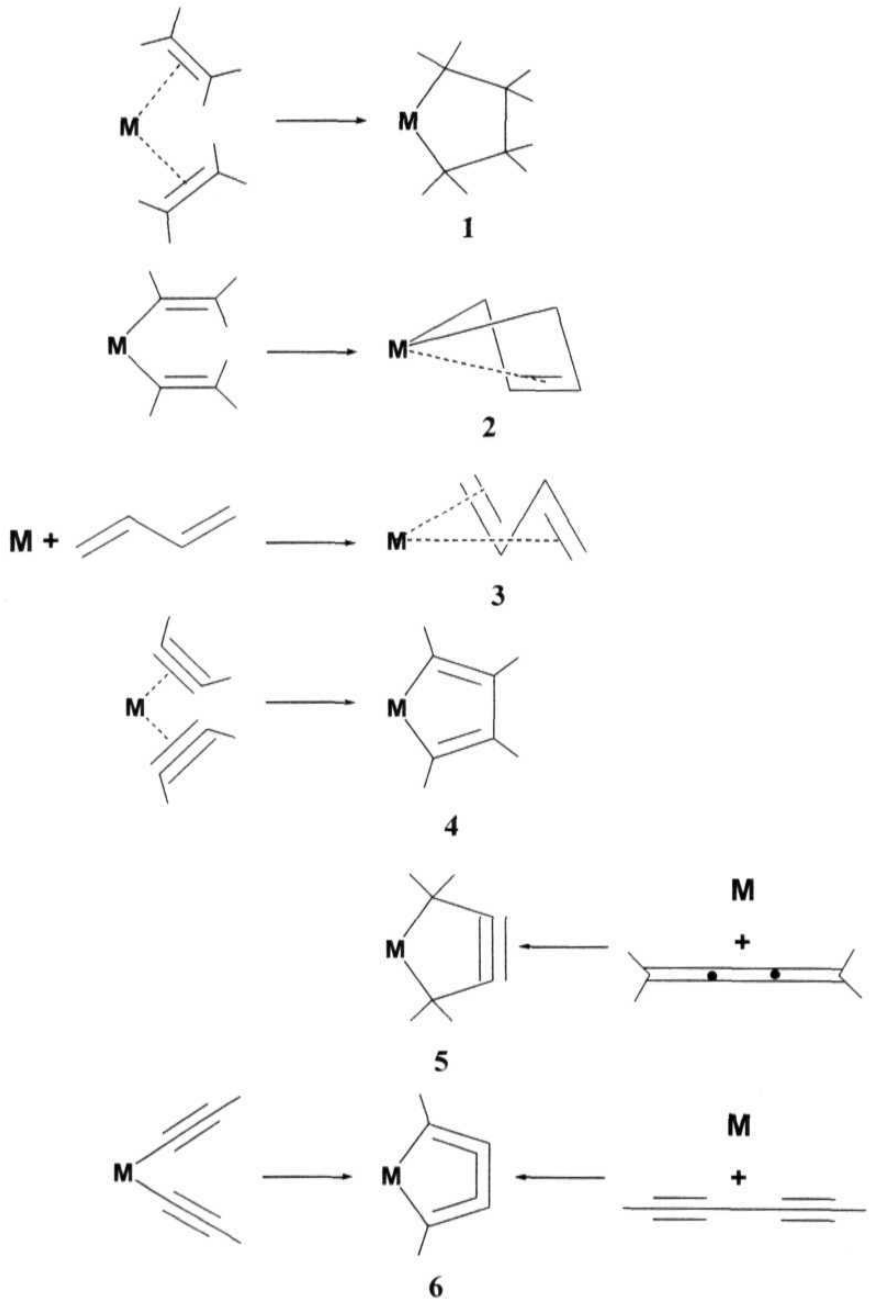

Scheme 2.2. Experimental approaches towards **1-6**

the treatment of *tert*-butyl substituted zirconocene dichloride with ethylene in the presence of *n*-butyl lithium.[5] Complex **2** can be prepared by the 1:1 reaction of zirconocene dichloride with enediyl-magnesium in THF,[6] and **3** by the photocatalysis of diphenyl zirconocene in the presence of a conjugated diene.[7] The metallacyclopentadiene (**4**) can be formed by the photolysis of dimethyl zirconocene or titanocene in the presence of diphenyl acetylene.[8] The recently reported metallacyclopentyne **5** is prepared by the reaction of zirconocene dichloride with 2 equivalents of *n*-butyllithium or *n*-butyl Grignard reagent and (Z)-1,4-bis-trimethylsilyl-1,2,3-butatriene.[9a] Metallacyclocumulene **6** can be prepared by the treatment of titanocene and zirconocene bis(trimethylsilyl)acetylene with 1,3-butadiynes or by the photocatalytic rearrangement of permethylzirconocene bisacetylides.[10] The formation of **2** and **6** through the direct coupling of two vinylides or two acetylides is favoured thermodynamically, and the reverse C-C cleavage reactions were observed only under drastic conditions.[11] In contrast, the olefin and alkyne coupling products **1** and **4** were found to be less stable, and the reverse C-C cleavage and retro-cycloaddition often occur under very mild conditions.[12] For example, zirconacyclopentane very easily undergoes β-β′ carbon-carbon bond cleavage to give zirconocene bisolefin complex, $Cp_2Zr(CH_2{=}CH_2)_2$.[13]

While the complexes **1-4** are well known in metallocene chemistry, the more exotic examples **5** and **6** were characterized only recently; the organic counterparts of **5** and **6** have been elusive so far.[9,14] On the basis of single crystal X-ray structural data and IR spectra on 1-zirconacyclo-pent-3-yne (**5**) with $Si(CH_3)_3$ or $C(CH_3)_3$ as substituents, it was concluded that there is no considerable interaction between the metal center and the C–C triple bond.[9a] This is in contrast with the

metallacyclocumulene complex **6**, where there is substantial interaction between the metal and the middle C=C bond. The titanium counterpart of **5** is unknown so far.

There are few theoretical studies about the structure and bonding of these metallacycles.[15-17] An earlier study of a zirconocene-butadiene complex based on the extended Hückel method predicts strong interaction of the metal with the terminal carbon atoms for the *cis* isomer while strong metal-middle carbon interaction for the *trans* isomer.[15] An *ab initio* MO theoretical study on titanacyclopentadiene using a small basis set shows strong interaction between the metal center and the terminal carbon atoms while ruling out any significant interaction with the middle carbon atoms.[16] A recent density functional theory study on the *cis*- and *trans*-butadiene complexes of zirconocene concludes the same.[17] Another DFT study on the structure and stability of the recently synthesized zirconacyclopentyne complex **5** concludes that it is a resonance hybrid between a metallacyclopentyne form and a cumulene complex Lewis structure.[9b] This study shows effective interaction between the metal atom and the central C=C bond of the cumulene ligand. In this chapter, we have compared the structure and aromaticity of **1-6**. The bonding parameters of various experimentally known five-membered metallacycles is given in Table 2.1 for comparison. Our study based on geometric and magnetic properties shows strong metal-π interaction in these metallacycles. The NICS values of several complexes indicate that the delocalization of the π electrons to the Zr and Ti is substantial, leading to the description of neutral homoaromatic to **2**, **5** and **6**. Homo- and bishomoaromaticity are usually observed in charged species,[18] but neutral homoaromatic systems are very rare.[19] The transition metal complexes studied here are the first examples of neutral homoaromaticity.

Table 2.1. **Bond Parameters of Different Experimentally known Metallacycles of Ti and Zr with the Generic Ligand C_5H_5 or its Derivatives.**

M-C1	M-C2	C1-C2	C2-C2′	Ref.
		1Zr ($C_5R_5ZrC_4R_8$)		
2.307	3.065	1.547	1.502	5
2.346	3.010	1.551	1.332	15a
2.305	3.0	1.556	1.494	26a
		2Zr (*cis*-$C_5R_5ZrC_4R_6$)		
2.300	2.597	1.451	1.398	7
2.293	2.709	1.469	1.392	27
2.313	2.461	1.436	1.370	19
2.296	2.557	1.450	1.394	19
		3Zr (*trans*-$C_5R_5ZrC_4R_6$)		
2.509	2.391	1.435	1.467	29
2.453	2.352	1.402	1.393	30
		4Zr ($C_5R_5ZrC_4R_4$)		
2.265	3.05	1.359	1.499	8a
2.265	3.01	1.351	1.503	31a
2.264	2.945	1.362	1.512	31b
2.245	2.861	1.358	1.481	31b
2.271	3.015	1.358	1.488	31c
2.245	2.951	1.351	1.518	31d
		5Zr ($C_5R_5ZrC_4R_4$)		
2.50	2.29	1.415	1.206	9
		6Zr ($C_5R_5ZrC_4R_2$)		
2.434	2.320	1.285	1.326	10a
2.423	2.305	1.292	1.336	10b
2.344	2.328	1.304	1.327	10b
		1Ti ($C_5R_5TiC_4R_8$)		
2.194	3.017	1.532	1.529	15b
2.209	2.950	1.526	1.532	26b
2.215	3.0	1.537	1.550	26b
		4Ti ($C_5R_5TiC_4R_4$)		
2.141	2.951	1.371	1.496	8b
2.160	2.946	1.362	1.493	31e
2.165	2.996	1.373	1.488	10e
2.177	2.872	1.353	1.490	15c
		6Ti ($C_5R_5TiC_4R_2$)		
2.252	2.210	1.244	1.338	10e

[2.1.2] Computational Methods :

All the molecules (**1-6**) were fully optimized using the B3LYP density functional method.[20] We used the LANL2DZ basis set with the effective core potentials of Hay and Wadt and an additional set of polarization function.[21] Frequency calculations were carried out at the same level to characterize the nature of the optimized structures. The nature of bonding was studied through NBO analysis.[22] In order to judge the extent of cyclic delocalization of electrons in **1-6**, nucleus independent chemical shifts (NICS)[23] calculations were carried out at the geometrical center point of the ring. This gives an insight into the possible interaction between the Ti and Zr centers and the C=C or C≡C bonds in the metallacycles. Gaussian 94 suite of program was used for all the calculations.[24] The contour plots were obtained by using the MOLDEN visualization program.[25] We have used the same computational procedure for the other two sections of this chapter unless stated otherwise.

[2.1.3] Results and Discussion :

[2.1.3.1] Structure and Bonding of Metallacycles :

The optimized geometries of the parent metallacycles are given in Figure 2.1. The theoretical bond parameters and natural bond orbital analysis of all the parent metallacycles (**1-6**) are given in Tables 2.2-2.3 and of the metallacyclopentyne complex **5** with CH_3 and SiH_3 as the substituents in Table 2.4. Also, contour plots of the MOs corresponding to the in-plane metal C2-C2′ interaction in **1-6** are given in Figure 2.2 to study the nature of bonding in these metallacycles.

i) Metallacyclopentanes (1): The calculated bond parameters for **1Zr** and **1Ti** are found to be comparable with the available experimental data (Tables 2.1 and 2.2).

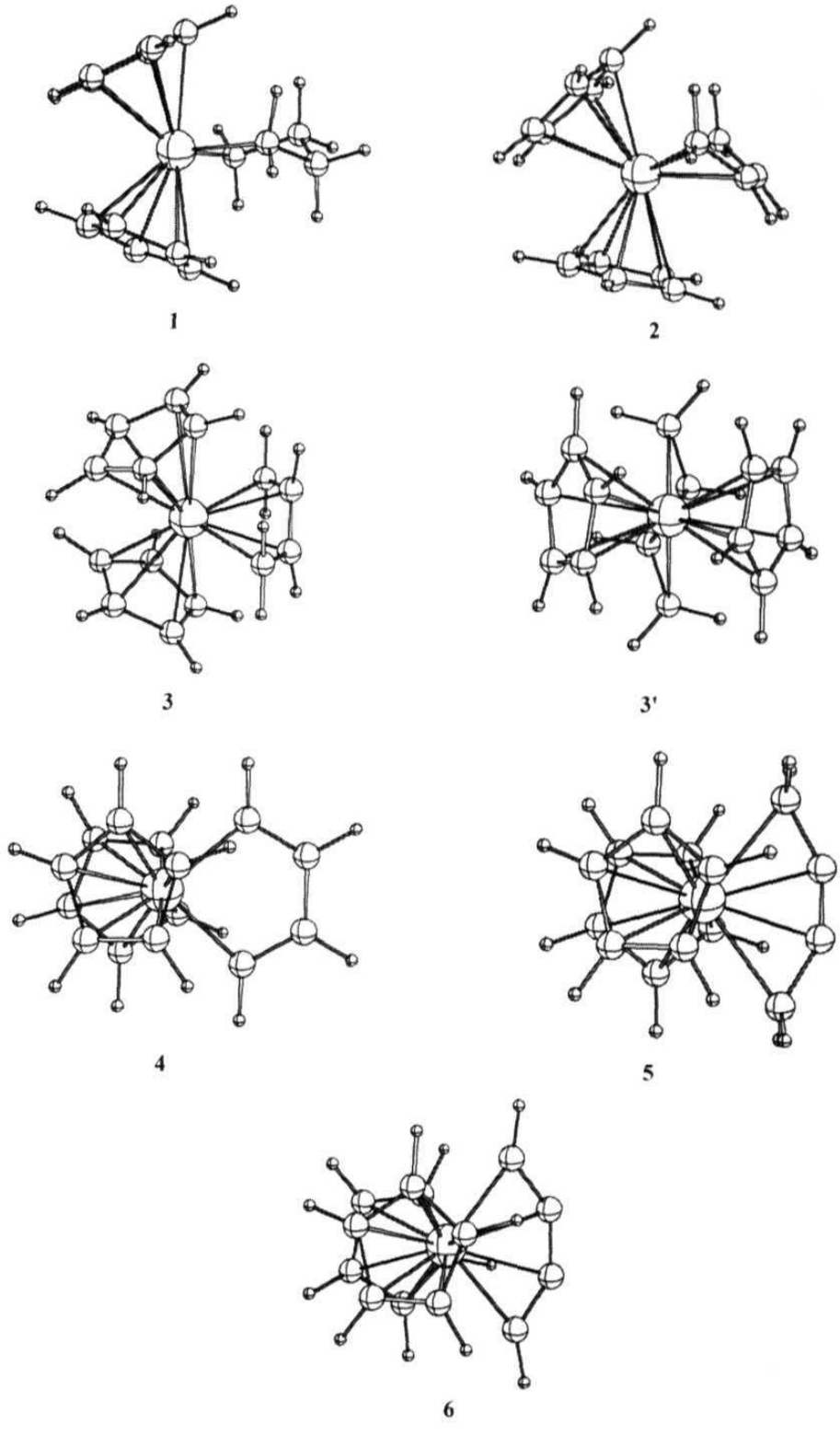

Figure 2.1. Optimized geometries of **1-6**. For a better understanding, the structure **3** is given in two different perspectives (**3** and **3'**).

Optimization gives a twisted five-membered ring (C_2 symmetry) for both complexes, and this agree well with the experimental findings.[12, 26] An NBO analysis shows a typical σ-bonding between M and C1, and no interaction between M and C2 is found (Table 2.3 and Figure 2.2). The M-C2 distance of 3.0 Å might serve as reference for no bonding. Therefore, **1** can be considered as a η^2-σ,σ-complex, in agreement with the discussion in the literature.[1, 9b] This M–C σ-bond length can be used as standard for comparison to all the other M-C distances.

ii) Metallacyclopentenes (2): Both the structures, **2Zr** and **2Ti**, were optimized as C_1 symmetry energy minima, although they are only slightly distorted from C_s symmetry. Due to the large interaction between the C=C double bond and the metal center, the five-membered ring is puckered rather than planar. The computed structural parameters for **2Zr** agree well with the available X-ray data for structures bearing methyl[7] or phenyl[27] substituents. In addition, the formal C=C double bond in **2Zr** of 1.399 Å is longer than that in parent cyclopentene (1.335 Å), but close to the benzene value (1.400 Å) at the same level. The Zr-C2 distance of 2.536 Å in **2Zr** is longer than in **5Zr** (2.330 Å), but shorter than in **1Zr** (3.045 Å), as given in Table 2.2. Although no experimental data are known for **2Ti**, the same trend of structural changes is found in the calculation for **2Ti**, as compared with **5Ti** and **1Ti**, and this indicates a strong Ti and C=C interaction in **2Ti**.

An NBO analysis (Table 2.3) shows a C=C double bond which interacts strongly with the metal center, and this results in a three-center and two electron (3c-2e) bonding. Figure 2.2 shows concentration of contour in the plane defined by the metal and the two middle carbon atoms of the metallacyclic ring in **2**. In **2Zr**, Zr

contributes 9.5%, Ti contributes somewhat more (12.0%) in **2Ti**. In these 3c-2e bondings, both carbon and metal are pure p or d orbital, and the calculated bond order for M-C2 and C=C are 0.538 and 1.717 for **2Zr,** and 0.420 and 1.687 for **2Ti**, respectively (Table 2.2). Therefore, **2** can be described as η^2-σ,σ + η^2-π complex. In addition to the puckered conformation, we have also computed the structure with planar five-membered ringfor **2Zr**. This planar structure (C_{2v}) is found to have an imaginary

Table 2.2. Theoretical Bond Parameters for the Parent Metallacycles (1-6). The NLMO Bond Order is Given Within Parenthesis.

	M-C1	M-C2	C1-C2	C2-C2′
1Zr	2.313	3.045	1.558	1.550
	(0.542)	(0.066)	(0.997)	(1.008)
2Zr	2.439	2.536	1.455	1.399
	(0.338)	(0.538)	(1.090)	(1.717)
3Zr	2.504	2.403	1.432	1.423
	(0.510)	(0.351)	(1.154)	(1.539)
4Zr	2.260	2.955	1.367	1.488
	(0.613)	(0.110)	(1.855)	(1.055)
5Zr	2.440	2.330	1.424	1.259
	(0.502)	(0.353)	(1.098)	(2.579)
6Zr	2.345	2.351	1.310	1.335
	(0.625)	(0.366)	(1.887)	(1.745)
1Ti	2.201	2.993	1.548	1.542
	(0.779)	(0.053)	(0.999)	(1.008)
2Ti	2.227	2.447	1.443	1.397
	(0.771)	(0.420)	(1.112)	(1.687)
3Ti	2.435	2.297	1.413	1.431
	(0.520)	(0.323)	(1.415)	(1.229)
4Ti	2.126	2.902	1.364	1.474
	(0.823)	(0.078)	(1.843)	(1.075)
5Ti	2.341	2.201	1.406	1.259
	(0.633)	(0.401)	(1.139)	(2.516)
6Ti	2.212	2.227	1.297	1.337
	(0.710)	(0.419)	(1.929)	(1.698)

Table 2.3. Hybridization and Orbital Occupancy (%) of the Parent Metallacycles (1-6)

	M-C1/σ	C1-C2/σ	C1-C2/π	C2-C2′/σ	C2-C2′/π
1Zr	$sd^{8.3}$ (Zr, 24.3%) $sp^{3.0}$ (C1, 73.6%)	$sp^{2.7}$ (C1, 48.5%) $sp^{2.8}$ (C2, 49.6%)		$sp^{2.8}$(C2+C2′,99.2%)	
2Zr	$sd^{15.2}$ (Zr, 25.0%) $sp^{5.2}$ (C1, 66.1%) p (C2+C2′,7.3%)	$sp^{2.6}$ (C1, 48.0%) $sp^{2.0}$ (C2, 50.1%)		$sp^{2.1}$(C2+C2′,98.8%)	d (Zr, 9.5%) p(C2+C2′, 85.8%)
3Zr	$sd^{21.8}$ (Zr, 26.3%) $sp^{6.3}$ (C1, 59.6%) p(C2+C2′,12.0%)	$sp^{2.5}$ (C1, 47.7%) $sp^{2.0}$ (C2, 50.9%)		$sp^{2.1}$(C2+C2′,98.4%)	d (Zr, 12.2%) p (C2+C2′, 81.4%) $sp^{11.6}$(C1+C1′,4.2%)
4Zr	$sd^{7.0}$ (Zr, 24.4%) $sp^{2.0}$ (C1, 73.3%)	$sp^{1.9}$ (C1, 48.3%) $sp^{1.8}$ (C2, 50.3%)	d (Zr, 2.2%) p(C1,45.0%) p(C2,48.5%)	$sp^{2.1}$(C2+C2′,98.8%)	
5Zr	$sd^{16.9}$ (Zr, 23.9%) $sp^{4.4}$ (C1, 64.5%) p(C2+C2′,10.0%)	$sp^{3.0}$ (C1, 46.4%) $sp^{1.1}$ (C2, 51.7%)		$sp^{1.3}$(C2+C2′,98.8%)	d (Zr, 4.0%) p (C2 + C2′, 92.4%) d (Zr, 9.2%) p (C2 + C2′, 87.0%)
6Zr	$sd^{12.5}$ (Zr, 23.6%) $sp^{2.2}$ (C1, 64.9%) p(C2+C2′,10.4%)	$sp^{2.3}$ (C1, 46.4%) $sp^{1.0}$ (C2, 52.0%)	d (Zr, 3.4%) p(C1,42.6%) p(C2,48.4%)	$sp^{1.4}$(C2+C2′,98.6%)	d (Zr, 9.6%) p (C2 + C2′, 85.6%)
1Ti	$sd^{15.0}$ (Ti, 36.5%) $sp^{3.4}$ (C1, 61.2%)	$sp^{2.6}$ (C1, 48.5%) $sp^{2.8}$ (C2, 49.7%)		$sp^{2.8}$(C2+C2′,99.2%)	
2Ti	d (Ti, 33.5%) $sp^{5.9}$ (C1, 56.4%) p (C2+C2′, 6.6%)	$sp^{2.5}$ (C1, 47.9%) $sp^{2.0}$ (C2, 50.1%)		$sp^{2.1}$(C2+C2′,98.8%)	d (Ti, 12.0%) p (C2 + C2′, 80.8%) $sp^{11.4}$(C1+C1′,4.8%)
3Ti	d (Ti, 38.0%) $sp^{8.6}$ (C1, 49.3%) p(C2 + C2′,8.1%)	d (Ti, 37.7%) p (C1, 38.6%) p(C1+C1′,12.0%) p (C2, 9.3%)		$sp^{2.7}$(C2,47.9%) $sp^{2.2}$(C2′,51.1%)	$sd^{10.6}$ (Ti, 11.7%) $sp^{8.6}$ (C1, 45.4%) p (C2, 38.2%)
4Ti	$sd^{14.6}$ (Ti, 36.2%) $sp^{2.2}$ (C1, 61.2%)	$sp^{1.8}$ (C1, 48.3%) $sp^{1.9}$ (C2, 50.2%)	d (Ti, 1.5%) p(C1,44.5%) p(C2,49.1%)	$sp^{2.2}$(C2+C2′,98.8%)	
5Ti	d (Ti, 33.7%) $sp^{5.4}$ (C1, 54.9%) p(C2+C2′,10.0%)	$sp^{2.9}$ (C1, 46.6%) $sp^{1.2}$ (C2, 51.6%)		$sp^{1.3}$(C2+C2′,99.0%)	d (Ti, 5.1%) p(C2+C2′, 91.4%) d (Ti, 12.8%) p(C2+C2′, 80.4%) $sp^{5.9}$(C1+C1′,4.6%)
6Ti	d (Ti, 33.7%) $sp^{2.4}$ (C1, 54.5%) p(C2+C2′,10.5%)	$sp^{2.2}$ (C1, 46.4%) $sp^{1.0}$ (C2, 52.0%)	d (Ti, 2.9%) p(C1,42.8%) p(C2,48.2%)	$sp^{1.4}$(C2+C2′,98.8%)	d (Ti, 13.2%) p(C2+ C2′, 79.0%) $sp^{4.5}$(C1+C1′, 4.8%)

vibrational frequency (–89i cm^{-1}) and therefore is a transition state on the potential energy surface. Following the imaginary mode leads to the puckered C_1 structure. The computed barrier ($\Delta G^{\neq}$, 298K) for the ring pocking is 9.0 kcal/mol, and this is close to the estimated 12.8 kcal/mol at 268 K on the basis of dynamic ^{13}C NMR measurements.[27]

iii) Complexes with *s-trans*-η^4-butadiene (3): It is found experimentally that **2Zr** equilibrates with its s-*trans*-η^4 isomer (**3Zr**) with a ratio of 45 (**2Zr**) to 55 (**3Zr**) at 298 K in C_6D_6.[28] This ratio indicates that both isomers are very close in energy. At the same level of theory, the computed difference in free energy between **2Zr** and **3Zr** is only 0.2 kcal/mol at 298 K, and this agree well with the experiment and gives also the error limit of theory to be less than 0.5 kcal/mol. The optimized structural parameters for **3Zr** agree at least with one set of the X-ray data for the 1,4-diphenyl-*trans*-butadiene,[29] since there are two independent molecules in the unit cell. It is shown both theoretically and experimentally that the Zr-C2 distance in **3Zr** is shorter than the Zr-C1 bond,[30] and this is in contrast to those in **2Zr**, in which the Zr-C1 bond is shorter than the Zr-C2 distance. In comparison with free *trans*-butadiene (1.341, 1.458 Å), the C-C bond lengths in **3Zr** are nearly equal (1.432 and 1.423 Å), and therefore it is hard to ascribe **3Zr** simply as an η^4-complex.

In contrast to **3Zr**, the corresponding **3Ti** complex is not known experimentally and no direct comparison is possible. The energy difference between **2Ti** and **3Ti** is much larger than that bet-ween **2Zr** and **3Zr**. At the same level of theory, **3Ti** is 5.6 kcal/mol more stable than **2Ti**, and the difference in free energy at 298 K is 4.6 kcal/mol. The absence of either of them points to some inherent unfavorability of Ti in

these geometries. This may be related to the smaller size of Ti in relation to Zr. For example, on reaction with $Me_3SiC{\equiv}C{-}C{\equiv}CSiMe_3$, Cp^*_2Ti forms the three-membered titanacyclopropene (η^2-complex) $Cp^*_2Ti(\eta^2\text{-}1,2\text{-}Me_3SiC_2C{\equiv}CSiMe_3)$ while Cp^*_2Zr produces the five-membered zirconacyclocumulene (η^4-complex) $Cp^*_2Zr(\eta^4\text{-}1,2,3,4\text{-}Me_3SiC_4SiMe_3)$.[10b]

NBO analysis supports a bonding description which is similar to that of **2Zr**, i.e., a strong Zr-C1 σ bond and a 3c-2e bonding between Zr center and the middle C=C double bond (Table 2.3). Compared to **2Zr**, the Zr-C interactions in **3Zr** involves contribution from the terminal carbon atoms also. Therefore, one can conclude that the bonding in the formal η^4-*s-trans*-butadiene **3Zr** can be described as η^2-σ,σ + η^2-π-complex between Zr and *trans*-1,4-but-2-endiyl.

iv) Metallacyclopentadienes (4): Both the computed and experimental[8,31] structural parameters for **4Zr** (Tables 2.1 and 2.2) reveal the delocalized bonding pattern as in the case of cyclopentadiene (1.349 and 1.479 Å). Both C-C bond lengths (1.367 and 1.488 Å) and NBO analysis (Table 2.3) show double bond character between C1 and C2, while conjugated single bond between C2 and C2′. Zr contributes only slightly (2.2%) to the C1-C2 double bond. A contour plot of **4** shows σ bonding between the metal and the terminal carbon atoms while no bonding interaction is found with the middle carbon atoms (Figure 2.2). Therefore, bonding in complex **4** can be described as η^2-σ,σ. The same is found for the Ti analog (**4Ti**). The computed and X-ray bond parameters show that M-C1 bond is of σ character and the C4 unit has typical butadiene characteristics, as evidenced by our NBO analysis and in tune with earlier theoretical studies.[16]

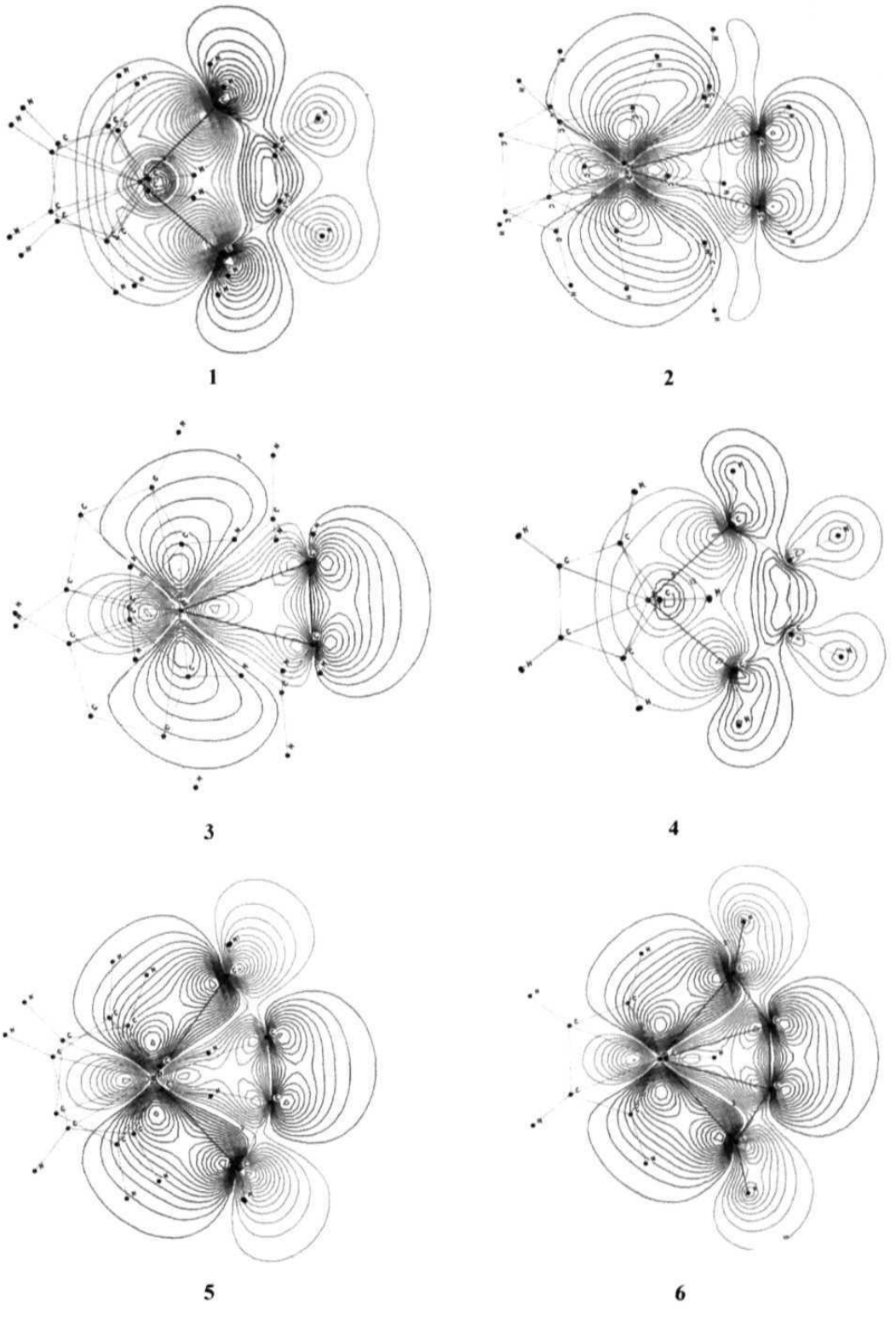

Figure 2.2. Contour plots of the MOs corresponding to the interaction of the metal and C2-C2′ for structures **1-6**.

v) 1-Zirconacyclopent-3-ynes (5Zr): Recently, Suzuki and co-workers reported the synthesis of a zirconacyclopentyne complex (**5**) with trimethylsilyl or *tert*-butyl group as the substituents.[9a] The X-ray structure of **5** shows an unusually short C-C middle bond (1.206 Å) prompting them to call it a metallacyclopentyne. The Zr-C2 and Zr-C3 bonds (2.29 Å) are shorter than Zr-C1 and Zr-C4 bonds (2.50 Å). The *cis* and *trans* conformations of **5Zr** with R = CH_3 or SiH_3 as the substituents were optimized under the C_s and C_2 symmetry constraints, respectively and they were found to be minima on the potential energy surface. The *trans* isomers are found to be only slightly more stable than the *cis* one, and the difference in free energy (ΔG°) is only 0.2 kcal/mol for R = SiH_3 or CH_3. This agrees well with the experimental findings. At room temperature, for example, equilibrium *cis/trans* ratios of 36/64 and 12/88 are found for R = $SiMe_3$ and *tert*-CMe_3, indicating that the *trans* isomers are slightly more populated than the *cis* one.

Table 2.4 lists a set of computed bond parameters for the parent and substituted **5Zr**. The bond parameters around the five-membered ring do not depend considerably on conformations (*cis/trans*) and substituents (R = SiH_3 or CH_3), and the only significant change is found for the Zr-C1 distance with R = H. Our calculations show that theory agrees reasonably well with the experiment, except for the formal C2-C2′ triple bond which is calculated to be longer (1.259 Å) than that found experimentally (1.206 Å) by Suzuki and coworkers.[9a] In addition, the computed stretch frequencies of the triple bonds of 2018 (R = SiH_3) and 2010 cm^{-1} (R = CH_3) also agree with the experimental values of 2014 (R = $SiMe_3$) and 2011 cm^{-1} (R = $C(CH_3)_3$), respectively. The shortening of the C≡C bond led Suzuki and coworkers to conclude that Zr does not interact considerably with the triple bond and **5Zr** prefers the η^2-σ,σ- (**A**) rather than

the η^2-π,π bonding (**B**), as shown in Scheme 2.3. However, the agreement of all other calculated geometric parameters with experiment makes one feel that the calculated C2-C2′ bond length is closer to reality. This led to the conclusion that while there may be small contribution from structures

Table 2.4. Computed Bond Parameters and NLMO Bond Orders (in *italics*) for the Parent as well as Substituted 1-Zirconacyclopent-3-yne (5Zr) and 1-Titanacyclopent-3-yne (5Ti).

Ligand (R)	M-C1	M-C2	C1-C2	C2-C2′	C1C2C2′
5Zr	2.440	2.330	1.424	1.259	151.2
(R = H)	*0.502*	*0.353*	*1.098*	*2.579*	
5Zr-*cis*	2.482	2.336	1.422	1.261	152.9
(R = CH_3)	*0.499*	*0.355*	*1.095*	*2.573*	
5Zr-*trans*	2.483	2.337	1.421	1.261	152.0
(R = CH_3)	*0.498*	*0.358*	*1.103*	*2.570*	
5Zr-*cis*	2.501	2.333	1.418	1.259	153.9
(R = SiH_3)	*0.461*	*0.365*	*1.122*	*2.565*	
5Zr-*trans*	2.503	2.333	1.417	1.259	154.0
(R = SiH_3)	*0.458*	*0.366*	*1.127*	*2.567*	
5Ti	2.341	2.201	1.406	1.259	150.9
(R = H)	*0.633*	*0.401*	*1.139*	*2.516*	
5Ti-*cis*	2.435	2.220	1.399	1.259	154.6
(R = CH_3)	*0.578*	*0.626*	*1.143*	*2.515*	
5Ti-*trans*	2.421	2.215	1.400	1.261	154.2
(R = CH_3)	0.627	0.404	1.144	2.508	
5Ti-*cis*	2.454	2.216	1.397	1.258	155.8
(R = SiH_3)	*0.564*	*0.565*	*1.164*	*2.505*	
5Ti-*trans*	2.447	2.213	1.398	1.259	155.5
(R = SiH_3)	*0.587*	*0.563*	*1.169*	*2.503*	

corresponding to **A** and **B**, major contribution to the actual structure must come from **C** (Scheme 2.3). A diffraction experiment at lower temperatures may lead to a longer C2-C2′ distance.[32]

In addition to the results discussed above, the interaction between Zr center and the triple bond was also analyzed. As shown in Table 2.2, all Zr-C2 bonds are shorter than Zr-C1. In comparison with 2-butyne (1.473 and 1.219 Å) which is calculated at the same level of theory, the C1-C2 distance in **5Zr** of 1.424 Å is shorter, while the C2-C2′ triple bond of 1.259 Å is longer. Since the ligand in **5Zr** is bent rather than linear, calculation was also performed on bent 2-butyne with the same CCC angle of 151.2° as

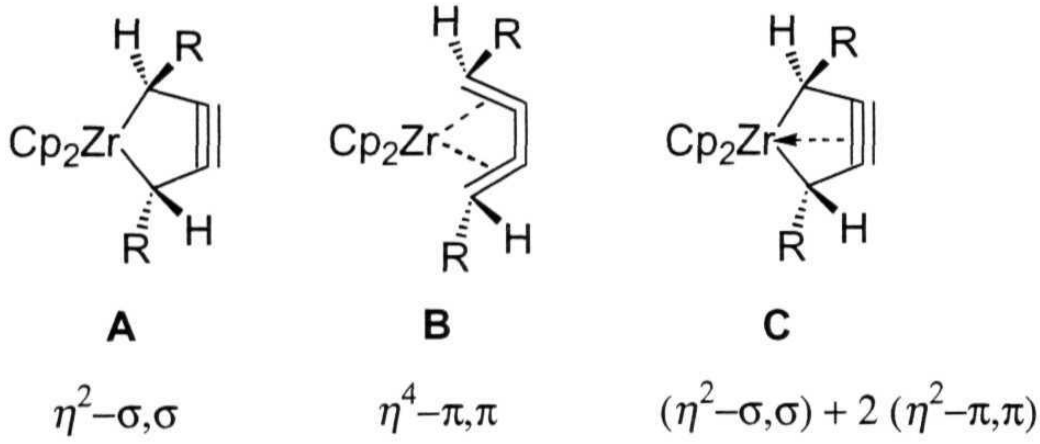

Scheme 2.3. Possible resonance structures (**A-C**) for **5**.

found in **5Zr**. The computed C-C triple bond length in bent 2-butyne of 1.226 Å is somewhat longer than in free 2-butyne, but still much shorter than in **5Zr**. Therefore, the elongation of the C-C triple bond in **5Zr** is mainly due to the interaction with metal rather than bending.

The strong interaction between Zr center and the triple bond is also indicated by the calculated bond order (Table 2.4), with or without substituents. Taking the plane of the five-membered ring as reference, there are two possible Zr-π interactions: the in-plane and the out-of-plane. As shown in Table 2.3, only σ bonds are found for Zr-C1 and C1-C2, but two types of three-center and two-electron interactions (3c-2e) are

found between Zr and the triple bond. Detailed analysis shows that the in-plane interaction is stronger than the out-of-plane one, as indicated by the contribution from Zr center. A contour plot of the frontier MOs of **5** also shows strong cyclic delocalization of electrons in the ring (Figure 2.2). On this basis, one can conclude that the bonding in **5Zr** is η^2-σ,σ + 2 (η^2-π,π) and structure **C** (Scheme 2.3) should be a reasonable resonance structure. In addition, the calculated C1-C2 and C2-C2' distances also do not support the cumulenic resonance form (**B**). For example, the C1-C2 (1.422 Å) and C2-C2' (1.259 Å) bonds in **5Zr** is too longer and too shorter than the corresponding cumulated C=C bonds in *cis*-RHC=C=C=CRH (R = H (1.330 vs. 1.281 Å), CH_3 (1.332 vs. 1.281 Å), and SiH_3 (1.333 vs. 1.282 Å), respectively). On the other hand, a cumulenic C=C double bond in interaction with a metal center should be much longer than in its free form, as indicated by central C-C bond length of 1.399 Å in **2Zr**, and this is not the case in **5Zr**. Therefore, our analysis is in contrast with the work by Lin et al where they have emphasized the importance of resonance structures **A** and **B**.[9b] Such co-existing in-plane and out-of-plane cyclic delocalized systems were considered as double aromatic, as found in 3,5-dehydrophenyl cation and cyclo[6]carbon.[33] Therefore, **5Zr** can be double aromatic, indeed neutral bishomoaromatic.

vi) 1-Titanacyclopent-3-ynes (5Ti): In contrast to **5Zr**, the corresponding **5Ti** is yet to be synthesized. However, similar bonding characteristics are found for **5Ti** and **5Zr**. For example, as given in Table 2.4, the C2-C2' triple bond in **5Ti** is also elongated and has nearly the same bond order as in **5Zr**. In addition, population analysis also shows that Ti interacts strongly with the triple bond and forms the in-plane and out-of-plane 3c-2e interaction (Table 2.3). Therefore, **5Ti** with a η^2-σ,σ + 2 (η^2-π,π) bonding as **5Zr**

should also be bishomoaromatic. It is found that Ti (+0.295) is less positively charged in **5Ti** than Zr in **5Zr** (+1.282).

Computation was also performed on the substituted **5Ti** with R = CH_3 and SiH_3 to aid the experimental investigators. The *trans* isomers are of C_2 symmetry, while the *cis* isomers have C_1 symmetry. The C_s symmetrical *cis* isomers with one imaginary frequency for the rotation of C_5H_5 rings are less than 0.2 kcal/mol higher in energy for both R = CH_3 and SiH_3. Therefore, the C_s structures are used for analysis. The calculated bond parameters are summarized in Table 2.4. As in the case of **5Zr**, both the *trans* isomers are favored energetically than the *cis* ones, and the calculated free energy difference at 298 K is 1.5 kcal/mol for R = SiH_3 and 1.3 kcal/mol for R = CH_3, respectively. The calculated stretching frequencies of the formal triple bonds in **5Ti** (2047 cm^{-1}, R = SiH_3) are slightly higher than those found in **5Zr**.

vii) Metallacyclopentatrienes (6): For both **6Zr** and **6Ti**, the computed bond parameters are comparable to those found experimentally (Tables 2.1 and 2.2).[10] The metal atom and the four carbon atoms of the metallacyclocumulene ring are coplanar. The bonding properties have been analyzed and strong interaction between the metal and the in-plane π bond is found.[34] The computed bond indexes and populations (Tables 2.2 and 2.3) reveal the cumulenic nature in **6Zr**. The additional in-plane interaction is also a 3c-2e bonding in which Zr contributes 9.6%, comparable with those in **2Zr** and **5Zr**. The contour plot of **6** shows significant delocalization of electrons in the ring similar to that in **5** (Figure 2.2). In agreement with X-ray results, similar structural pattern is found for **6Ti**. The similarity in the bonding pattern of **5** and **6** is exemplified by the frontier orbitals of **5** and **6** (Figure 2.3). This was subsequently reinforced by the work of Lin and co-workers.[9b]

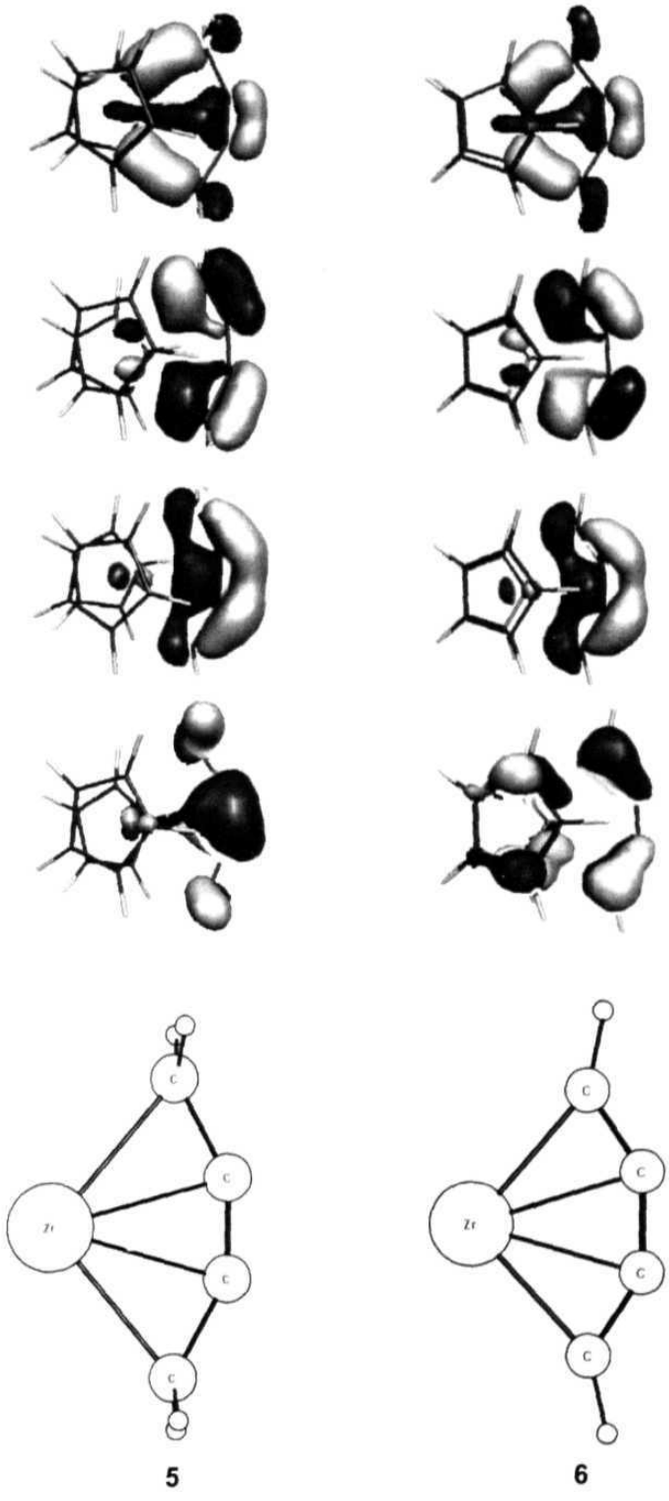

Figure 2.3. The three highest occupied in-plane π-type MOs of structures **5** and **6** are given at the top. The highest occupied π MOs in the perpendicular plane are given below this.

A better understanding of the structure **6** is obtained from a fragment molecular orbital approach.[35] The metal fragment Cp_2M is in formal oxidation state of +2 with two valence electrons and three frontier orbitals, all of which are in the MC4 plane. The in-plane frontier orbitals of the HCCCCH fragment are formed from the *sp* hybrid orbitals on the end carbon atoms, C1 and C4, and the two in-plane *p* orbitals on the two middle carbon atoms. These form four linear combinations, much the same in symmetry as the π orbitals of butadiene. The lowest two orbitals among these are filled. The next MO, the LUMO of the C_4H_2 fragment, corresponds to the LUMO of the butadiene in symmetry and is bonding between C2 and C3. The strongest stabilizing interaction between the Cp_2M fragment and the C_4H_2 takes place between this LUMO of C_4H_2 and the HOMO of Cp_2M. This interaction stabilizes the C2-C3 bond. The consequence of this bonding is tempered by the two π MOs perpendicular to the MC4 plane, typical of butadiene.

[2.1.3.2] Ring Strain in metallacycles (1-6) : The ring strain in the metallacycles were calculated by successive hydrogenation energies from the unsaturated metallacyclopentatriene (**6**) to the saturated metallacyclopentane (**1**). As given in Table 2.5, the two C=C double bond in cyclopentadiene (**$4CH_2$**, obtained by replacing the L_2M fragment of the metallacycles by CH_2 group) does not differ much as that in cyclopentene (**$2CH_2$**), since the hydrogenation energies are close to each other (23.1 and 25.8 kcal/mol, and the experimental values are 24.0 and 26.4 kcal/mol,[36] respectively). The same is also found for the **4Ti** and **2Ti** (20.1 and 19.8 kcal/mol), but their hydrogenation energies are smaller than those of **$4CH_2$** and **$2CH_2$**. In contrast, the hydrogenation energy of **4Zr** of 30.4 kcal/mol is larger than that of **2Zr** (13.1

kcal/mol). It is interesting to note that the hydrogenation energy of **2Ti** is larger that that of **2Zr**, but that of **4Ti** is smaller than **4Zr**.

Table 2.5. Successive Hydrogenation Energies (kcal/mol)[a]

M	2 → 1	4 → 2	5 → 2	6 → 4
CH_2[b]	25.8 (23.1)	23.1 (25.8)	106.3	123.4
Cp_2Ti	19.8	20.1	20.7	38.5
Cp_2Zr	13.1	30.4	24.7	31.5

[a]At B3LYP/LANL2DZp + ZPE (B3LYP/LANL2DZp; [b]The energies of the hydrocarbon equivalents (obtained by replacing the L_2M fragment with CH_2) of the metallacycles are given for comparison. The numbers within parenthesis indicate the experimental values.

As expected, the C-C triple bond in cyclopentyne (**5CH$_2$**) and the C-C cumulenic bond in cyclopentatriene (**6CH$_2$**) have huge hydrogenation energies (106.3 and 123.4 kcal/mol), which are more than four and five times the value of cyclopentadiene. Such large differences indicates the enhanced strain in both **5CH$_2$** and **6CH$_2$** and this is not very surprising why they are still elusive.

In contrast to the parent hydrocarbons, the hydrogenation energy of **5Ti** is very close to those of **2Ti** and **4Ti**, while that of **6Ti** is about double of those of **2Ti**, **4Ti** and **5Ti**, respectively. That both **4Ti** and **6Ti** are known in the experimental literature, the currently elusive **5Ti** should be the target for experimental realization. The small hydrogenation energies for both **5Zr** and **6Zr**, which are close to that of **4Zr**, indicate that these molecules are not strained as pointed out by Lin and co-workers.[9b] These reduced hydrogenation energies can be ascribed to the very strong stabilization interaction between the metal center and the ligands, as indicated by the NBO analysis, and the aromatic stabilization as discussed below.

[2.1.3.3] NICS Characterization: NICS calculations (Table 2.6) give a fair idea about cyclic delocalization of electrons or aromaticity[23] as well as possible interaction between the metal and the C=C bond in these metallacycles. As expected, the saturated metallacyclopentanes (**1**) are non-aromatic. This is also indicated by the calculated NICS values at the ring center, NICS (0), and 1 Å above the ring center, NICS (1). Similarly, metallacyclopentadienes **4Zr** and

Table 2.6. Calculated NICS (*x*) Values for Five-Membered Metallacycles.[a]

	NICS (0)	NICS (0.5)	NICS (1)	NICS (1.5)
1Zr	−5.8	−5.1	−3.5	−1.2
2Zr	−32.0	−18.2[b]	−11.9[b]	−8.7[b]
		(−31.6)[c]	(−18.1)[c]	(−12.0)[c]
4Zr	+0.3	−0.7	−1.5	−1.8
5Zr	−49.4	−37.2	−19.8	−11.5
6Zr	−34.4	−26.3	−15.0	−9.6
1Ti	−8.3	−6.6	−3.4	−1.0
2Ti	−33.2	−16.8[b]	−10.6[b]	−7.9[b]
		(−35.0)[c]	(−21.7)[c]	(−16.3)[c]
4Ti	−3.2	−3.4	−2.8	−2.0
5Ti	−53.3	−40.2	−21.3	−12.5
6Ti	−36.2	−28.3	−16.7	−11.4

a) Calculated at the center (0) and above the ring center (0.5 to 1.5Å).
b) At the convex side. c) At the concave side

4Ti with small NICS (**1**) values of −1.5 and −2.8 are also not aromatic which is in agreement with their geometric parameters.

In contrast, very strong metal-π interaction is found in both **2Zr** and **2Ti**, as indicated by their large NICS(0) and NICS (1) values. These are due to the 3c-2e bonding. The NICS (1) values for the concave (−18.1 vs. −21.7) side and convex (−11.9 vs. −10.6) side are larger or close to the benzene value. Thus, one might conclude that they are neutral bishomoaromatic, as compared tothe parent 4-

cyclopentenyl cation.[37] As given in Table 2.6, cyclocumulene complexes **6Zr** and **6Ti** have nearly the same NICS(0) values (–34.4 and –36.2) as cyclopentene derivatives **2Zr** (–32.0) and **2Ti** (–33.2). This is due to the fact that they have the in-plane 3c-2e interaction as indicated in the population analysis (Table 2.3). Therefore, complex **6** can be considered to be in-plane aromatic.

From the population analysis in Table 2.3, we found two 3c-2e interaction in the metallacyclo-pentyne complexes (**5Zr** and **5Ti**), the in-plane and the out-of-plane types. Therefore, it is expected that the NICS values at the ring centers in **5Zr** and **5Ti** should be more negative than those in **2** and **6**. Indeed, we found more negative NICS (0) values for **5Zr** (–49.4) and **5Ti** (–53.3), and one might conclude that they are neutral bishomoaromatic.

[2.1.4] Conclusions :

A comparison of the structure and bonding of the metallacycles **1-6** shows that there is consider-able metal-π interactions in **2**, **5**, and **6**. Our analysis of geometric and magnetic properties (NICS) shows the presence of strong delocalization in these systems including that of the metallacyclopentyne (**5**), which is contrary to previous conclusions.[9] The metallacyclopentene (**2**) and metallacyclopentyne (**5**) are found to be neutral bishomoaromatic, while the metallacyclocumulene (**6**) is in-plane aromatic. A comparison of the hydrogenation energies of the parent carbocycles and metallacycles shows that the strain present in cyclopentynes and cyclopentatrienes is practically removed when the CH_2 group is replaced by a Cp_2M fragment (M = Ti, Zr).

[2.2] Dependence of the Structure and Stability of Cyclocumulenes and Cyclopropenes on the replacement of CH_2 group by Titanocene and Zirconocene

[2.2.1] Introduction :

After discussing the structure, bonding, aromaticity and ring strain of various metallacycles in the previous section, we move on to compare the stability of some hydrocarbons with their organometallic counterparts. The replacement of small groups in organic structures by transition metal fragments results in a broad class of organometallic compounds which are extensively used in industry.[4] The transformation of the organic moiety as a result of the attachment of a metal fragment is so delicate and specific that apparently similar fragments make large changes in the system.[38] Here, we consider, the relative thermodynamic stabilities of cyclocumulene (**1**), alkynylcyclopropene (**2**), dialkynylmethane (**3**) and the isomers obtained by the replacement of the CH_2 group by Cp_2Ti and Cp_2Zr. The resulting metallacyclocumulenes (**4**), metallacyclopropenes (**5**), and metal bisacetylides (**6**) are important intermediates in the transformations of conjugated and non-conjugated alkadiynes by Cp_2Ti and Cp_2Zr.[4f,39] The reactivity of the Ti and the Zr complexes differ dramatically. Using similar reaction conditions where **4** is generated, Ti forms the C-C coupled structure **7** whereas Zr favors the structure **8**, where coupling between the two internal carbon atoms are absent. A three membered metallacyclopropene **5** with M = Ti and $R^1 = R^2 = SiMe_3$ has been reported recently.[10b] The attempt to synthesize similar complexes for Zr has been unsuccessful so far. On the otherhand, the five membered metallacyclocumulene complex, **4**, as well as the bisacetylide complex, **6**, are known for both Ti and Zr.[10, 40, 41] The experimentally reported structures of **4**, **5** and **6** are given in Scheme 2.4.

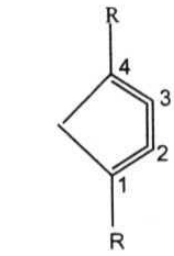

1

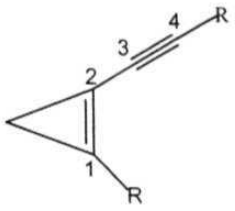

2

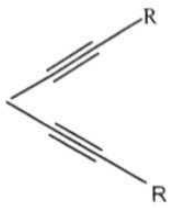

3

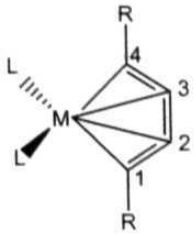

4

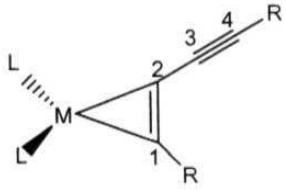

5

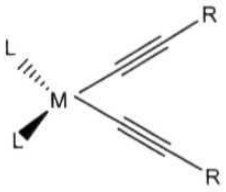

6

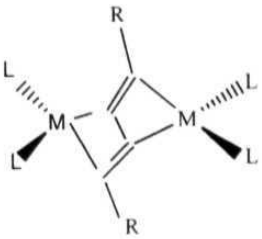

7

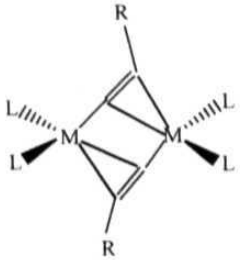

8

Scheme 2.4

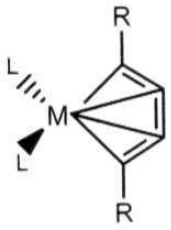

4

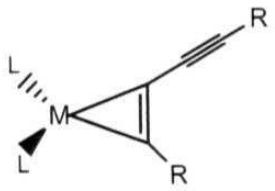

5

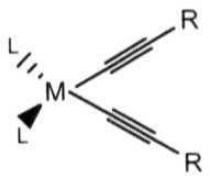

6

	M	L	R	4	5	6	ref.
i)	Ti	Cp	^{t}Bu	4			7
ii)	Ti	Cp*	$SiMe_3$		5		5
iii)	Ti	$C_5H_4(SiMe_3)$	$SiMe_3$			6	9b
iv)	Zr	Cp	^{t}Bu	4			6
v)	Zr	Cp*	Ph	4			5
vi)	Zr	Cp*	$SiMe_3$	4			5
vii)	Zr	Cp*	Ph			6	9c
viii)	Zr	Cp	CH_3			6	9a
ix)	Zr	$C_5(Me)_4H$	$SiMe_3$			6	9d

The metallacyclocumulenes (**4**) exist in a dynamic equilibrium with their respective three membered (η^2-) isomer, **5** (Scheme 2.5). The metallacyclopropenes (**5**) may also convert to the degenerate alternative through a sliding of the metallocene unit along the butadiyne chain.[10a] The bis (σ-alkynyl) complexes of Ti and Zr (**6**) are known to undergo photochemical rearrangement to the cyclocumulenic complex (**4**).[10c, 41] These bisacetylide complexes were used for the preparation of homo and heterobinuclear complexes containing bridging σ–π alkynyl groups between the metal centers.[42] Experimental and theoretical studies are unraveling the details of these intricate set of reactions.[4f,10, 38] While the relative energies of the organic isomers are part of general knowledge in organic chemistry, similar understanding is only beginning to take shape in transition metal organometallics.

Scheme 2.5

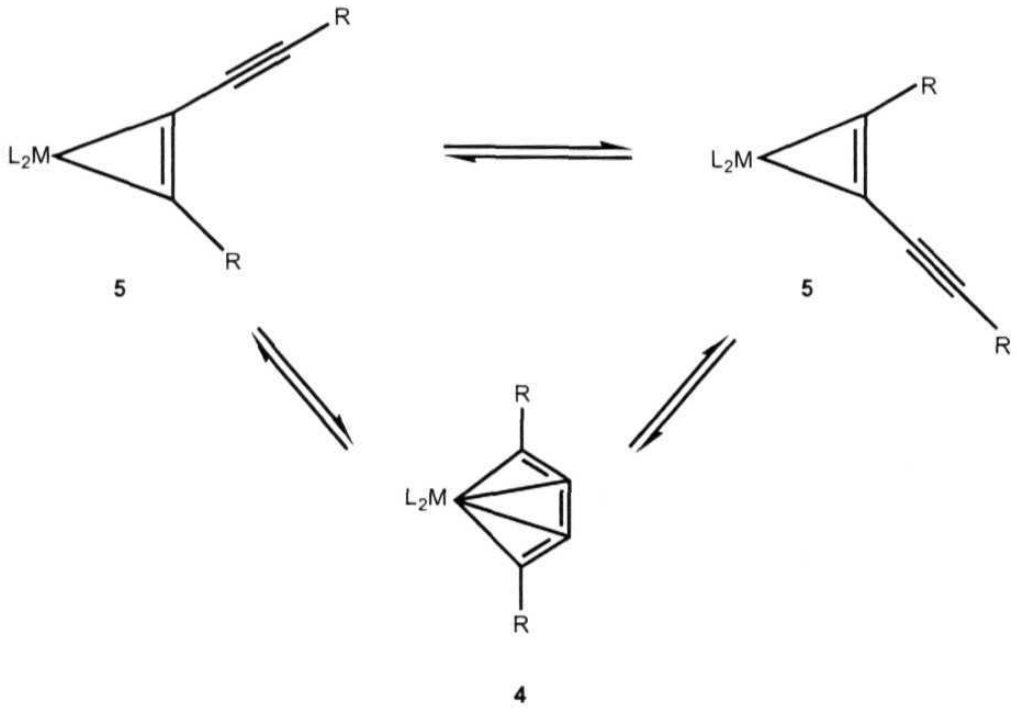

[2.2.2] Results and Discussion :

i) Relative stability of 1 - 6 and TS connecting 4 and 5 : The relative energies of the organic molecules are as anticipated. Assigning a zero value for the least strained acyclic species **3**,[43] the cyclocumulene derivative **1** is higher in energy by 51.6 kcal/mol and the cyclopropene derivative **2** is higher in energy by 16.7 kcal/mol. Such clear spread of energy between the three structures vanishes with the Cp_2Ti and Cp_2Zr analogue (Table 2.7 and Figure 2.4). The introduction of a metal brings in dramatic change in the stability of these molecules. The three cumulative double bonds are

Table 2.7: Relative Energies in Kcal/mol for the Cp_2M Substituted Cumulene (4), Cyclopropene (5), Bis(acetylide) (6), and the Transition State (TS) Connecting 4 and 5 at the B3LYP/LANL2DZ Level Including ZPVE

Metal	Ligand	Substituent (R)	4	5	6	TS
Ti	Cp	H	0.0	-8.1	0.93	6.2
		F	0.0	3.3	22.5	15.3
		CN	0.0	-10.3	0.16	1.9
Zr	Cp	H	0.0	4.7	1.1	16.8
		F	0.0	14.8	22.8	24.7
		CN	0.0	1.5	1.9	12.2
	C_5H_4[a]		0.0 (**1**)	-34.9 (**2**)	-51.6 (**3**)	

[a]The energies of the hydrocarbon equivalent of **4**, **5**, and **6**, i.e., cyclocumulene (**1**), alkynylcyclopropene (**2**) and dialkynylmethane (**3**) are given for comparison.

highly strained in the organic structure **1**. In the metallacyclocumulene **4**, the in-plane π orbitals are stabilized by their interaction with the in-plane orbitals of the metal atom (Figure 2.7). Such a stabilization in the cyclopropene derivative **2** corresponds to typical ethylene π donation and back bonding. Another component of the reduction in strain in going from the organic molecules to the metal substituted ones arises from the longer M-C bonds as opposed to the corresponding C-C bonds. The C1-C2-C3 angle in

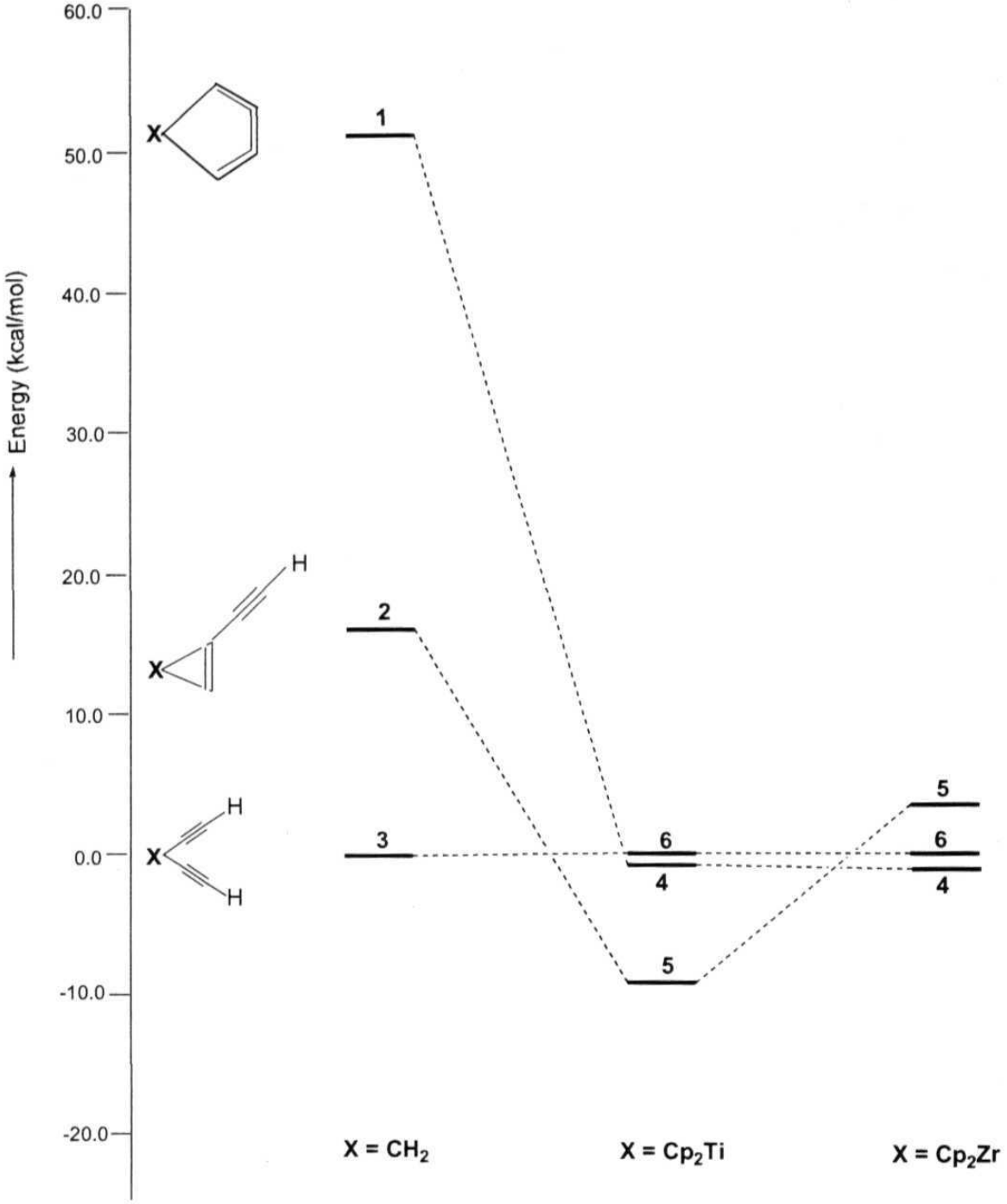

Figure 2.4. Comparison of relative energies (kcal/mol) of **1**, **2**, and **3** with that of **4**, **5**, and **6** respectively at the B3LYP level. Structures of **3** and **6** are kept at the reference value of 0.0.

1 of 114.7° is far away from the ideal linearity anticipated for cumulenes. The complexation with metal increases this to 145.1° in **4** (with M = Ti and R = H). Calculations indicate that the cyclocumulene **4** as well as the bisacetylide **6** are comparable in energy for both Ti and Zr. The difference between Ti and Zr is shown up in the relative energies of the metallacyclopropene derivative. The titanacyclopropene is lower in energy than the other two isomers, while the zirconacyclopropene is higher in energy. How do these relate to experiments? The in situ generated metallocene fragment reacts with butadiyne to give either a metallacyclocumulene (**4**) or a metallacyclopropene (**5**). It also forms the isomeric bisacetylide complex (**6**). It is clearly seen from the experiments so far that the Cp_2Ti fragment prefers a metallacyclopropene structure. Several products implied in reactions (Scheme 2.6) indicates the presence of **5** with Ti as the metal.[10d, 4e] On the other hand, similar experiments with Zr gives no indication of products arising from **5**; instead, a structure **9** is observed which may be derived from **4**.[10b, 4e] For M = Ti and R = H and CN, the structure **5** is lower in energy than **4** by 8.2 and 10.3 kcal/mol respectively (Figure 2.5). Substitution of the R group by F increases the energy of **5** for both Ti and Zr. The higher stability of the CN substituted η^2-complexes (**5**) may come from extended conjugation of the CN group with the MC_4 skeleton.

We located a transition state (**TS**) connecting **4** and **5** (Figure 2.6), and the magnitude of the barrier height which dictates the ease of interconversion of these complexes. The barrier for the process **4** $\rightarrow$ **5** with different butadiyne substituents increases in the order CN<H<F for both Ti and Zr. The relatively low barrier height of the complexes with M = Ti, enables them to exist in a dynamic equilibrium as found experimentally (Scheme 2.5).[10b] It should be possible to shift the equilibrium by fine

Scheme 2.6

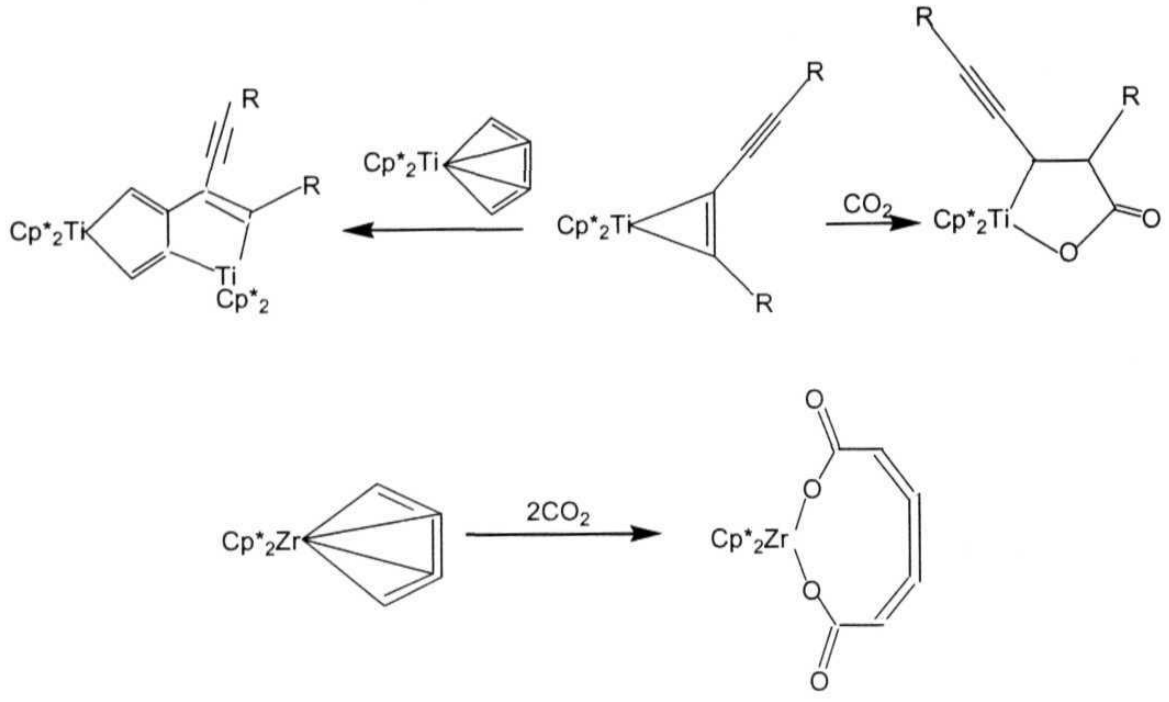

9

tuning the substituents on the Cp rings. The computed barrier height for the process **4→5** is much lower than what is known experimentally. For Ti, the experimental barrier height is found to be approximately 10.7 Kcal/mol, while the computed values are 6.2 and 1.9 kcal/mol with R = H and CN respectively. This difference may come from the change in ligand and the butadiyne substituent in our calculations compared to those in the experimental system. The structure **5** can also be stabilized for Zr by choosing the proper butadiyne substituents. The calculations show that this can be achieved by using cyanide (**CN**) as the substituent. The unusual stability of **5** results from simultaneous π bonding and metal back bonding. This is reflected in the longer C–C bond length as well as in the C–C stretching frequency of the three membered ring (ν_{C-C} = 1683 cm^{-1} (H) and 1753 cm^{-1} (CN) for M = Ti; 1587 cm^{-1} (H) and 1664 cm^{-1} (CN) for M = Zr). The lower frequencies for the Zr complex indicates the strong back bonding and consequent greater stability.

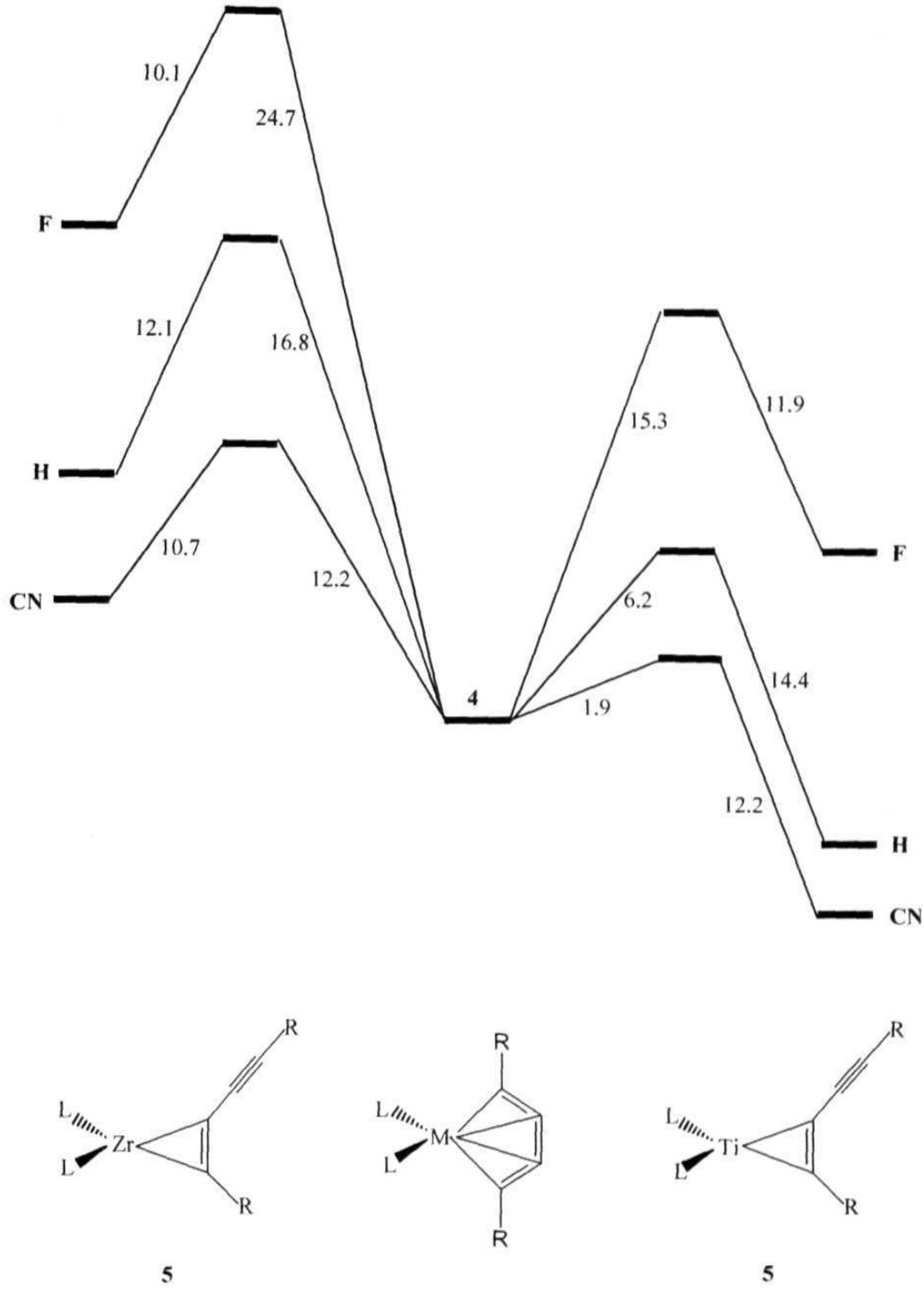

Figure 2.5. Potential energy diagram for the isomerization of **4** → **5** at the B3LYP/LANL2DZ level. Structure **4** is kept at the reference value of 0.0. The labels at the extreme right and left hand side of the figure indicates the substituents on butadiyne, viz., **H**, **F**, and **CN**.

ii) Structure and Bonding Analysis of 4, 5, and the TS Connecting 4 and 5 :

The structures and the geometrical parameters of all the complexes are given in Figure 2.6 and Table 2.8 respectively. The metal-carbon and the carbon-carbon bond distances obtained for these models are comparable to those found experimentally. The three C-C bond lengths in **4** are almost equal. All the M-C bonds are within the bonding range and the middle M-C bonds are marginally longer than the end ones. The bite angle, i.e., the angle between the the geometrical center point of the Cp rings and the metal is about 132°. The M-C1-C2 angle does not vary much with the change in the metal. However, when the substituent is F, it increases from 74° to 80°. The M-C1 and M-C4 bonds are more polarized toward the carbon atom, more so when M = Zr, having a weightage of more than 72% on the carbon atom as against 60% when M = Ti. This polarization of the M-C bonds increases with different butadiyne substituent in the order H<F<CN. An analysis of the natural charge obtained from the NBO indicates the same. The positive charge on the Zr atom (1.2) is more than that in Ti (0.2), indicating greater Zr to C4 back bonding.

All the C–C bond lengths in **5** are within the expected range. Both the M-C bonds are of almost equal order as evident from the Wiberg Bond Indexes (WBI). There is a marked reduction in the bite angle from the experimental value of 141.4°, the calculated bite angle is 135.0°. This reduction in the bite angle may arise because the experiments were done with Cp^*. There is no interaction between the C3-C4 bond and the metal in **5** as evident from the near linearity of the C2-C3-C4 angle of 176.0°. The natural charge analysis computes a higher positive charge on the metal than in the η^4-complexes. The total charge on the Cp ligand is identical to that in **4**, viz., about 0.0 in Ti complexes and -0.3 in Zr complexes.

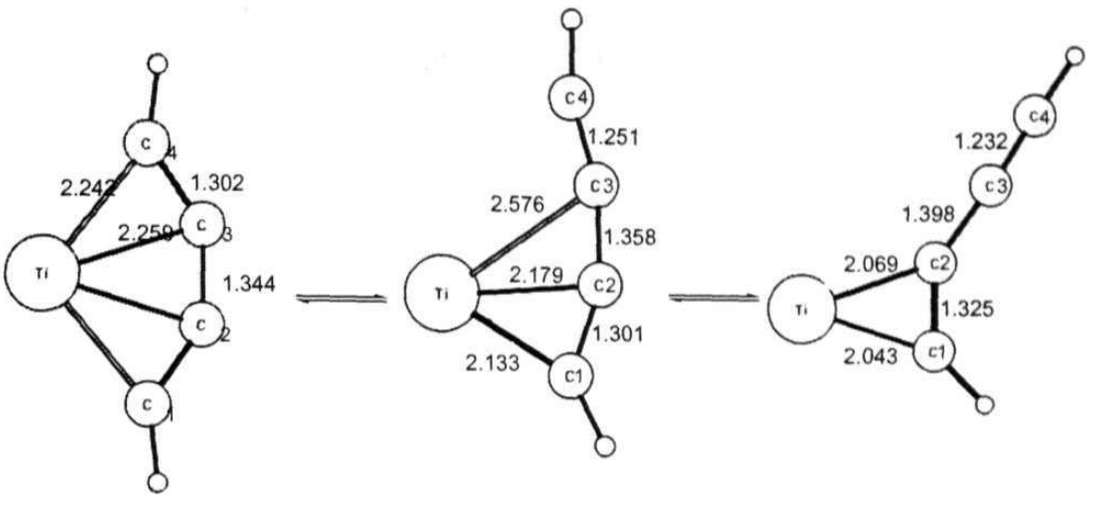

4 **TS** **5**

Figure 2.6. The transition state (**TS**) connecting **4** and **5**. The bond lengths (in Å) are given for M = Ti , L = Cp and R = H. The Cp rings are omitted for clarity.

In going from **4** to **5** through the transition state, the following changes take place in the M-C and C-C bond distances (Figure 2.6). For example, when M = Ti and R = H, the M-C3 bond changes from 2.259Å (**4**)→2.576Å (**TS**)→3.312 (**5**); the C2-C3 bond distance goes from 1.344Å (**4**)→1.358Å (**TS**)→1.398Å (**5**); the C1-C2-C3 angle changes from 145.1° (**4**)→160.9° (**TS**)→144.8° (**5**).

Although the M-C3 bond is somewhat elongated, it is still within the bonding distance as indicated by the WBI of 0.114 (Table 2.8). Similar changes were noticed with the other substituents (F and CN) for both Ti and Zr. The Cp ligand shows similar electronic effects as in **4**, **5 and 6**. A correlation diagram was constructed to understand the changes in the frontier orbitals in going from **4** to **5** via the transition state (**TS**) as shown in Figure 2.7. Even though many bonds appear to be breaking and many formed, the overall M-C_4H_2 bonding is not affected considerably. The only orbital that goes up substantially during the reaction is the HOMO. Even this MO is

Table 2.8: Important Geometric Parameters of the Structures at the B3LYP/LANL2DZ Level. The numbers in italics indicate Wiberg Bond Index (WBI).

Molecule	M	L	R	M-Cp	M-C1	M-C2	M-C3	C1-C2	C2-C3	C3-C4	L-M-L	M-C1-C2	C1-C2-C3	C2-C3-C4
4	Ti	Cp	H	2.144	2.242	2.259		1.302	1.344		130.9	73.9	145.1	
					0.663	*0.338*		*2.047*	*1.467*					
			F	2.126	2.153	2.337		1.318	1.337		132.1	80.7	138.8	
					0.698	*0.305*		*1.871*	*1.574*					
			CN	2.118	2.267	2.284		1.308	1.327		132.1	74.0	145.7	
					0.549	*0.314*		*1.858*	*1.559*					
	Zr	Cp	H	2.292	2.353	2.373		1.316	1.342		130.3	74.7	146.6	
					0.624	*0.294*		*1.992*	*1.554*					
			F	2.276	2.30	2.450		1.327	1.335		131.6	80.1	141.8	
					0.647	*0.261*		*1.861*	*1.637*					
			CN	2.268	2.379	2.40		1.320	1.325		131.7	74.8	147.1	
					0.519	*0.265*		*1.820*	*1.644*					
5	Ti	Cp	H	2.124	2.043	2.069	3.312	1.325	1.398	1.232	134.9		144.8	176.2
					0.792	*0.692*	*0.030*	*1.837*	*1.205*	*2.722*				
			F	2.115	2.010	2.092	3.339	1.319	1.396	1.221	134.8		146.3	176.3
					0.822	*0.692*	*0.029*	*1.769*	*1.194*	*2.623*				
			CN	2.097	2.064	2.085	3.320	1.332	1.381	1.238	136.3		143.7	175.1
					0.676	*0.643*	*0.029*	*1.694*	*1.265*	*2.437*				
	Zr	Cp	H	2.295	2.179	2.197	3.484	1.349	1.405	1.232	134.1		138.8	176.1
					0.784	*0.704*	*0.028*	*1.783*	*1.194*	*2.733*				
			F	2.288	2.159	2.227	3.517	1.339	1.404	1.221	134.0		140.1	176.2
					0.796	*0.669*	*0.027*	*1.758*	*1.179*	*2.639*				
			CN	2.271	2.203	2.221	3.492	1.353	1.388	1.237	135.8		138.6	174.9
					0.654	*0.626*	*0.027*	*1.664*	*1.253*	*2.447*				
TS	Ti	Cp	H	2.116	2.133	2.179	2.576	1.301	1.358	1.251	133.8		160.9	165.0
					0.682	*0.476*	*0.144*	*1.995*	*1.322*	*2.448*				
			F	2.103	2.036	2.196	2.767	1.305	1.350	1.267	134.6		165.3	157.2
					0.784	*0.466*	*0.119*	*1.826*	*1.387*	*2.316*				
			CN	2.084	2.112	2.255	2.709	1.309	1.343	1.252	136.3		160.9	176.9
					0.606	*0.424*	*0.114*	*1.817*	*1.406*	*2.216*				
	Zr	Cp	H	2.275	2.256	2.240	2.860	1.316	1.362	1.251	133.9		175.9	164.0
					0.712	*0.514*	*0.104*	*1.913*	*1.330*	*2.480*				
			F	2.269	2.183	2.272	3.0	1.318	1.355	1.265	133.9		178.6	156.9
					0.767	*0.480*	*0.093*	*1.804*	*1.383*	*2.347*				
			CN	2.253	2.262	2.289	2.844	1.320	1.338	1.259	134.6		171.9	166.8
					0.608	*0.429*	*0.108*	*1.754*	*1.447*	*2.181*				

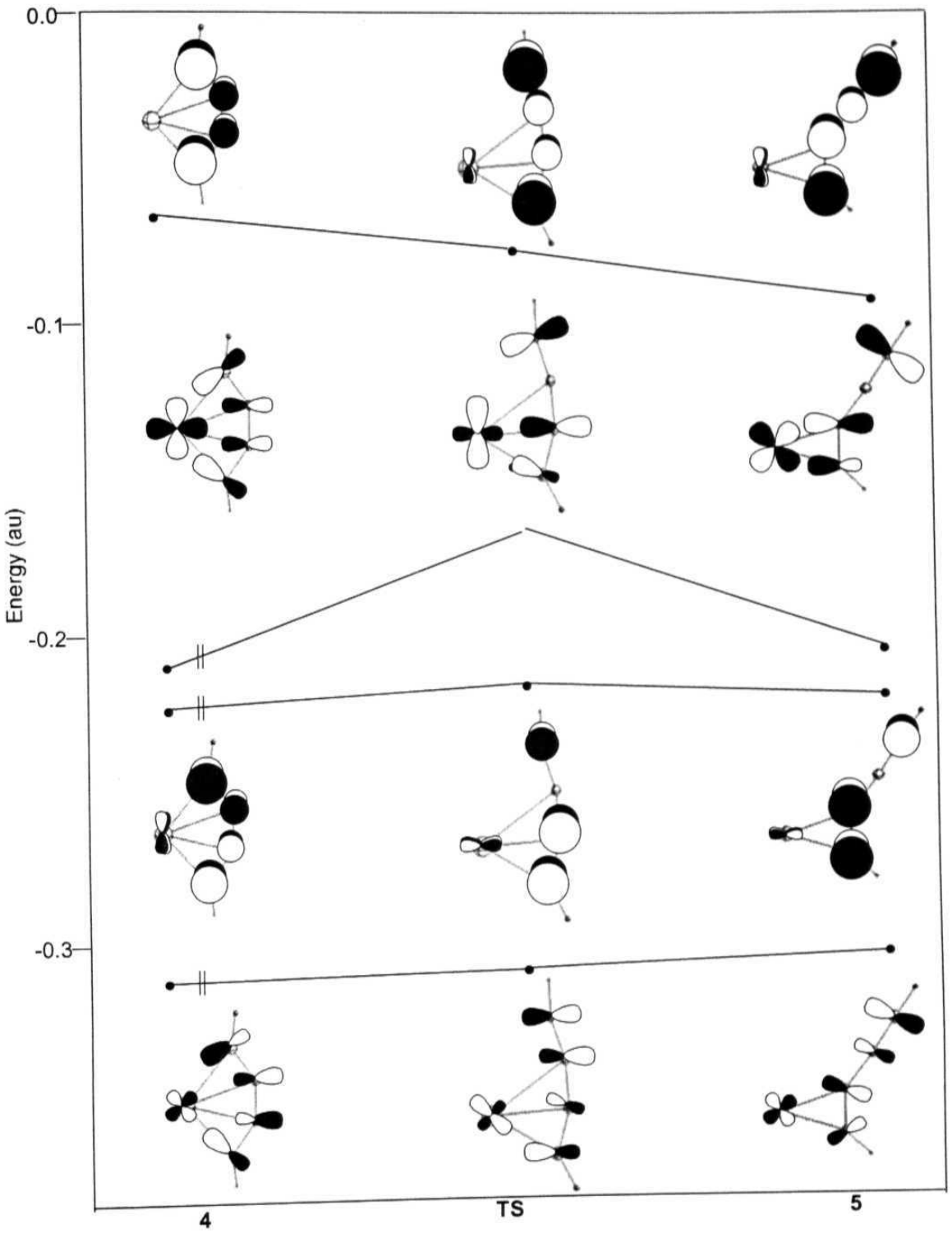

Figure 2.7. Correlation diagram for the conversion of **4** to **5** via the transition state (**TS**). The ligands (Cp) are omitted for clarity.

stabilized by the incipient C3-C4 triple bond formation (see the decrease in this bond length, Figure 2.6). Similarly, there is a weak M-C4 bonding interaction even in the TS. The retention of major bonding interactions even in the **TS** explains the low barrier for the transformation.

[2.2.3] Conclusions :

A comparison of the energetics of metallacyclocumulene (**4**), metallacyclopropene (**5**) and bis-acetylide (**6**) with their hydrocarbon analogs (**1**, **2** and **3**) show that the metal fragment has a dramatic impact on the relative energies. The replacement of the CH_2 group by Cp_2M (M = Ti, Zr) makes structures **4**, **5** and **6** comparable in energy. Our calculations support the experimental observation that the metallacyclopropene (**5**) is more favorable for the Ti complex. Under similar reaction conditions, Ti reacts through the cyclopropene structure **4** whereas Zr reacts through the cumulenic structure **5**.[10a] However, it should be possible to obtain both the cyclocumulene (**4**) and cyclopropene (**5**) type complexes for Ti and Zr by using the proper substituent on the carbon skeleton. The transition state connecting **4** and **5** retains most of the M-C bonding interactions leading to low barrier for conversion.

[2.3] Structure and Bonding of Metallacyclocumulenes, Radialenes, Butadiyne Complexes and their Possible Interconversion

[2.3.1] Introduction :

The Dewar-Chatt-Duncanson (DCD) model gave an elegant and simple description of the transition metal-alkene bonding in terms of π donation and metal back-donation.[44] The properties of a complexed double bond depend on the extent of back bonding.[45] We consider here a π bond which is flanked by π bonds on either side in an orthogonal plane as in cumulenes. Metallacyclocumulenes (**1** and **2**), obtained from Cp_2Ti and Cp_2Zr fragments contain such π bonds (Scheme 2.7).[1, 10] The Ti complex also dimerizes to give a radialene derivative (**4**), arising from a 2+2 cycloaddition of the middle π bond.[46] However, this structural type is not known for Zr (**5**). In principle, a cycloreversion of **4** could lead to the bis(butadiyne) complex (**7** or **8**). This structural pattern is indeed known, but with the metal Ni (**9**).[47] Yet, neither the metallacyclocumulene **3** nor the radialene **6** is known with Ni. In this section, the nature of bonding of the middle π-bond in the metallacyclocumulene complexes **1**, **2**, and **3**, correlation diagrams for its dimerization to the radialenes **4** and **5**, and its isomeric butadiyne structures of Ti and Ni (**7** and **9**) are discussed. The electronic structure of the titanium substituted radialene (**4**) and the ways to get similar complexes for zirconium using different substituents at the 1,4-position of the butadiyne are also probed. Moreover, the electronic structure of butadiyne bridged nickel complex (**9**) and the dimerization energy for the process **1** → **4** are presented briefly.

Initial studies involving Cp_2Ti, Cp_2Zr, Cl_2Ti and Cl_2Zr fragments have indicated that the energetic trends are reproduced by the dichloro derivatives.[38b, 48]

Scheme 2.7

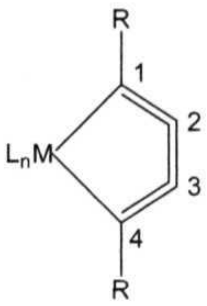

1 ; M = Ti ; L = Cp ; n=2
2 ; M = Zr ; L = Cp ; n=2
3 ; M = Ni ; L = NH_3 ; n=1

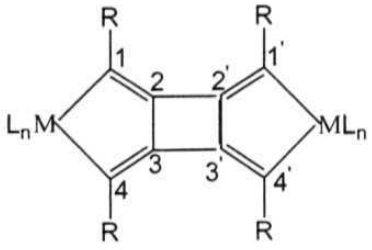

4 ; M = Ti ; L = Cp ; n=2
5 ; M = Zr ; L = Cp ; n=2
6 ; M = Ni ; L = NH_3 ; n=1

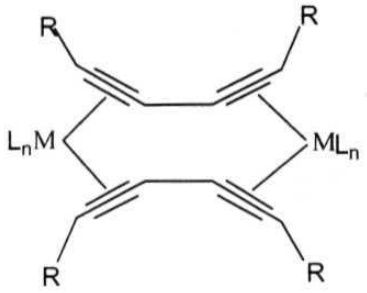

7 ; M = Ti ; L = Cp ; n=2
8 ; M = Zr ; L = Cp ; n=2
9 ; M = Ni ; L = NH_3 ; n=1

However, absolute comparisons between Cp_2Ti and Cp_2Zr systems required Cp ligands. Since this is not practical with our computational facilities to optimize the dimers (**4-9**) with four Cp rings, we have used Cl in place of Cp. The bis(butadiyne) complex of Ni (**9**) and the hypothetical structure **3** were optimized by modeling pyridine with NH_3. We used H, OH and NH_2 as the butadiyne substituents, R^1 and R^2, in complexes **1** to **5**. For all other structures, H is used as the substituent.

[2.3.2] Results and Discussion :

The structure and bonding of the cyclocumulenes will be discussed first followed by description of the dimerization reactions and finally the nature of bonding in these metal substituted radialenes.

i) Structure and Bonding of Metallacyclocumulenes (M=Ti, Zr and Ni) :

The structure and bonding of metallacyclocumulenes, **1** and **2**, are already discussed in greater detail in the first section of this Chapter. However, few points will

be made about their bonding characteristics in contrast to the hypothetical nickellacyclocumulene structure **3**.

All the three metallacyclocumulenes, **1**, **2**, and **3** are planar with the four carbon atoms and the metal atom lying in the same plane. For M=Ti (**1**) and Zr (**2**), all the three C–C bond lengths are of almost equal order (≅1.3 Å) and they are within the range of C–C distance expected for a sp^2–sp bond (Table 2.9). The geometrical features of the Zr complex **2**, is similar to that of **1**.[10e] However, our calculated bond lengths differ from that of the experimental structure.[10b] While the calculated M-C distances (**1** : M-C1 = 2.11, M-C2 = 2.14 and **2** : M-C1 = 2.264, M-C2 = 2.298) are shorter than those from the experimental geometry (**1** : M-C1 = 2.252, M-C2 = 2.209 and **2** : M-C1 = 2.357, M-C2 = 2.303), the C-C bond lengths (**1** : C1-C2 = 1.311, C2-C3 = 1.347 and **2** : C1-C2 = 1.324, C2-C3 = 1.343) are longer (**1** : C1-C2 = 1.243, C2-C3 = 1.339 and **2** : C1-C2 = 1.28, C2-C3 = 1.31). The experimental structures have Cp or Cp* as the ligand and ^{t}Bu, Ph or $SiMe_3$ as substituents, whereas calculations were performed using Cl instead of Cp and H in place of ^{t}Bu, Ph or $SiMe_3$. These would contribute to the differences in the geometries between the model structures calculated and the experimental values. The middle C–C bond in the hypothetical nickel complex is longer than the other two C–C bond, thereby showing back-bonding interaction between the filled metal d-orbitals and the in-plane empty π^* orbital of the middle C–C bond. This is also reflected in the length of the Ni-C bonds. The Ni-C2 bond is shorter than the Ni-C1 bond by 0.17 Å. Thus the Ni complex, **3**, has the typical DCD bonding. The bonding of the middle C–C bond in both the Ti and Ni complexes can be described in terms of the DCD model except that there are no electrons in the metal orbitals of the Ti complex for back bonding with the in-plane π-orbitals. Interaction diagrams

constructed using the calculated geometries at the extended Hückel level exemplifies this anticipation. The $1A_1$ and $1B_2$ (Figure 2.8, i and ii) of the Ti complex corresponds to the in-plane and out of plane combination of the σ-hybrid orbitals of the end carbons

Table 2.9: Important Geometric Parameters of the Metallacyclocumulenes at the B3LYP/LANL2DZ Level of Theory. The Numbers in *italics* Indicate Wiberg Bond Index (WBI).

M	L	R	M-C1	M-C2	C1-C2	C2-C3	C1-M-C4	M-C1-C2	C1-C2-C3
Ti	**Cl**	**H**	2.11	2.14	1.311	1.347	108.5	73.3	142.4
			0.737	*0.404*	*1.979*	*1.487*			
		OH	2.069	2.163	1.332	1.338	109.3	75.5	139.8
			0.755	*0.419*	*1.757*	*1.570*			
		NH_2	2.078	2.125	1.338	1.331	110.7	73.4	141.3
			0.758	*0.469*	*1.676*	*1.604*			
Zr	**Cl**	**H**	2.264	2.298	1.324	1.343	101.4	74.5	144.7
			0.695	*0.343*	*1.948*	*1.574*			
		OH	2.232	2.326	1.341	1.336	101.7	76.5	142.4
			0.691	*0.346*	*1.757*	*1.647*			
		NH_2	2.242	2.284	1.347	1.330	103.1	74.4	144.0
			0.695	*0.389*	*1.678*	*1.676*			
Ni	**NH_3**	**H**	2.19	2.02	1.287	1.369	110.2	65.1	149.8
			0.351	*0.183*	*2.358*	*1.378*			
		OH	2.116	2.036	1.302	1.365	112.0	68.4	145.5
			0.353	*0.188*	*2.153*	*1.446*			
		NH_2	2.156	2.027	1.305	1.365	111.6	66.5	146.9
			0.328	*0.193*	*2.104*	*1.445*			

of the cumulenic unit interacting with the metal orbitals. On the other hand, back donation plays a very dominant role in the Ni complex where the metal is formally d^8. The corresponding MOs are shown in Figure 2.8 (iii and iv). With an intact middle π bond, which is in the σ plane, **1** and **2** are expected to dimerize. The geometrical parameters of the parent metallacycles **1**, **2**, and **3** are mostly unaffected by the change of substituents from H to OH and NH_2. The variations in the dimerization energy of the π bond is discussed next.

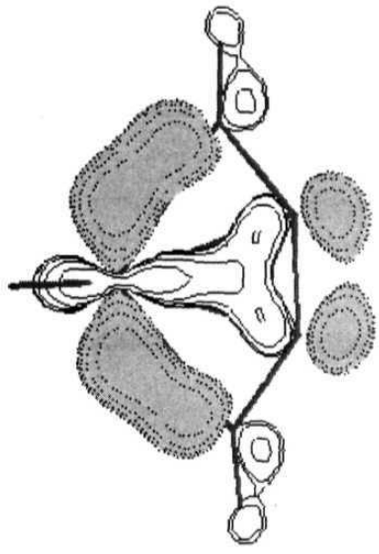

$1A_1$

(i)

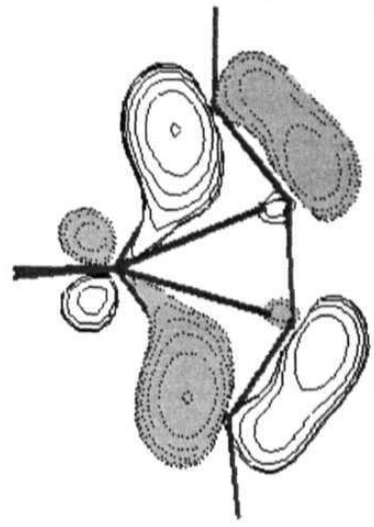

$2B_2$

(ii)

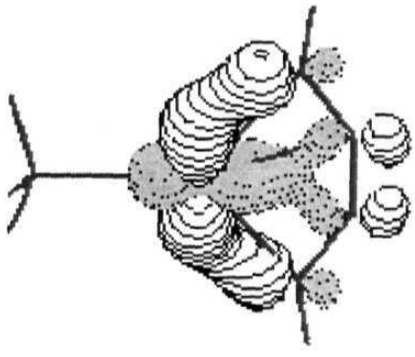

3A′

(iii)

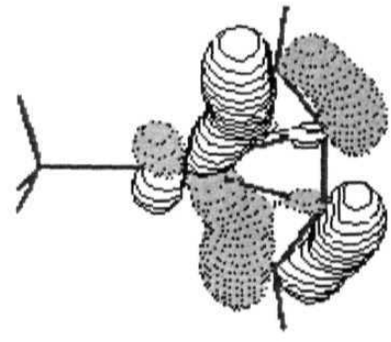

4A″

(iv)

Figure 2.8. Three dimensional drawings of molecular orbitals showing the "bonding" and "back-bonding" interaction between the metal and the middle C-C bond. (i) and (ii) shows the metal- carbon bonding in the Ti complex and (iii) and (iv) represents the π bonding and back-donation in the Ni complex respectively.

ii) Dimerization Energies for the Process 1 → 4 and the Structure and Bonding of Metal Substituted Radialenes :

The first point to note here is that experimentally a Zr based cumulene structure is not known to give a radialene, even though the dimerization of the Ti complex is well known. Calculations on the model complexes **1**, **2**, and their dimers **4** and **5** indicate that these are minima. The difference between the two dimerization energies is small; it is not possible to assign any specific explanation for the experimental observation. Calculations using the cyclopentadienyl ligands could change this small energy difference. Estimation of the barrier heights for dimerization is required to explain the difference in behavior of Ti and Zr complexes. The dimerization energies of different combinations of metal and substituent is shown in Table 2.10. To provide a comparison with the parent hydrocarbon systems, we calculated the dimerization energies of ethylene and cumulene at the same level of theory (Scheme 2.8). The dimerization energy of cumulene is more than that of ethylene. The sp hybridized middle C=C π bond of cumulene releases more energy upon dimerization. The unavoidable closed shell repulsions between the π bond and the psuedo CH_2 π orbital on either side may be destabilizing this π bond. This is also evident from a comparison of the hydrogenation of ethylene to ethane and cumulene to 1,3-butadiene (eqns. 3 and 4). The hydrogenation energy of cumulene is more exothermic than that of ethylene by −11.0 kcal/mol. Further, the radialene is stabilized by the cyclic delocalization of π-electrons of the four exocyclic C=C bonds around the ring, which is absent in the parent cyclobutane. On the other hand, the dimerization energies of **1** and **2**, where the metal is formally d^0, are less than that of cumulene (eqn. 5). This reduction in the dimerization energy comes from the delocalization of perpendicular π orbitals of the

carbon atoms to the vacant d levels of Ti and Zr. It is also possible that the destabilization of the middle C-C π bond mentioned above is not as high in **1** and **2** as in the parent cumulene because of the nonlinearity of the carbon string in **1** and **2**.

Table 2.10 : Dimerization Energies of the Metal Substituted Radialenes at B3LYP/ LANL2DZ Level of Theory Including ZPVE. The energies of C_2H_4, C_4H_4 and their Dimers are given for Comparison.

M	L	R	$E_{monomer}$ (au)	E_{dimer}(au)	Dimerization Energy (Kcal/mol)
Ti	Cl	H	-241.57810	-483.22853	-45.4
		OH	-391.98639	-784.07610	-64.8
		NH_2	-352.27406	-704.61738	-43.5
Zr	Cl	H	-230.09988	-460.27737	-48.7
		OH	-380.50955	-761.12674	-67.5
		NH_2	-340.79346	-681.65573	-43.2
Ni	NH_3	H	-379.25407	-758.59569	-54.9
		OH	-529.65470	-1059.39810	-55.6
		NH_2	-489.92064	-979.91701	-47.5
	C_2H_4		-78.52689	-157.07658	-14.3
	C_4H_4		-154.64576	-309.37967	-55.3

The dimerization energies are dependent on the butadiyne substituents. These increase in the order NH_2<H<OH. A contributor to the enhanced dimerization energy of the OH substituted complex is the O–H---O bonding. On the otherhand, hydrogen bonding is not very significant in NH_2 substituted complexes. The calculated geometrical parameters of the metal substituted radialenes are comparable to those found experimentally (Table 2.11). In the H and OH substituted complexes of Ti and Zr, the metal and all the four carbon atoms of the metallacycle are in the same plane. However, in the NH_2 substituted complexes , the metal atom is forced out of the plane of the metallacycle (Figure 2.9). With M=Zr and R=NH_2, the central cyclobutane ring

Scheme 2.8

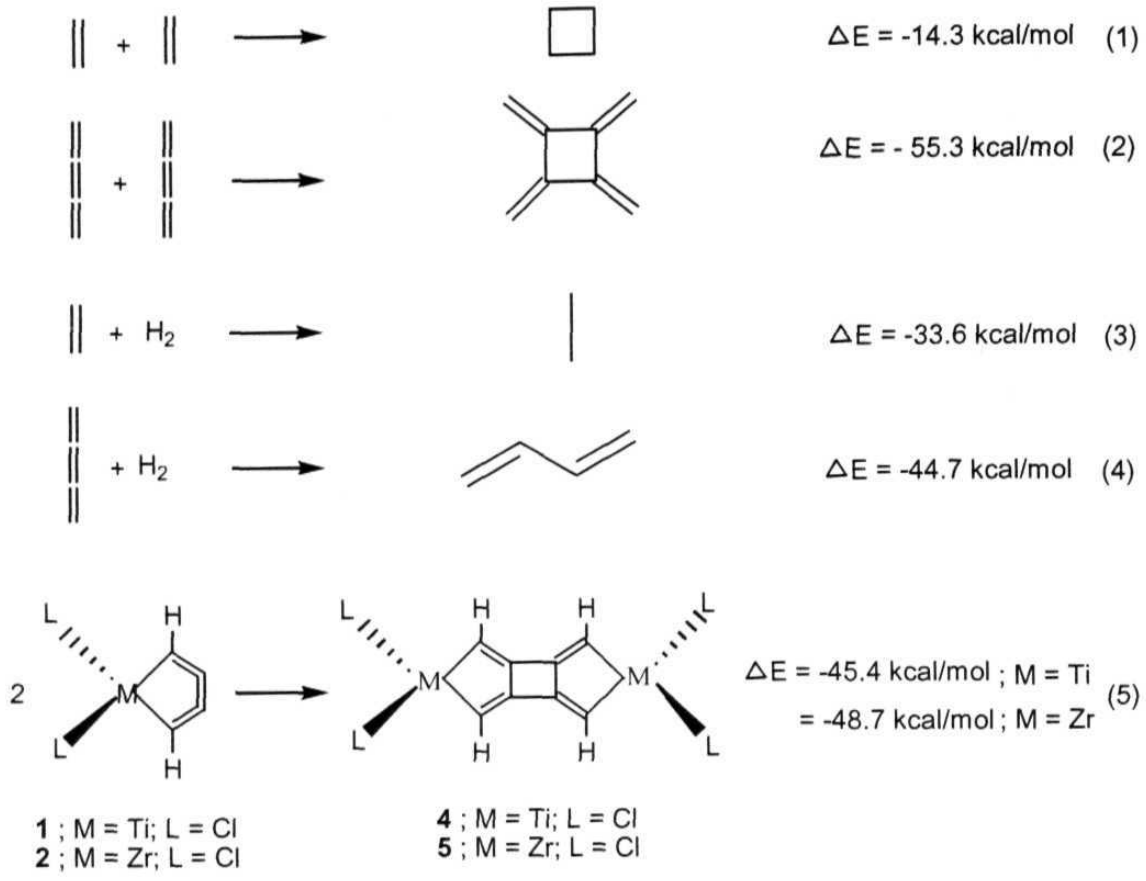

deviates from planarity by about 5°. However, such deviations are not found for the Ni complex **9**. The M-C bond is more polarized toward the carbon atom as expected, more so when the metal is Zr. A cycloreversion can in principle lead to a bis-(butadiyne) complex **7**, but this is not observed with **4**. Structure **3** or any other cumulene complex of Ni is not known experimentally. The radialene structure of Ni (**6**) on optimization collapses to the bis(butadiyne) complex **9**. Such a complex has been synthesized by starting with a monomeric Ni complex, (2,6-$Me_2C_5H_3N$)Ni(η^1,η^2-C_7H_{12}).[10c] The model nickel complex, **9** with R=H, OH, and NH_2 and L=NH_3 calculated at the same level of theory is a planar molecule with both the Ni atoms bridged by two butadiyne units (Table 2.11). The nickel atoms are in zero oxidation

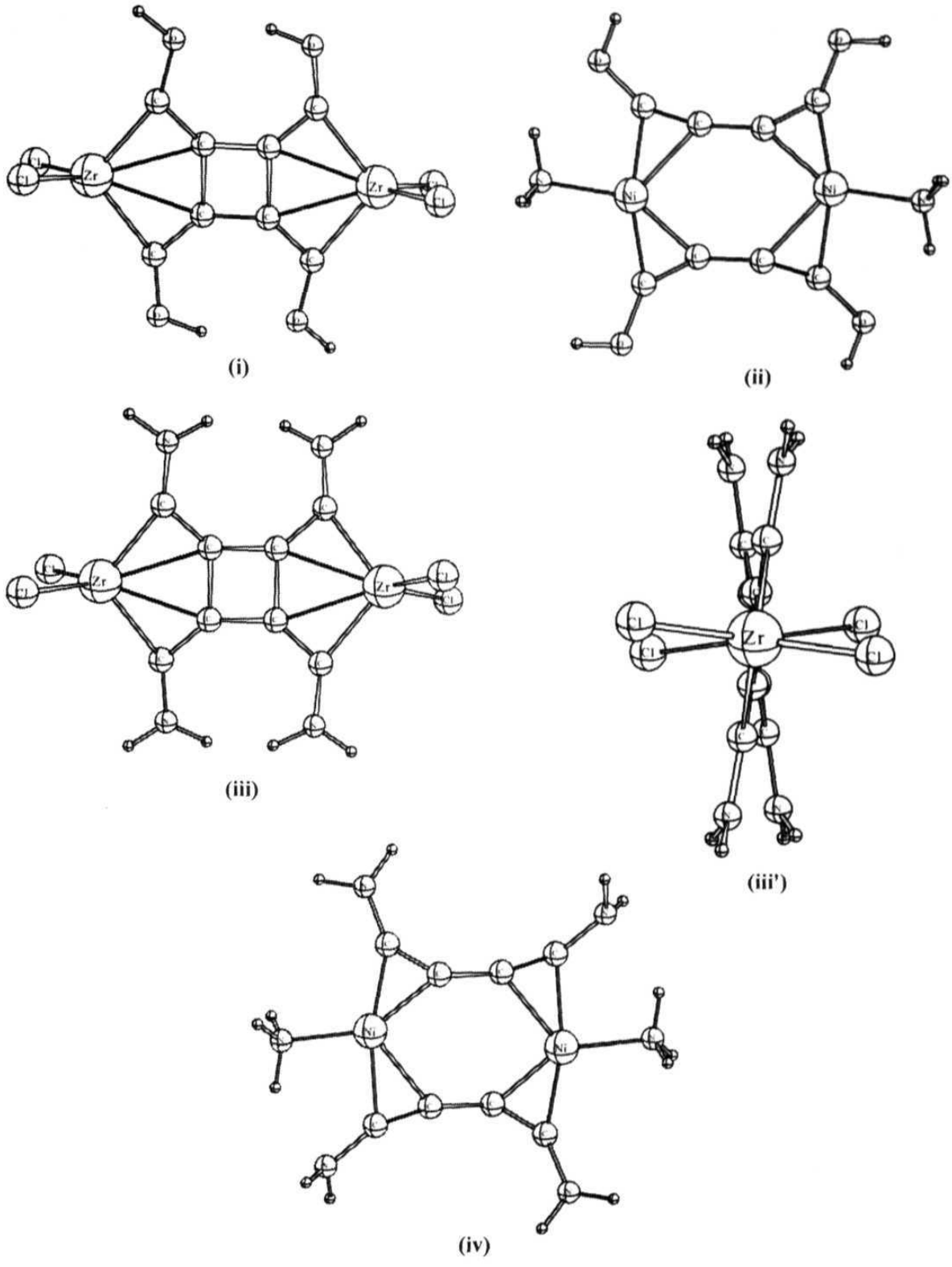

Figure 2.9. Optimized geometries of some of the metal substituted radialenes. The dramatic structural changes to the skeleton of Zr complex brought in by the NH_2 substituent is shown in (**iii**) for Zr. Structure (**iii'**) is the perpendicular view of (**iii**). Similar changes are found for the Ti complex as well.

state. The environment around both the nickel atom is trigonal planar with each Ni(0) atom coordinated to one NH_3 ligand and one each of the C≡C bonds of two different butadiyne units. The calculated Ni-C bond lengths are comparable to the experimental values[47] and indicate considerable delocalization of electrons between the metal atom and the butadiyne unit. The middle C-C bond in **8** varies between 1.40 Å -1.41 Å, as expected for a *sp–sp* bond.

Table 2.11 : Important Geometric Parameters of the Metal Substituted Radialenes at the B3LYP/LANL2DZ Level of Theory.[a] The numbers in *italics* Indicate Wiberg Bond Index (WBI).

M	L	R	M-C1	M-C2	C1-C2	C2-C3	C2-C2'	C1-M -C4	M-C1 -C2	C1-C2 -C3	C3-C2 -C2'
Ti	Cl	H	2.015	2.420	1.353	1.578	1.494	106.0	89.7	127.3	90.0
			0.903	*0.196*	*1.704*	*0.915*	*1.012*				
		OH	2.02	2.430	1.364	1.542	1.473	105.3	89.6	127.1	90.0
			0.892	*0.213*	*1.525*	*0.963*	*1.046*				
		NH_2	2.02	2.354	1.375	1.567	1.471	109.1	86.2	128.2	90.0
			0.859	*0.263*	*1.454*	*0.935*	*1.059*				
Zr	Cl	H	2.176	2.583	1.361	1.579	1.497	99.1	90.8	129.6	90.0
			0.792	*0.146*	*1.740*	*0.942*	*1.01*				
		OH	2.181	2.575	1.368	1.546	1.473	99.6	89.5	130.1	90.0
			0.784	*0.163*	*1.575*	*0.981*	*1.038*				
		NH_2	2.166	2.512	1.381	1.575	1.474	103.0	87.3	130.8	89.8
			0.765	*0.202*	*1.505*	*0.956*	*1.053*				
Ni	NH_3	H	1.956	1.989	1.286	1.284	1.412	164.2	72.5	115.5	90.2
			0.388	*0.307*	*2.289*	*2.299*	*1.170*				
		OH	1.912	1.941	1.268	1.302	1.40	163.1	81.0	118.1	92.4
			0.457	*0.384*	*2.260*	*2.059*	*1.194*				
		NH_2	1.902	1.926	1.261	1.318	1.398	165.5	74.5	116.3	85.2
			0.458	*0.438*	*2.255*	*1.932*	*1.224*				

[a] *For Ni, the C2-C3 bond lengths are replaced by that of C1'-C2'*

The inability to get optimized geometries corresponding to **6** and **7** prompted us to analyze the conservation of orbital symmetry during the transformation of **1** → **4** (Figure 2.10), **4** → **7** (Figure 2.11) and **6** → **9** (Figure 2.12). These are all found to be symmetry allowed processes. The specifics of individual reactions need to be studied

for further quantitative details. It is interesting to note that complexation with metal changed the symmetry disallowed dimerization of cumulene to an allowed one.

The difficulty in getting a radialene type structure for Ni may arise from the non availability of the in plane π orbitals of the middle C-C bond of the parent cyclocumulene which is already involved in bonding and back-bonding interaction with the metal d orbitals. But, in the Ti complex, where there is no back-bonding, these orbitals are readily available for interaction with another cyclocumulene unit. In view of these calculations, it is clear that the formation of the diyne structure **9** does not involve the cyclocumulene **3**. We suggest the following notional mechanistic steps for the formation of **9** (Scheme 2.9). The first step involves the coordination of a butadiyne molecule to the Ni atom forming the monoligand Ni(0) olefin-alkyne complex.[49] This is followed by coordination of one more molecule of butadiyne to the metal atom and subsequent removal of the diene moiety. There is precedence for such type of mechanism in the literature.[50, 51] In the third step, one more molecule of the initial monoligand Ni(0) diene complex attacks one of the two butadiyne unit available for coordination. The formation of such dinuclear complexes by coordination of two Ni(0) complex fragments at one 1,3 – diyne is well known.[51] In the last step, the diene unit is removed from the coordination sphere of the Ni atom and the bis(butadiyne) complex of Ni is formed.[47]

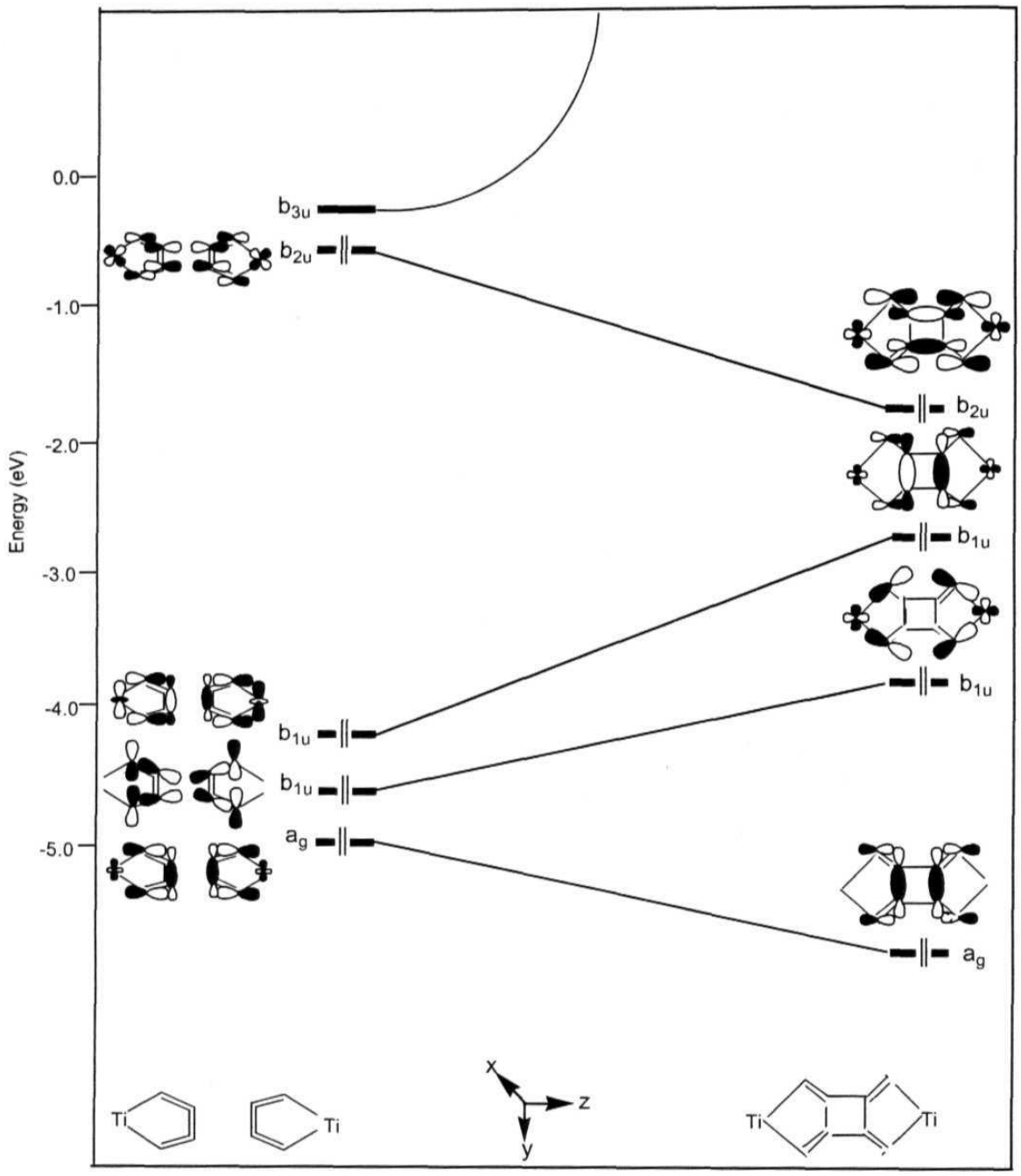

Figure 2.10. Correlation diagram for the dimerization of Ti substituted cumulene. The hydrogen atoms and the ligands (**Cl**) are omitted for clarity.

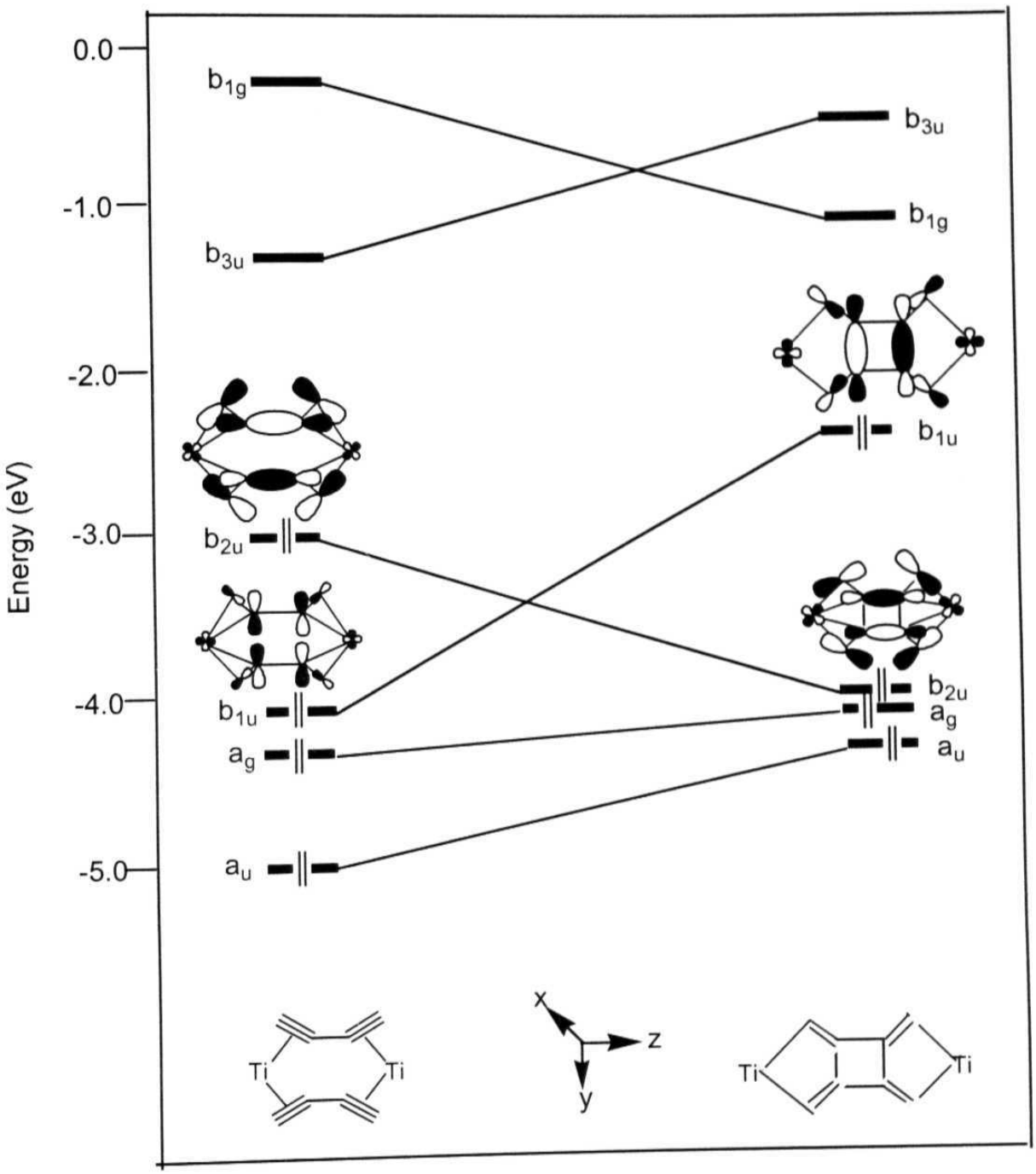

Figure 2.11. Correlation diagram for the process **4** → **7**. The hydrogen atoms and the ligands (**Cl**) are omitted for clarity.

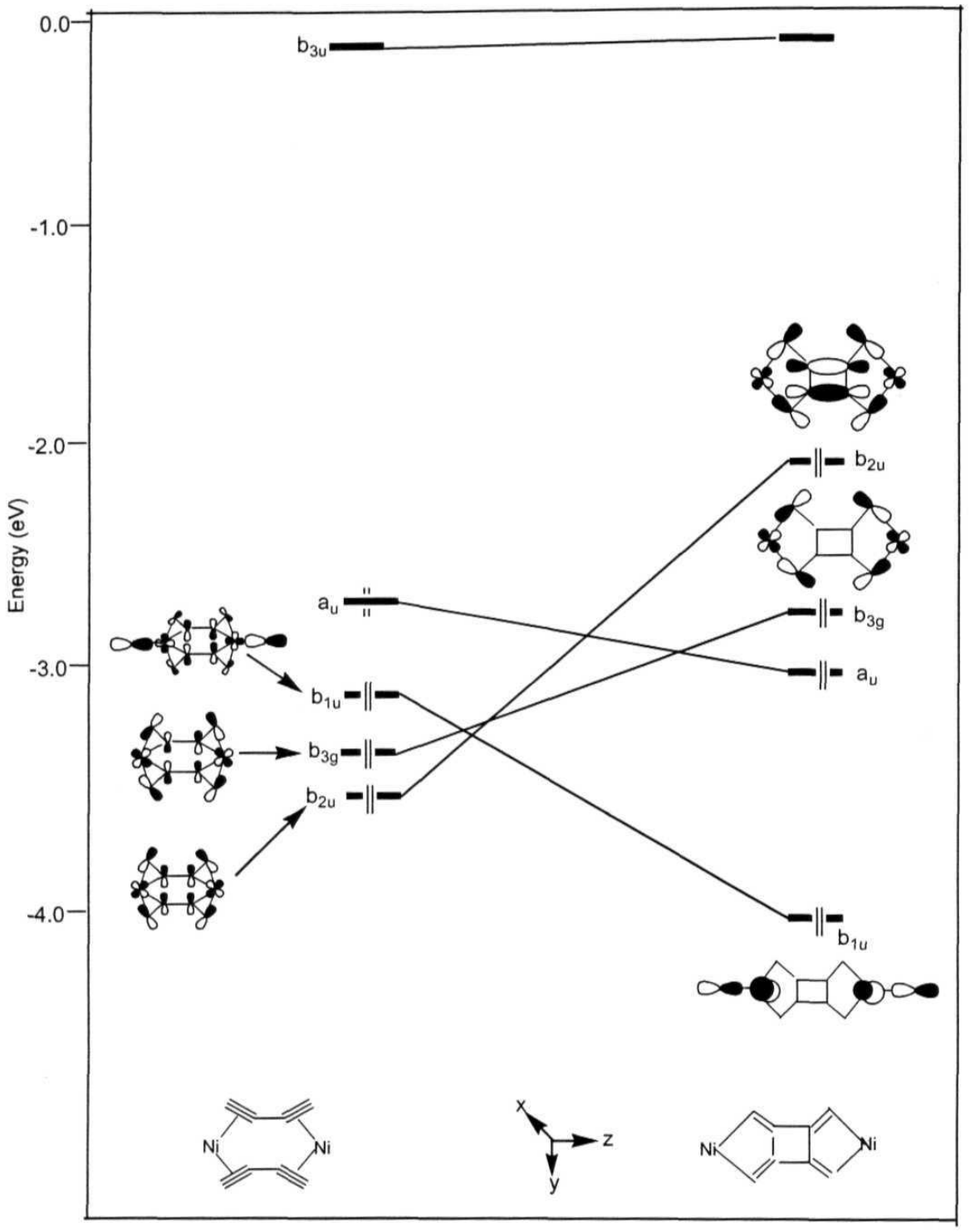

Figure 2.12. Correlation diagram for the process **6** → **9**. The hydrogen atoms and the ligands (pyridine) are omitted for clarity.

Scheme 2.9

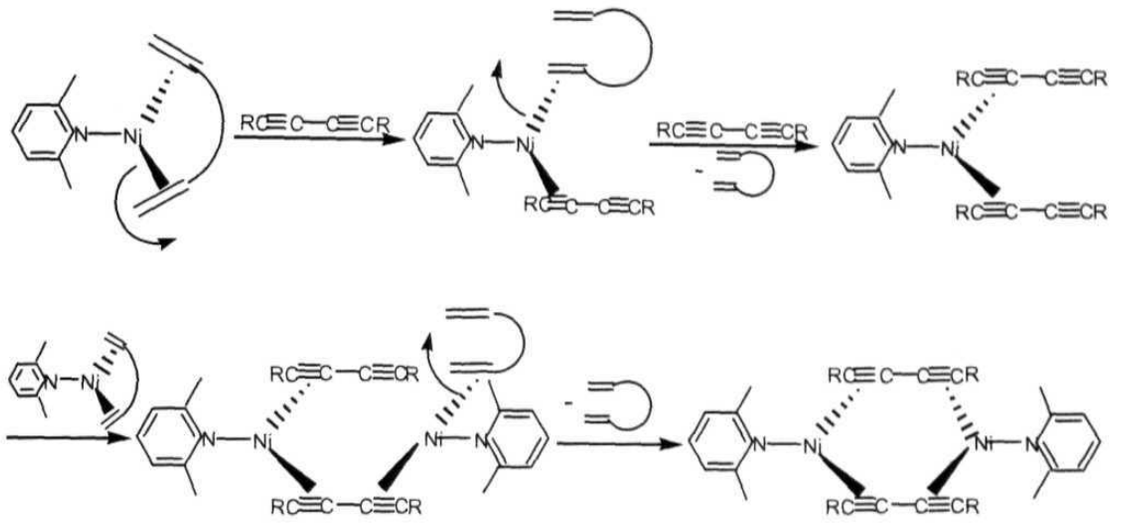

[2.3.3] Conclusions :

The Ti complex is found to dimerize to **4**, but such a process is not observed for Zr. Quantitative studies of the reaction barrier is needed to establish the details. With a d^0 electron count, the back-bonding part of the DCD model is not applicable here. Though the corresponding Ni complex, **3** is shown to be a minimum, its radialene dimer, **6**, is not even a stationary point. A bis(butadiyne) complex, **9**, is obtained instead. Corresponding complexes of Ti and Zr (**7** and **8**), on optimization, collapses to the radialenes **4** and **5**. Correlation diagrams constructed for the dimerization of **1** and **2** as well as for conversion of the radialene type structure to that of the bis(butadiyne) complex show that these are symmetry allowed. The effect of substituents on the dimerization of metallacyclocumulenes is also studied and it shows similar energetics for Ti and Zr.

[2.4] References

1. Lauher, J. W.; Hoffmann, R. *J. Am. Chem. Soc.* **1976**, *98*, 1729.
2. (a) Alt, H. G.; Köppl, A. *Chem. Rev.* **2000**, *100*, 1205. (b) Resconi, L.; Cavallo, L.; Fait, A.; Piemontesi, F. *Chem. Rev.* **2000**, *100*, 1253. (c) Kaminsky, W. *J. Chem. Soc. Dalton Trans.* **1998**, 1413. (d) Bochmann, M. *J. Chem. Soc., Dalton Trans.* **1996**, 255. (e) Brintzinger, H. H.; Fischer, D.; Mulhaupt, R.; Rieger, B.; Waymouth, R. M. *Angew. Chem. Int. Ed. Engl.* **1995**, *34*, 1143.
3. (a) Choukroun, R.; Donnadieu, B.; Zhao, J.-S.; Cassoux, P.; Lepetit, C.; Silvi, B. *Organometallics* **2000**, *19*, 1901. (b) Choukroun, R.; Cassoux, P. *Acc. Chem. Res.* **1999**, *32*, 494. (c) Danjoy, C.; Zhao, J. S.; Donnadieu, B.; Legros, J.-P.; Valade, L.; Choukroun, R.; Zwick, A.; Cassoux, P. *Chem. Eur. J.* **1998**, *4*, 1100.
4. (a) *Metallocenes: Synthesis, Reactivity, Applications*, Togni, A.; Halterman, R. L., Ed., Vols. 1 and 2, Wiley-VCH: Weinheim, 1998. (b) Crabtree, R. H. *The Organometallic Chemistry of The Transition Metals*; John Wiley: New York, 1994. (c) Diederich, F.; Oligoacetylenes. In *Modern Acetylene Chemistry*, Stang, P. J., Diederich, F., Eds.; Wiley-VCH: Weinheim, 1995; p 443-469. (d) Sato, F.; Urabe, H.; Okamoto, S. *Chem. Rev.* **2000**, *100*, 2835. (e) Rosenthal, U.; Pellny, P.-M.; Kirchbauer, F. G.; Burlakov, V. V. *Acc. Chem. Res.* **2000**, *33*, 119. (f) Ohff, A.; Pulst, S.; Peulecke, N.; Arndt, P; Burlakov, V. V.; Rosenthal, U. *Synlett* **1996**, 111. (g) Negishi, E.; Takahashi, T.; *Acc. Chem. Res.* **1994**, *27*, 124. (h) Buchwald, S. L.; Nielsen, R. B. *Chem. Rev.* **1988**, *88*, 1047. (i) Miura, K.; Funatsu, M.; Saito, H.; Ito, H.; Hosomi, A. *Tetrahedron Lett.* **1996**, *37*, 9059.
5. Takahashi, T.; Fischer, R.; Xi, Z.; Nakajima, K. *Chem. Lett.* **1996**, *241*, 357.

6. (a) Yasuda, H.; Kajihara, Y.; Mashima, K.; Lee, K.; Nakamura, A. *Chem. Lett.* **1981**, *226*, 519. (b) Erker, G.; Krüger, C.; Müller, G. *Adv. Organomet. Chem.* **1985**, *24*, 1. (c) Yasuda, H.; Nakamura, A. *Angew. Chem. Int. Ed. Engl.* **1987**, *26*, 723.

7. Erker, G.; Wicher, J.; Engel, K.; Rosenfeldt, F.; Dietrich, W.; Krüger, C. *J. Am. Chem. Soc.* **1980**, *102*, 6344.

8. (a) Hunter, W. E.; Atwood, J. L.; Fachinetti, G.; Floriani, C. *J. Organomet. Chem.* **1981**, *204*, 67. (b) Atwood, J. L.; Hunter, W. E.; Alt, H.; Rausch, M. D. *J. Am. Chem. Soc.* **1976**, *98*, 2454.

9. (a) Suzuki, N.; Nishiura, M.; Wakatsuki, Y. *Science* **2002**, *295*, 660. (b) Lam, K. C.; Lin, Z. *Organometallics* **2003**, *22*, 3466.

10. (a) Pellny, P.-M.; Burlakov, V. V; Arndt, P.; Baumann, W.; Spannenberg, A.; Rosenthal, U. *J. Am. Chem. Soc.* **2000,** *122*, 6317. (b) Pellny, P.-M.; Kirchbauer, F. G.; Burlakov, V. V; Baumann, W.; Spannenberg, A.; Rosenthal, U. *J. Am. Chem. Soc.* **1999,** *121*, 8313. (c) Pulst, S.; Arndt, P.; Heller, B.; Baumann, W.; Kempe, R.; Rosenthal, U. *Angew. Chem. Int. Ed. Engl.* **1996**, *35*, 1112. (d) Rosenthal, U.; Ohff, A.; Baumann, W.; Kempe, R.; Tillack, A.; Burlakov, V. V. *Angew. Chem. Int. Ed. Engl.* **1994**, *33*, 1605. (e) Burlakov, V. V.; Ohff, A.; Lefeber, C.; Tillack, A.; Baumann, W.; Kempe, R.; Rosenthal, U. *Chem. Ber.* **1995**, *128*, 967.

11. (a) Beckhaus, R. *Angew. Chem. Int. Ed. Engl.* **1997**, *36*, 686. (b) Jemmis, E. D.; Giju, K. T. *J. Am. Chem. Soc.* **1998**, *120*, 6952.

12. (a) Mansel, S.; Thomas, D.; Lefeber, C.; Heller, D.; Kempe, R.; Baumann, W.; Rosenthal, U. *Organometallics* **1997**, *16*, 2886. (b) Mashima, K.; Takaya, H. *Organometallics* **1985**, *4*, 1464. (c) Lefeber, C.; Ohff, A.; Tillack, A.; Baumann,

W.; Kempe, R.; Burlakov, V. V.; Rosenthal, U.; Görls, H. *J. Organomet. Chem.* **1995**, *501*, 179.

13. (a) Takahashi, T.; Tamura, M.; Saburi, M.; Uchida, Y.; Negishi, E. *J. Chem. Soc., Chem. Commun.* **1989,** 852. (b) Takahashi, T.; Suzuki, N.; Hasegawa, M.; Nitto, **Y.;** Aoyagi, K.; Saburi, M. *Chem. Lett.* **1992,** 331. (c) Suzuki, N.; Aoyagi, K.; Kotora, M.; Hasegawa, M.; Nitto, Y.; Saburi, M.; Takahashi, T. *J. Organomet. Chem.* **1994,** *473*, 117.
14. March, J. In *Advanced Organic Chemistry*, 4. Ed. John Wiley &Sons, p 158, **1992**, New York.
15. (a) Tatsumi, K.; Yasuda, H.; Nakamura, A. *Isr. J. Chem.* **1983**, *23*, 145. (b) Yasuda, H.; Tatsumi, K.; Nakamura, A. *Acc. Chem. Res.* **1985**, *18*, 120.
16. Knight, E. T.; Myers, L. K.; Thompson, M. E. *Organometallics* **1992**, *11*, 3691.
17. Green, J. C.; Green, M. L. H.; Taylor, G. C.; Saunders, J. *J. Chem. Soc., Dalton Trans.* **2000**, 317.
18. For leading reviews of homoaromaticity, see: (a) Williams, R. V. *Chem. Rev.* **2001**, *101*, 1185. (b) Williams, R. V. *Eur. J. Org. Chem.* **2001**, 227.
19. Stahl, F.; Schleyer, P. v. R. Jiao, H.; Schaefer III, H. F.; Chen. K. S.; Allinger, N. L. *J. Org. Chem.* **2002**, *67*, 6599.
20. (a) Becke, A. D. *J. Chem. Phys.* **1993**, *98*, 5648. (b) Becke, A. D. *Phys. Rev. A* **1988**, *38*, 2398. (c) Lee, C.; Yang, W.; Parr, R. G. *Phys. Rev. B* **1988**, *37*, 785.
21. (a) Hay, P. J.; Wadt, W. R. *J. Chem. Phys.* **1985**, *82*, 299. (b) Dunning, T. H. Jr.; Hay, P. J. *Modern Theoretical Chemistry*, H. F. Schaefer III. (Ed), Plenum; New York, 1976, 1. For polarization functions, see : Huzinaga, S.; Anzelm, J.; Klobukowski, M.; Radzio-Andzelm, E.; Sakai, Y.; Tatewaki, H., *Gaussian Basis Sets for Molecular Calculations*, Elsevier, Amsterdam, 1984.

22. (a) NBO Program 3.1, Glendening, E. D.; Reed, A. E.; Carpenter, J. E.; Weinhold, F. (b) Reed, A. E.; Weinhold, F.; Curtiss. L. A *Chem. Rev.* **1988**, *88*, 899.

23. (a) Schleyer, P. v. R.; Maerker, C.; Dransfeld, A.; Jiao, H.; Hommes, N. J. R. v. E. . *J. Am. Chem. Soc.* **1996**, *118*, 6317. (b) Schleyer, P.v. R.; Jiao, H.; Hommes, N. J. R. v. E.; Malkin, G. V.; Malkina, O. L. *J. Am. Chem. Soc.* **1997**, *119*, 12669. (c) Schleyer, P. v. R.; Manoharan, M.; Wang, Z.-X.; Kiran, B.; Jiao, H.; Puchta, R.; Hommes, N. J. R. v. E. *Org. Lett.* **2001**, *3*, 2465.

24. Frisch, M. J. Trucks, G. W.; Schlegel, H. B.; Scuseria, G. E.; Robb,M. A.; Cheeseman, J. R.; Zakrzewski, V. G.; Montgomery, J. A., Jr.; Stratmann, R. E.; Burant, J. C.; Dapprich, S.; Millam, J. M.; Daniels, A. D.; Kudin, K. N.; Strain, M. C.; Farkas, O.; Tomasi, J.; Barone, V.; Cossi, M.; Cammi, R.; Mennucci, B.; Pomelli, C.; Adamo, C.; Clifford, S.; Ochterski, J.; Petersson, G. A.; Ayala, P. Y.; Cui, Q.; Morokuma, K.; Malick, D. K.; Rabuck, A. D.; Raghavachari, K.; Foresman, J. B.; Cioslowski, J.; Ortiz, J. V.; Baboul, A. G.; Stefanov, B. B.; Liu, G.; Liashenko, A.; Piskorz, P.; Komaromi, I.; Gomperts, R.; Martin, R. L.; Fox, D. J.; Keith, T.; Al-Laham, M. A.; Peng, C. Y.; Nanayakkara, A.; Gonzalez, C.; Challacombe, M.; Gill, P. M. W.; Johnson, B.; Chen, W.; Wong, M. W.; Andres, J. L.; Gonzalez, C.; Head-Gordon, M.; Replogle, E. S.; Pople, J. A.; *Gaussian98*, Revision A.7; Gaussian, Inc.: Pittsburgh, PA, **1998**.

25. Shaftenaar, G. MOLDEN 3.6; CAOS/CAMM Center Nijmegen, Toernooiveld, Nijmegen, The Netherlands, 1991.

26. (a) Lee, L. W. M.; Piers, W. E.; Parvez, M.; Rettig, S. J.; Young, V. G. *Organometallics* **1999**, *18*, 3904. (b) Horáček, M.; Štěpnička, P.; Gyepes, R.;

Císařová, I.; Tišlerová, I.; Zemánek, J.; Kubišta, J.; Mach, K. *Chem. Eur. J.* **2000**, *6*, 2397.

27. Erker, G.; Engel, K.; Krüger, C.; Chiang, A.-P. *Chem. Ber.* **1982**, *115*, 3311.
28. Erker, G.; Wicher, J.; Engel, K.; Krüger, C. *Chem. Ber.* **1982**, *115*, 3300.
29. Kai, Y.; Kanehisa, N.; Miki, K.; Kasai, N.; Mashima, K.; Nagasuna, K.; Yasuda, H.; Nakamura, A. *J. Chem. Soc. Chem. Commun.* **1982**, 191.
30. Dahlmann, M.; Erker, G.; Fröhlich, R.; Meyer, O. *Organometallics* **1999**, *18*, 4459.
31. (a) Jones, S. B.; Petersen, J. L. *Organometallics* **1985**, *4*, 966. (b) Erker, G.; Zwettler, R.; Krüger, C.; Kryspin, I. H.; Gleiter, R. *Organometallics* **1990**, *9*, 524. (c) Kempe, R.; Spannenberg, A.; Peulecke, N.; Rosenthal, U. *Z. Krist.* **1998**, *213*, 789. (d) Westerhausen, M.; Digeser, M. H.; Gückel, C.; Nöth, H.; Knizek, J.; Ponikwar, W. *Organometallics* **1999**, *18*, 2491. (e) Peulecke, N.; Baumann, W.; Kempe, R.; Burlakov, V. V.; Rosenthal, U. *Eur. J. Inorg. Chem.* **1998**, 419.
32. The quality of the crystal structure is indicated by the C-C distance of the cyclopentadienyl rings in the range of 1.36 – 1.43 Å, see the Supplementary Material of Ref. 9a.
33. Schleyer, P.v. R.; Jiao, H.; Glukhovtsev, M. N.; Chandrasekhar, J.; Kraka, E. *J. Am. Chem. Soc.* **1994**, *116*, 7429
34. (a) Jemmis, E. D.; Phukan, A. K.; Giju, K. T. *Organometallics* **2002**, *21*, 2254. (b) Jemmis, E. D.; Phukan, A. K.; Rosenthal, U. *J. Organomet. Chem.* **2001**, *635*, 204.

35. (a) Hoffmann, R. *J. Chem. Phys.* **1963**, *39*, 1397. (b) Hoffmann, R.; Lipscomb, W. N. *ibid*, **1962**, *36*, 2179. (c) Fujimoto, H.; Hoffmann, R. *J. Phys. Chem.* **1974**, *78*, 1167.

36. CRC *Handbook of Chemsitry and Physis*, David R. Lide, Editor in Chief, 80 Th. 1999-2000

37. Winstein, S.; Sonnenberg, J. de Vries, L. *J. Am. Chem. Soc.* **1959**, *81*, 6532.

38. (a) Jemmis, E. D.; Giju, K. T. *Angew. Chem. Int. Ed. Engl.* **1997**, *36*, 606. (b) Jemmis, E. D.; Giju, K. T. *J. Am. Chem. Soc.* **1998**, *120*, 6952.

39. (a) Takahashi, T.; Kotora, M.; Xi, Z.F. *J. Chem. Soc., Chem. Commun.* **1995**, 361. (b) Fagan, P. J.; Nugent, W.A.; Calabrese, J.C. *J. Am. Chem. Soc.* **1994**, *116*, 1880. (c) Cardin, D. J.; Lappert, M. F.; Raston, C. L. *Chemistry of Organozirconium and Hafnium Compounds*; John Wiley: New York, 1994. (d) Ashe, A. J.; Kampf, J. W.; Altaweel, S. M. *J. Am. Chem. Soc.* **1992**, *114*, 372.

40. Lang, H.; Blau, S.; Nuber, B.; Zsolnai, L. *Organometallics* **1995**, *14*, 3216.

41. (a) Erker, G.; Frömberg, W.; Benn, R.; Mynott, R.; Angermund, K.; Krüger, C. *Organometallics* **1989**, *8*, 911. (b) Lang, H.; Herres, M.; Zsolnai, L.; Imhof, W. *J. Organomet. Chem.* **1991**, *409*, C7. (c) Hou, Z.; Breen, T. L.; Stephan, D. W. *Organometallics* **1993**, *12*, 3158. (d) Varga, V.; Hiller, J.; Thewalt, U.; Polasck, M.; Mach, K. *J. Organomet. Chem.* **1998**, *553*, 15.

42. Berenguer, J. R.; Falvello, L. R.; Forniés, J.; Lalinde, E.; Tomás, M. *Organometallics* **1993**, *12*, 6.

43. (a) Haumann, T.; Boese, R.; Kozhushkov, S. I.; Rauch, K.; Meijere, A. de; *Liebigs Ann. Chem.* **1997**, 2047. (b) Anderson, H. L.; Boudon, C.; Diederich, F.; Gisselbrecht, J.-P.; Gross, M.; Seiler, P. *Angew. Chem. Int. Ed. Engl.* **1994**, *33*, 1628.

44. Dewar, M. J. S. ; *Bull. Soc. Chim. Fr.* **1951**, C71-C79; Chatt, J.; Duncanson, L. A. *J. Chem. Soc.* **1953**, 2939.

45. Eisenstein, O. ; Hoffmann, R. *J. Am. Chem. Soc.* **1981**, *103*, 4308-4320.

46. Pellny, P.–M.; Burlakov, V. V.; Peulecke, N.; Burlakov, V. V.; Spannenberg, A.; Kempe, R.; Francke, V. Rosenthal, U. *J. Organomet. Chem.* **1999**, *578*, 125-132.

47. Rosenthal, U.; Pulst, S.; Kempe, R.; Pörschke, K. R.; Goddard, R.; Proft, B. *Tetrahedron* **1998**, *54*, 1277.

48. Koga, N.; Morokuma, K. *Chem. Rev.* **1991**, *91*, 823 and references therein.

49. (a) Pörschke, K. R. *J. Am. Chem. Soc.* **1989**, *111*, 5691. (b) Krause, J.; Cestaric, G.; Haack, K. J.; Seevogel, K.; Storm, W.; Pörschke, K. R. *J. Am. Chem. Soc.* **1999**, *121*, 9807.

50. Proft, B.; Pörschke, K. R.; Lutz, F.; Crüger, C. *Chem. Ber.* **1994**, *127*, 653.

51. Rosenthal, U.; Pulst, S.; Arndt, P.; Baumann, W.; Tillack, A.; Kempe, R.; *Z. Naturforsch. B* **1995**, 50, 368, 377.

CHAPTER 3

AROMATICITY AND REACTIVITY OF BENZENOID AROMATICS AND THEIR B-N ANALOGUES

[3.0] ABSTRACT :

The extent of aromaticity in benzene and borazine is evaluated by using energetic criteria. A comparison of the energetics of the formation of σ- complex of benzene and borazine shows that they differ only in the quantitative details. This is in tune with the recent experimental evidence for the electrophilic aromatic substitution reaction of borazine in the gas phase. The calculated geometric parameters of both the cyclic and open chain compounds of the hydrocarbon and the corresponding B-N compound also show similar parallel behaviour. Stability of the σ- complex is another parameter, which is used to judge the extent of aromaticity. Even though borazine shows aromatic character and reactivity pattern parallel to benzene, its condensed derivatives show different pattern from that of its hydrocarbon equivalents. As per the nucleus independent chemical shift (NICS) values in acenes, the aromaticity of the inner rings is more than that of benzene, whereas in BN-acenes, there is no substantial change in the aromaticity of the individual rings.

[3.1.] Introduction :

The inorganic benzene, borazine, is a textbook example of six π–electron six membered ring.[1] Compared to benzene, the cyclic delocalization of electrons in the borazine ring is reduced due to the large electronegativity difference between boron and nitrogen. Even though, like benzene, borazine has equal B-N bond lengths like benzene, the polarity of the BN bond causes borazine to show different reactivity pattern from that of benzene. Thus, it is natural that the chemistry of borazine is dominated by addition reactions.[1] However, recent experiments of Chiavarino et al demonstrate that borazine undergoes electrophilic aromatic substitution in the gas phase similar to its organic counterpart.[2] The electrophiles first attack at nitrogen centers and form corresponding conjugate acid, $H_3B_3N_3H_3E^+$ (E = electrophile; H^+, CH_3^+ etc.) similar to the benzonium ion[3] and, under basic conditions, substitution reactions occur.[2] This new experimental data prompted us to re-examine the criteria used to understand the aromatic nature of borazine and related systems. The benzenoid aromatics are characterized by the formation of σ- and π- complex as intermediates in eletrophilic aromatic substitution reactions. However, the nature of the σ- and π-complex in the parent system and the thermodynamic contributions to their stability are still open questions.[3]

Energetic criterion has been used to estimate the extent of aromaticity of borazine. Early studies by Fink, Gordon and others using homodesmotic equations, led to the conclusion that borazine has non negligible resonance energy (9.6 kcal/mol) which is close to half of the value for benzene (21.9 kcal/mol) thus indicating substantial aromaticity.[4,5a] Following the studies on benzenoid aromatics, the idea of ring current and resulting magnetic properties have been used to describe aromaticity.

However, the different magnetic criteria used to understand the nature of the ring current indicate that borazine is not aromatic.[5] Neither the diamagnetic susceptibility exaltation (-1.7 for borazine and 13.7 for benzene),[5d] nor the ^{1}H chemical shifts of H(B) and H(N) (5.0 and 5.5), nor nucleus independent chemical shift (NICS) computations (-2.1 for borazine and -11.5 for benzene) indicate the presence of appreciable ring current. Krygowski et. al., in a discussion of geometric indices, observed that borazine derivatives are less aromatic compared to the benzene analogues,[6] but not non-aromatic.

Thus, the theoretical evaluations of aromaticity (magnetic, energetic and geometric) do not go parallel to each other.[7] While the magnetic criterion is useful in describing the aromaticity of hydrocarbon systems, the reactivity criterion is more important in describing the same for more polar BN systems. There are few theoretical studies which have taken *reactivity* as a criterion of aromaticity.[8] The present computational study shows parallel behavior in hydrocarbon systems and BN systems towards protonation and methylation. In view of the traditional emphasis of substitution rather than addition as a hallmark of aromaticity, the energetics of these reactions are important in the evaluation of aromaticity.

While the chemistry of benzene and its linearly annelated compounds is well developed,[9] the corresponding B-N analogues are relatively unknown. There is a renewed interest in the study of borazine based polycyclic compounds because of their use as precursors for boron containing polymers and ceramics.[10] Also, the linearly annelated benzene rings, also known as the polycyclic aromatic hydrocarbons (PAHs) or acenes, have recently received much attention because of their role as pollutants, and

in particular, as carcinogens.[11] Owing to their remarkable stability, these PAHs are found in substantial quantities in the interstellar space[12] and are of substantial chemical interest. Almost four decades ago, Laubengayer and co-workers[13] reported the isolation of the BN analogues of naphthalene and biphenyl, viz. borazanaphthalene ($B_5N_5H_8$) and diborazine ($B_6N_6H_{10}$) respectively. These were further detected in the gas-phase mass spectrometric analysis of borazine.[14] Recently, Sneddon and co-workers reported the synthesis and X-ray characterization of these two molecules.[15] To the best of our knowledge, there is only one theoretical report on the structure and aromaticity of BN-analogues of PAHs, viz., that of BN-naphthalene.[16]

In this chapter, we present a comparison of the energetics of σ- complex formation in borazine, benzene and related systems. We also discuss the aromaticity of linearly condensed compounds of benzene and their B-N analogues. The emphasis is to compare and contrast the properties of the borazines with those of their PAH counterparts. We considered two sets of molecules for our study: cyclobutadiene, 1,3-butadiene, benzene, 1,3,5-hexatriene and their protonated and methylated species form the first set for the evaluation of relative aromaticity of benzene and borazine and the corresponding B–N analogues. Naphthalene, anthracene, tetracene, pentacene along with their *trans*-perhydro derivatives as well as cyclohexene and 1,3-cyclohexadiene constitutes the second set for the study of aromaticity of acenes and their B-N analogues. The B-N analogues of the hydrocarbons are obtained by replacing the carbon atoms with alternating B and N atoms.

[3.2.] Computational Methods :

All the structures (**1-46**, Figure 3.1, 3.5, 3.6) are fully optimized using the hybrid HF-DFT method B3LYP as implemented in the Gaussian 94 suite of

programs.[17, 18] The frequencies for the molecules **1-24** are evaluated at the same level. Only the minimum energy structures were included in the energy evaluations. Further, single point calculations at the CCSD(T)/6-31G* level are carried out for **1-24** to gauge the reliability of the relative energies obtained at the B3LYP/6-311+G** level. Due to the lack of computational resources, the frequency analysis of the structures of **25-46** are carried out at B3LYP/6-31+G* level by taking the optimized geometries from calculation at B3LYP/6-311+G** level. The total energies are calculated by adding the zero point vibrational energy (ZPVE) obtained from B3LYP/6-31+G* level to the energy values obtained from B3LYP/6-311+G** level. The condensed polycyclic hydrocarbons and their BN counterparts were optimized under the D_{2h} and C_{2v} symmetry constraints respectively. We performed NICS[19] calculations for benzene, borazine and their poly-condensed derivatives to judge the aromaticity of the individual rings.

[3.3.] Results and Discussions :

The parallel aromatic behavior of benzene and borazine will be discussed first on the basis of their protonation and methylation energies which will be followed by a comparison of the aromaticity of acenes and their B-N analogues.

[3.3.1.] Parallel Aromatic Behavior of Benzene and Borazine :

The protonation and methylation energies are evaluated using the equations 1-8 (Scheme 3.1). Though isolated protonation energies are not helpful in understanding the delocalized nature of electrons, useful comparisons can be made with open chain and antiaromatic systems. This provides a clear picture of the stabilities and

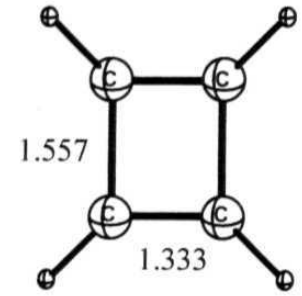

1

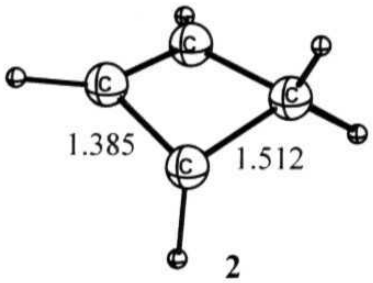

2

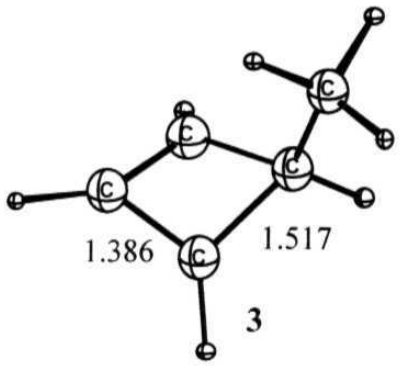

3

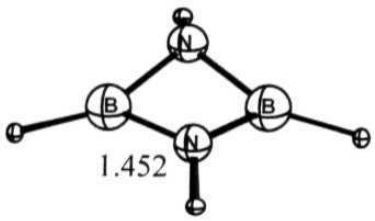

4

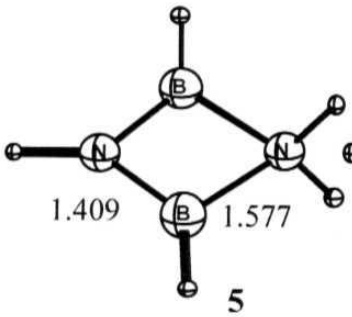

5

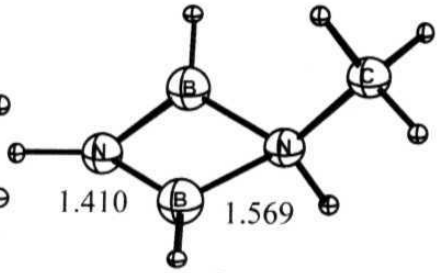

6

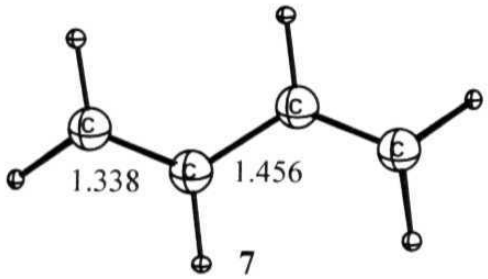

7

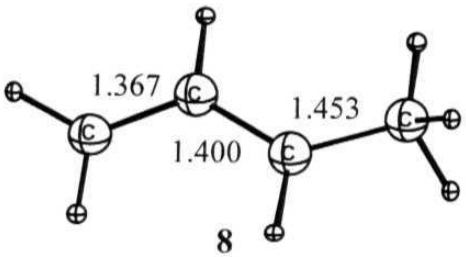

8

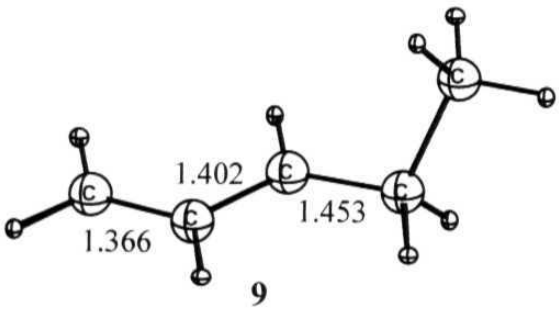

9

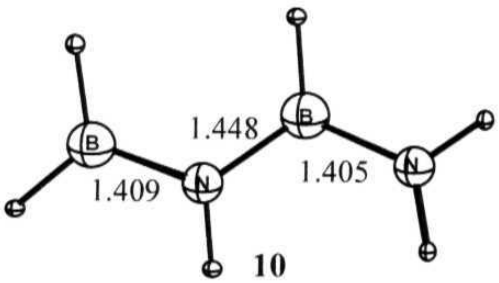

10

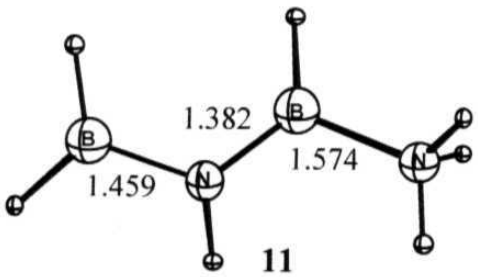

11

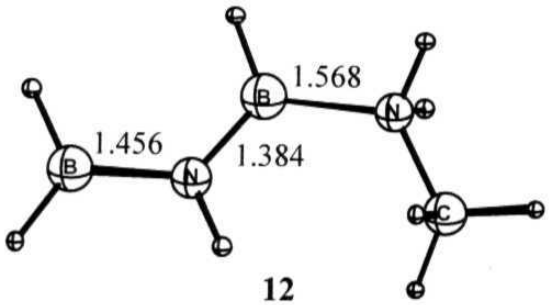

12

(Contd.)

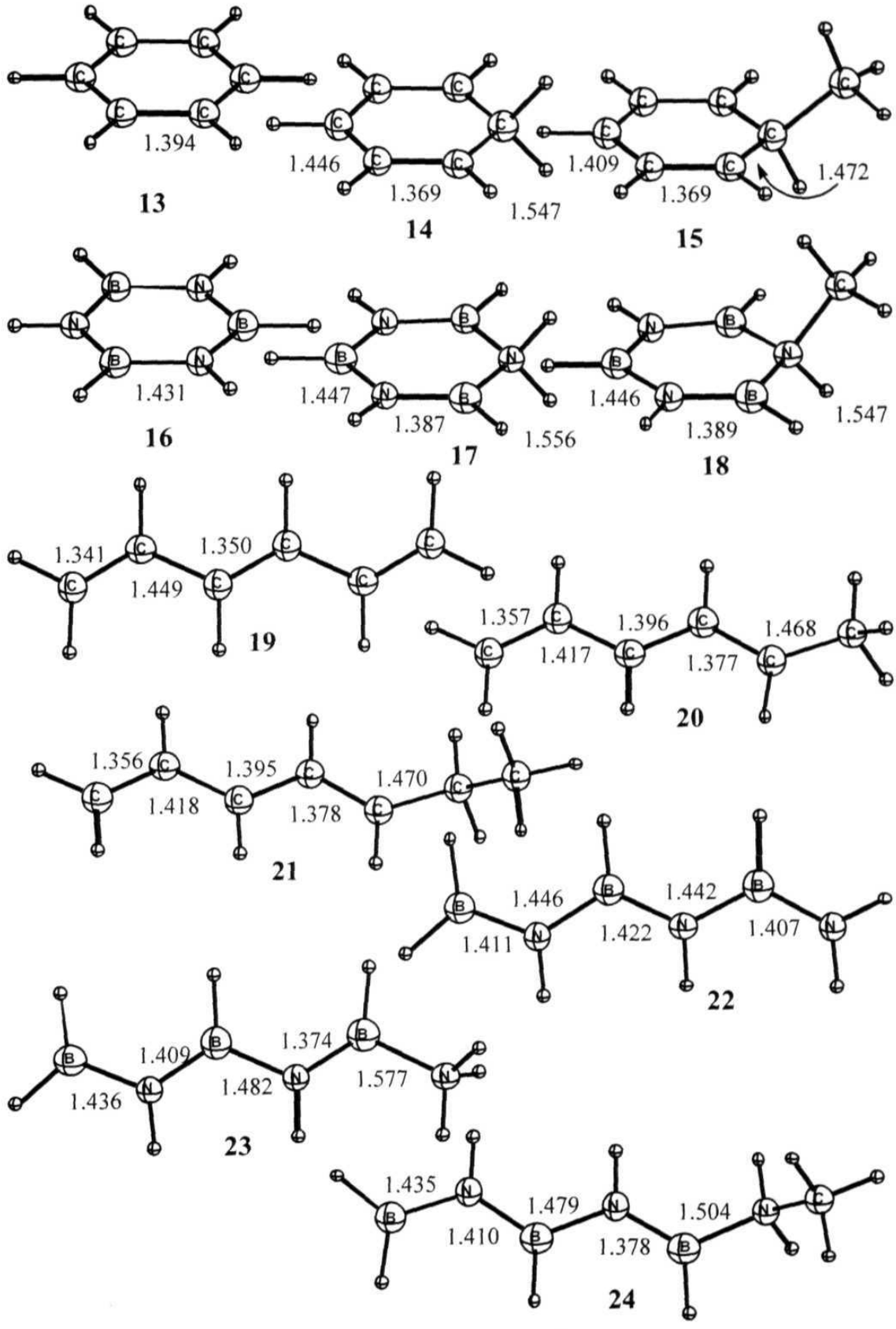

Figure 3.1. Optimized structures (**1-24**) along with important bond lengths (Å)

Scheme 3.1[a]

Equations	H		CH_3	
	ΔE	ΔE_{rel}	ΔE	ΔE_{rel}
(1).  **13**	-181.9 (-182.6)	0.0 (0.0)	-79.7 (-81.9)	0.0 (0.0)
(2). 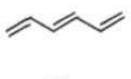 **19**	-208.8 (-207.1)	-26.9 (-24.5)	-106.6 (-105.6)	-26.9 (-23.7)
(3).  **1**	-226.2 (-227.9)	-44.3 (-45.3)	-128.6 (-131.6)	-48.9 (-49.2)
(4). 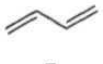 **7**	191.7 (-190.8)	-9.8 (-8.2)	-90.2 (-90.0)	-10.5 (-8.1)
(5).  **16**	-190.1 (-193.9)	0.0 (0.0)	-83.7 (-89.8)	0.0 (0.0)
(6). 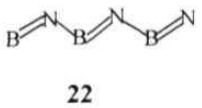 **22**	-198.4 (-204.5)	-8.3 (-10.6)	-94.1 (-101.6)	-10.4 (-11.8)
(7).  **4**	-206.5 (-210.0)	-16.4 (-16.1)	-102.1 (-107.5)	-18.4 (-17.7)
(8). 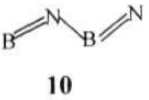 **10**	-193.7 (-199.2)	-3.6 (-5.3)	-89.1 (-96.0)	-5.4 (-6.2)

[a]*The energy values within parentheses are given at the CCSD(T)/6-31G*//B3LYP/6-311+G** level.*

reactivities of the systems involved. The magnitude of protonation energy is an indication of the stability of the polyene; the lower the magnitude, the more stable is the polyene. As expected, the lowest value of protonation energies are calculated for benzene. This is lower than that of hexatriene by 24.5 kcal/mol, a reflection of the lack

of aromatic stabilization in the linear system. Butadiene with two π electrons has less delocalisation energy. However, butadiene has a lower protonation energy than hexatriene. This is due to an additional factor that controls the protonation energy. The cation generated by protonation of butadiene is less favourable because of the size effect. A larger molecule can accommodate a charge better. For this reason, protonation energies of molecules of widely varying sizes cannot be used directly for drawing general inferences. Comparison between molecules of similar size, however, helps in understanding relative stabilities. The large magnitude of the antiaromaticity of cyclobutadiene is gauged by comparing its protonation energy with that of butadiene. Among the B-N systems under study, borazine, as anticipated, has the lowest protonation energy. The hexatriene equivalent, $B_3N_3H_8$ (**22**), has the relative protonation energy of –10.6 kcal/mol. Obviously, the stabilization in the cyclic π-electron system, $B_3N_3H_6$, is considerably lower than that in benzene. The antiaromaticity in the cyclobutadiene equivalent, $B_2N_2H_4$ (**4**), is also low as indicated by the relative protonation energy. It is found that protonation at boron centers is less favourable and therefore not considered here.

A graphical representation of the relative protonation and methylation energies (Figures 3.2 and 3.3), shows a striking similarity between the hydrocarbon and the B-N analogues. The changes observed are only in the quantitative detail. The aromaticity of benzene and the antiaromaticity of cyclobutadiene are reflected in their B-N analogues, albeit to a lower extent. Thus, in terms of the stability of the σ- complex, an acknowledged indicator of aromatic systems, both benzene and borazine behave similarly, the differences are only in quantitative detail.

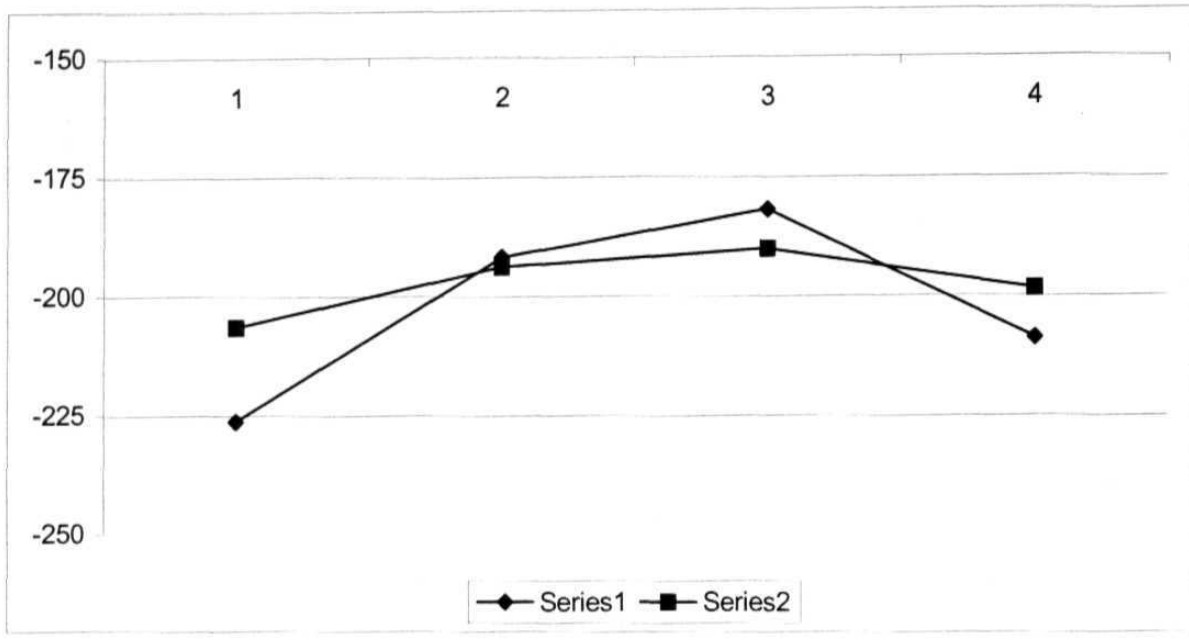

Figure 3.2 Protonation energies (Kcal/mol) of CH and BN systems **1-4**. Series 1 indicates the hydrocarbon systems and series 2 indicates the corresponding B-N systems. The molecules considered were cyclobutadiene (**1**), 1,3-butadiene (**2**), benzene (**3**) and 1,3,5-hexatriene (**4**) and their B-N analogues.

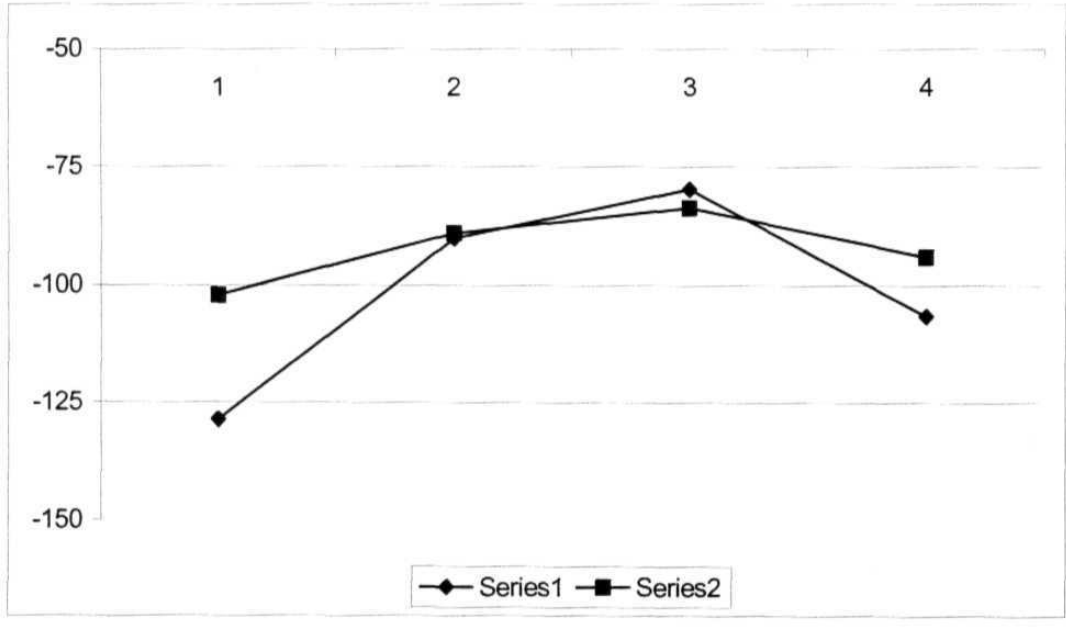

Figure 3.3. Methylation energies (Kcal/mol) of CH and BN systems **1-4**. Series 1 indicates the hydrocarbon systems and series 2 indicates the corresponding B-N systems. The molecules considered were cyclobutadiene (**1**), 1,3-butadiene (**2**), benzene (**3**) and 1,3,5-hexatriene (**4**) and their B-N analogues.

The reaction energies (Table 3.1) can also be used to estimate the aromatic stabilization energies (ASE). For example, the ASE of benzene is the difference in protonation energy between **13+20** and **19+14** (26.9 Kcal/mol). The ASE is close to the earlier estimates that had employed different reference molecules. Similarly, for borazine, the ASE is 8.2 Kcal/mol (from **16+23** and **17+22**) which is very close to the other estimates. The antiaromatic destabilization energy (ADE) of C_4H_4 is -34.5 Kcal/mol (**1+8** and **2+7**) and for $B_2N_2H_4$, ADE is -12.8 Kcal/mol (**4+11** and **5+10**). The reaction energies considered here confirm that borazine is less aromatic than benzene, but sufficient enough to show similar gas phase reactivity pattern. Similarly, the antiaromaticity in $B_2N_2H_4$ is one third of that in cyclobutadiene.

The parallel behavior observed in reaction energies of CH and BN systems is reflected in their geometries as well. Protonation or methylation of all these systems result in a chain of alternating single and double bonds starting from the site of the electrophile attack. The extent of variation in the bond lengths before and after protonation is shown in Figure 3.4. As observed in the case of energies, the bond length variations of CH and BN systems also go in parallel. With the exception of the antiaromatic molecules, both open chain and aromatic molecules have similar geometrical features. C_4H_4 is planar with localized single (1.557Å) and double bonds (1.333Å), but $B_2N_2H_4$ is puckered (C_{2v}) with equal bond lengths (1.452Å). The puckering in $B_2N_2H_4$ is due to the pyramidalization of the two lone pairs on nitrogen atoms and, by symmetry, it shows equal B-N bond lengths. This also reduces the antibonding π-interaction. Such an option is not available for cyclobutadiene. Reaction with electrophiles reverses the geometrical features. While protonated cyclobutadiene is puckered, with developing 1-3 interaction (C1-C3 = 1.77Å, Wiberg

Table 3.1. Total Energies of all the Molecules (1-24) Calculated at the B3LYP/6-311+G Level of Theory Including Zero Point Vibrational Energy (ZPVE) Correction**

Molecule	Total Energy (au)
C_4H_4 (**1**)	-154.65995
C_4H_4-H^+ (**2**)	-155.02050
C_4H_4-Me^+ (**3**)	-194.32509
$B_2N_2H_4$ (**4**)	-161.69763
$B_2N_2H_4$-H^+ (**5**)	-162.02667
$B_2N_2H_4$-Me^+ (**6**)	-201.32051
C_4H_6 (**7**)	-155.95606
C_4H_6-H^+ (**8**)	-156.26157
C_4H_6-Me^+ (**9**)	-195.56005
$B_2N_2H_6$ (**10**)	-162.90598
$B_2N_2H_6$-H^+ (**11**)	-163.21462
$B_2N_2H_6$-Me^+ (**12**)	-202.50816
C_6H_6 (**13**)	-232.21118
C_6H_6-H^+ (**14**)	-232.50113
C_6H_6-Me^+ (**15**)	-271.79843
$B_3N_3H_6$ (**16**)	-242.65535
$B_3N_3H_6$-H^+ (**17**)	-242.95836
$B_3N_3H_6$-Me^+ (**18**)	-282.24890
C_6H_8 (**19**)	-233.34954
C_6H_8-H^+ (**20**)	-233.68234
C_6H_8-Me^+ (**21**)	-272.97961
$B_3N_3H_8$ (**22**)	-243.78849
$B_3N_3H_8$-H^+(**23**)	-244.10464
$B_3N_3H_8$-Me^+ (**24**)	-283.39873

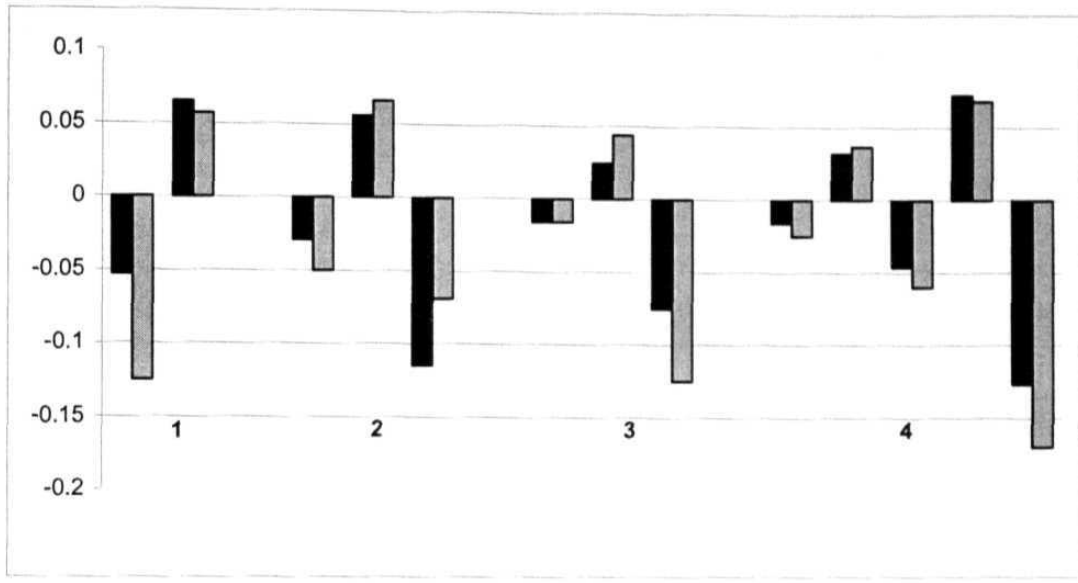

Figure 3.4. Variation in the bond lengths of hydrocarbon systems (dark) and the corresponding B-N systems (shaded) for molecules **1-4.**

Bond Index = 0.41, an indication of developing homoaromaticity[20]), the BN analogue is planar. The apparent dichotomy in the geometrical features of C_4H_4 and $B_2N_2H_4$ is the result of the tendency for pyramidalization by the nitrogen lone pair when not involved in stabilizing delocalization. All observations made here are applicable to methylation energies with minor variations.

The observations from energetic and geometric behavior of CH and BN systems differ from the conclusion obtained from magnetic criteria which point out that borazine is not aromatic. Anomalous magnetic properties associated with aromatic molecules are mainly due to the cyclic π electrons. However, the structure, energy and reactivity are determined by both σ and π electrons.[21] Localized lone pairs in borazine do not generate any ring current, but the stabilized B-N bonds, as shown by 9 kcal/mol resonance energy, does play a role in reactivity. It is a common practice to use both aromaticity and ring current interchangeably. Aromaticity is a concept best represented

by a cluster of properties: energetics, structure, reactivity, magnetic properties etc. Aromatic molecules exhibit anomalous behavior compared to the nonaromatic molecules in the above said properties. The ring current represents only the magnetic peculiarities of aromatic molecules. The failure to recognize a suitable, alternative criterion of aromaticity made the ring current model the fingerprint of aromaticity. Though it is difficult to uniquely define resonance energy, we emphasize that energetic criterion is equally important in understanding the aromatic nature of a given molecule.

[3.3.2.] Aromaticity of Acenes and Their B-N Analogues :

The optimized geometries of the hydrocarbons (**13**, **25-35**) and their BN counterparts (**16**, **36-46**) are shown in Figures 3.5 and 3.6 respectively. The calculated C–C bond lengths which range from 1.363 to 1.455Å, are comparable to those reported earlier.[22] Compared to the acenes, the changes in the corresponding B–N bond lengths of the BN-acenes are very small (1.425 Å to 1.460 Å). The stabilization or resonance energies of the linear acenes and their BN analogues were evaluated by using Eqn. (3) as suggested by Schleyer and co-workers.[23]

E (*n* 1, 3-cyclohexadiene) + E (*trans*-perhydroacene) = E (acene) + E (*n* cyclohexene)

(n =3,5,7…)

It is seen that the resonance energies of both the acenes and their BN analogues increase linearly from benzene (**1**) to pentacene (**5**) and from borazine (**13**) to BN-pentacene (**17**) respectively (Table 3.2). However, the resonance energies per π electron ($\mathbf{RE}_\pi$) of the two systems do not go parallel to each other. While the $\mathbf{RE}_\pi$ of the acenes is almost constant throughout the series, that of the BN analogues increases non-uniformly in going from borazine to BN-pentacene. It increases significantly from

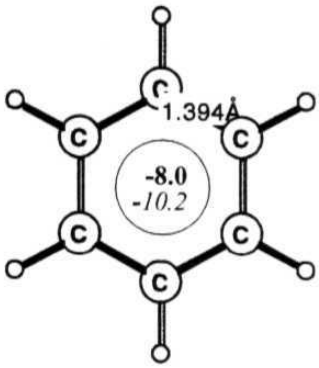

13

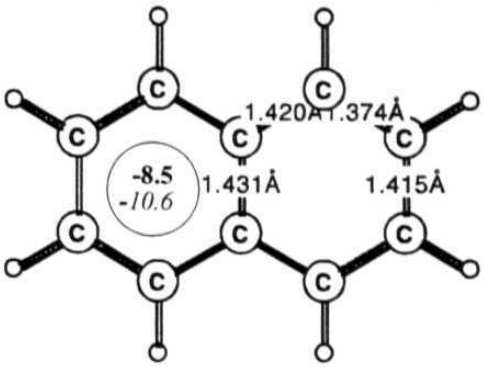

25

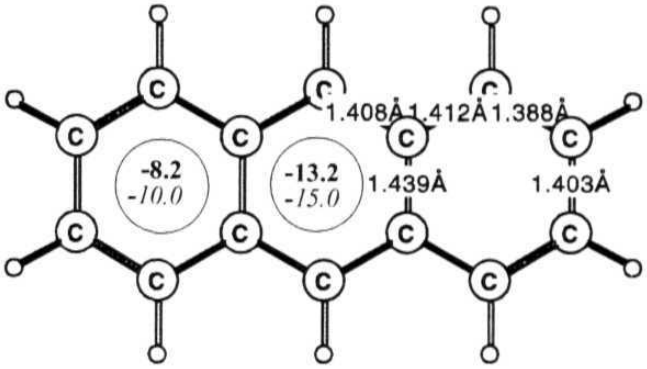

26

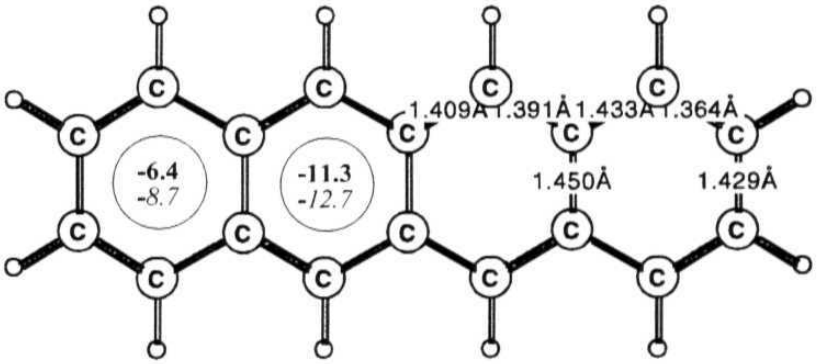

27

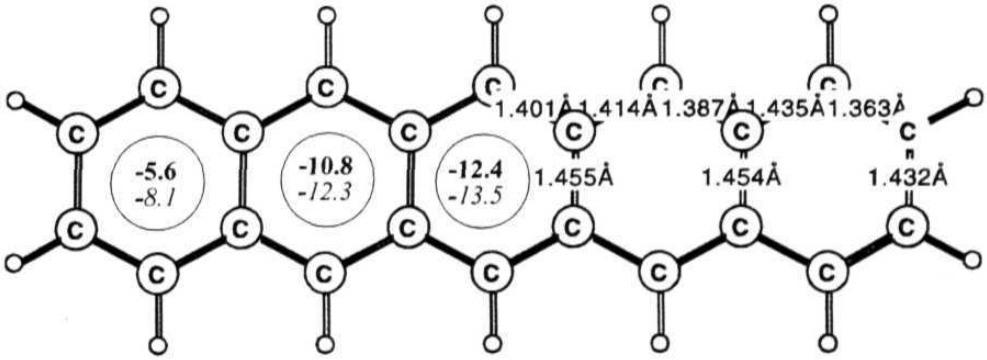

28

(Contd.)

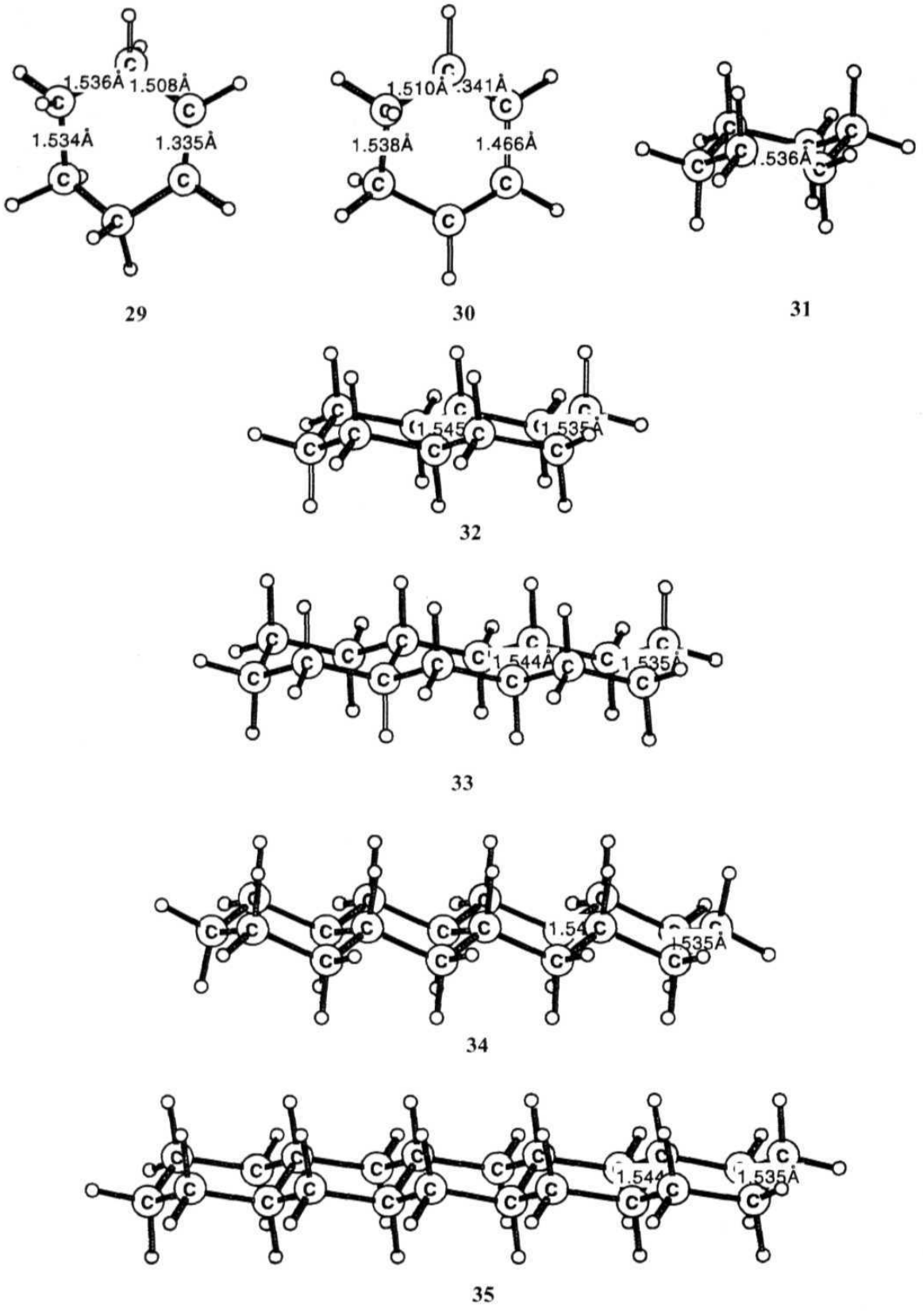

Figure 3.5. Optimized (B3LYP/6-311+G**) structures for the hydrocarbons (**1-12**) along with important bond lengths (Å). NICS values for the individual rings were given within the circle. The upper number in bold and the lower number in italics indicate the NICS values in the plane and 1 Å above the plane of the ring respectively.

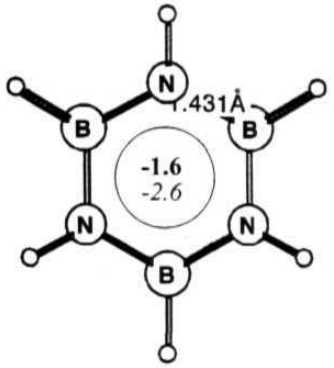

16

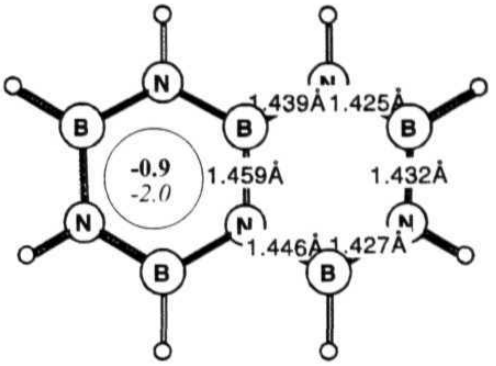

36

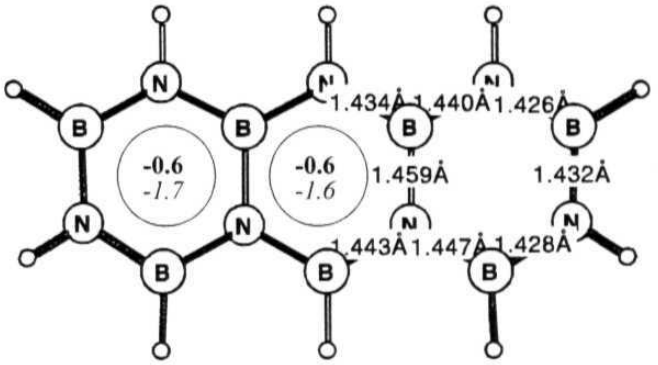

37

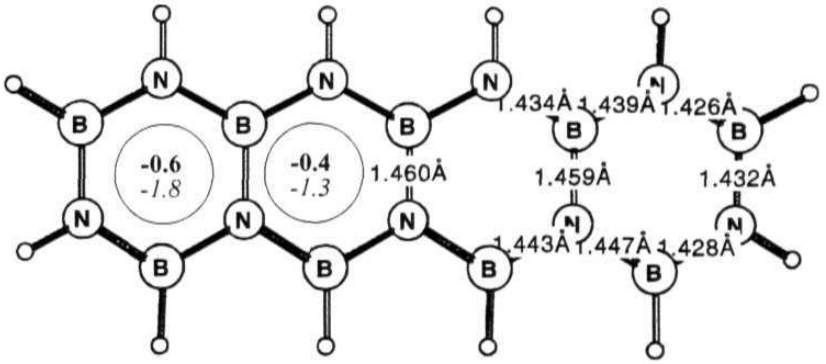

38

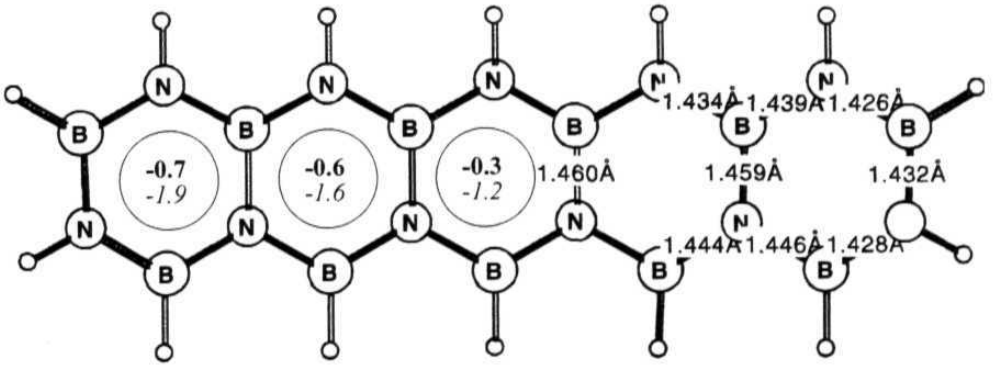

39

(Contd.)

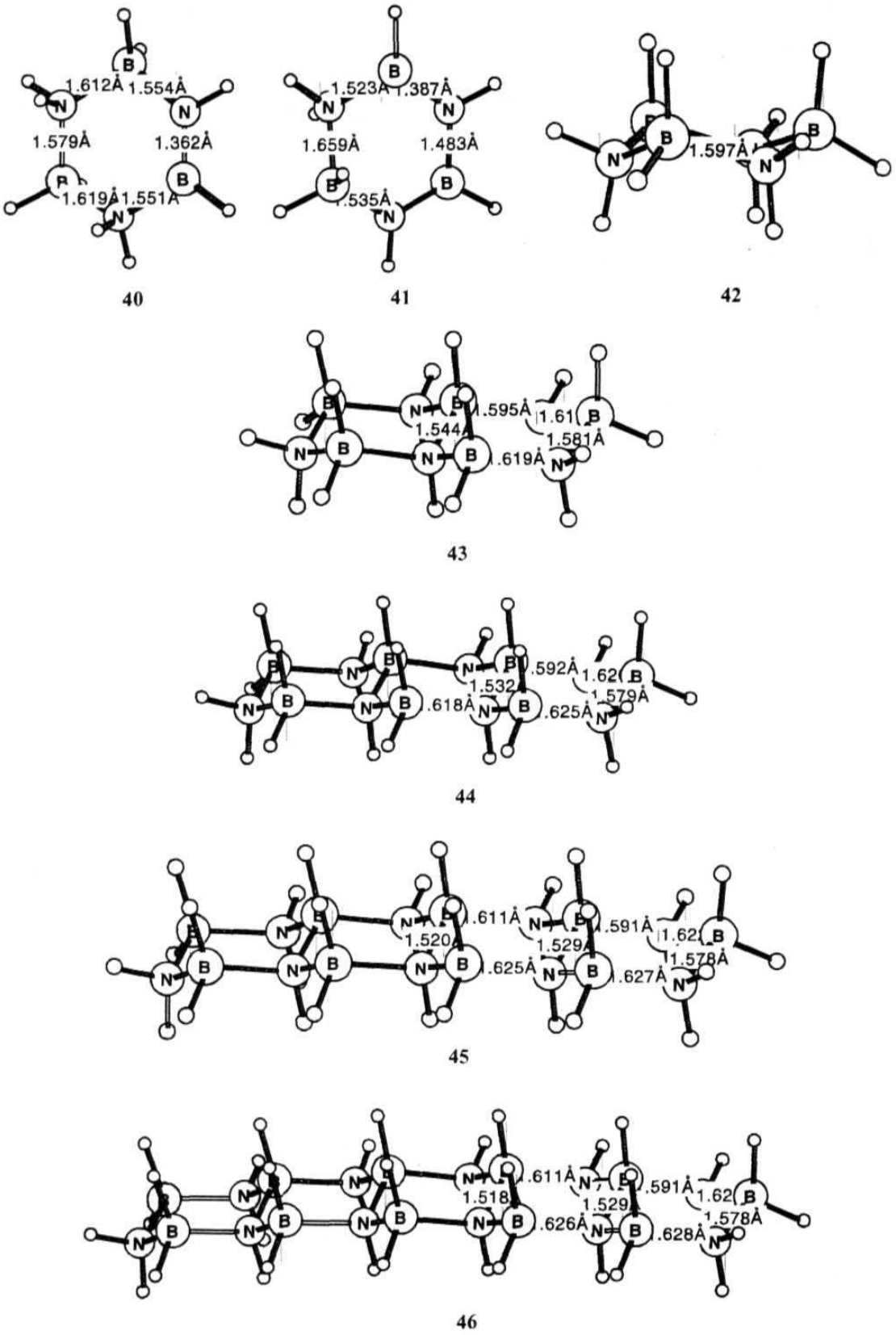

Figure 3.6. Optimized (B3LYP/6-311+G**) structures for the BN analogues of the hydrocarbons (**13-24**) along with important bond lengths (Å). NICS values for the individual rings were given within the circle. The upper number in bold and the lower number in italics indicate the NICS values in the plane and 1 Å above the plane of the ring respectively.

Table 3.2. **Total Energies (B3LYP/6-311+G**) Including Zero Point Vibrational Energy (B3LYP/6-31+G*) of all the Molecules (1-24) and Resonance Energies (Kcal/mol), Total (RE_t) and per π (RE_π) Electron for the Aromatic Hydrocarbons and their Corresponding B-N Analogues**

Molecule	Total Energy (a.u.)	RE_T (RE_π)
C_6H_6 (**13**)	-232.21071	32.7 (5.45)
$C_{10}H_8$ (**25**)	-385.84115	59.8 (5.98)
$C_{14}H_{10}$ (**26**)	-539.46601	83.5 (5.96)
$C_{18}H_{12}$ (**27**)	-693.08850	105.5 (5.86)
$C_{22}H_{14}$ (**28**)	-846.70984	127.6 (5.80)
C_6H_{10} (**29**)	-234.56659	
C_6H_8 (**30**)	-233.36139	
Trans-C_6H_{12} (**31**)	-235.77422	
Trans-$C_{10}H_{18}$ (**32**)	-391.77179	
Trans-$C_{14}H_{24}$ (**33**)	-547.76935	
Trans-$C_{18}H_{30}$ (**34**)	-703.76709	
Trans-$C_{22}H_{36}$ (**35**)	-860.30943	
$B_3N_3H_6$ (**16**)	-242.65525	13.3 (2.22)
$B_5N_5H_8$ (**36**)	-403.27502	33.2 (3.32)
$B_7N_7H_{10}$ (**37**)	-563.89443	56.2 (4.0)
$B_9N_9H_{12}$ (**38**)	-724.51386	80.1 (4.45)
$B_{11}N_{11}H_{14}$ (**39**)	-885.13313	104.2 (4.74)
$B_3N_3H_{10}$ (**40**)	-244.93255	
$B_3N_3H_8$ (**41**)	-243.77339	
trans-$B_3N_3H_{12}$ (**42**)	-246.11068	
trans-$B_5N_5H_{18}$ (**43**)	-409.01641	
trans-$B_7N_7H_{24}$ (**44**)	-571.91685	
trans-$B_9N_9H_{30}$ (**45**)	-734.81591	
trans-$B_{11}N_{11}H_{36}$ (**46**)	-897.71453	

(**13**) to (**14**) and then uniformly to (**17**). This dramatic change in RE_π in going from (**13**) to (**17**) may be attributed to difference in the degree of electron delocalization in these systems.

We attempted to quantify the extent of electron delocalization in each ring with the help of NICS calculations.[19] A negative NICS value indicates aromatic character while a positive value indicates antiaromatic character. Among the acenes, the middle ring of anthracene has the highest negative NICS values, –13.2 and –15.0 in the plane and 1Å above the plane of the ring respectively (Figure 3.5). It is found that the inner rings of all the acenes are more aromatic than the terminal ones. This is in contrast with the trends for BN acenes. Among the BN analogues, borazine (**13**) is endowed with the highest negative NICS values, –1.6 and –2.6 (Figure 3.6), which decrease rather gradually in the series. This indicates that unlike the benzenoid rings, there is no appreciable change in the aromaticity of the individual rings of BN-acenes.

[3.3.3] Conclusions :

The protonation and methylation energies of C_6H_6, C_4H_4, $B_3N_3H_6$ and $B_2N_2H_4$ are calculated theoretically. The results show that the stability of the σ- complex obtained from protonation or methylation is a good indicator of aromaticity. Even though there are quantitative differences between hydrocarbons and the B-N analogues, the general trends show that $B_3N_3H_6$ is a stable species in the context of σ- complex. While the contribution of the σ- and π- electrons to the stability of the σ- complex cannot be separated easily, this stabilization is a characteristic, useful in estimating aromaticity. According to this criterion, $B_3N_3H_6$ should be considered aromatic,

though only half as much as benzene, which is in agreement with earlier theoretical results.[4]

The stability and aromaticity of benzene (**13**), naphthalene (**25**), anthracene (**26**), tetracene (**27**), pentacene (**28**) and their BN analogues (**16, 36-39**) are evaluated by using density functional theory. Even though the stabilization energy of the acenes and their BN analogues increases linearly from **13**→**25**→**26**→**27**→**28** and **13**→**36**→**37**→**38**→**39** respectively, the resonance energy per π electron remains constant for the acenes. However, it increases steadily for the BN-acenes. On the other hand, NICS calculations show that the aromaticity of the inner rings of the acenes is more than that of benzene, but the aromaticity of the individual rings in the BN-acenes remains constant and they are less than that of borazine.

[3.4] References :

1. (a) Huheey, J. E.; Keiter, A. E.; Keiter, R. L. *Inorganic Chemistry: Principles of Structure and Reactivity*; Harper Collins College Publishers: New York, 1993. (b) Cotton, F. A.; Wilkinson, G.; *Advanced Inorganic Chemistry*, Wiley: New York, 1988. (c) *The Chemistry of Inorganic Ring Systems*; Steudel, R.; Ed.; Elsevier: New York, 1992. (d) *The Chemistry of Inorganic Homo- and Heterocycles*, Haiduc, I.; Sowerby, D. B. Ed., vols. 1 and 2, Academic Press, London, 1987 (e) Stock, A; Pohland, E. *Chem. Ber.* **1926**, *59*, 2215.
2. (a) Chiavarino, B.; Crestoni, M. E.; Fornarini, S. *J. Am. Chem. Soc.* **1999**, *121*, 2619. (b) Chiavarino, B.; Crestoni, M. E.; Marzio, A. D.; Fornarini, S.; Rosi, M. *J. Am. Chem. Soc.* **1999**, *121*, 11204.
3. (a) Hubig, S. M.; Kochi, J. K. *J. Org. Chem.* **2000**, *65*, 6807. (b) Tarakeshwar, P.; Lee, J.Y.; Kim, K. S. *J. Phys. Chem. A*. **1998**, *102*, 2253. (c) Osamura, Y.; Terada, K.; Kobayashi, Y.; Okazaki, R.; Ishiyama, Y. *J. Mol. Struct. (THEOCHEM)* **1999**, *462*, 399. (d) Wang, D.;Z.; Streitwieser, A. *Theor. Chim. Acta* **1999**, *102*, 78. (e) Tarakeshwar, P.; Kim, K. S. *J. Phys. Chem. A*. **1999**, *103*, 9116.
4. (a) Fink, W. H.; Richards, J. C. *J. Am. Chem. Soc.* **1991,** *113*, 3393. (b) Matsunaga, N.; Gordon, M. S. *Am. Chem. Soc.* **1994,** *116*, 11407. (c) Matsunaga, N.; Cundari, T. R.; Schmidt, M. W.; Gordon, M. S. *Theor. Chim. Acta* **1992**, *83*, 57. (d) Haddon, R. C. *Pure Appl. Chem.* **1982**, *54*, 1129.
5. (a) Jemmis, E. D.; Kiran, B. *Inorg. Chem.* **1998**, *37*, 2110. (b) Boyd, R. J.; Choi, S. C.; Hale, C. C. *Chem. Phys. Lett.* **1984**, *112*, 136. (c) Boese, R.; Maulitz, A. H.; Stellberg, P. *Chem. Ber.* **1994**, *127*, 1887.(d) Schleyer, P.v. R.; Jiao, H. *Pure Appl. Chem.* **1996**, *68*, 209.(e) Fowler, P. W.; Steiner, E. *J. Phys. Chem. A.*

1997, *101*, 1409.(f) Schleyer, P.v. R.; Jiao, H.; Hommes, N. J. R. v. E.; Malkin, G. V.; Malkina, O. L. *J. Am. Chem. Soc.* **1997**, *119*, 12669.

6. Madura, I.; Krygowski, T. M.; Cyrañski, M. K. *Tetrahedron* **1998**, *54*, 14913.
7. (a) Katritzky, A. R.; Karelson, M.; Sild, S.; Krygowski, T. M.; Jug, K. *J. Org. Chem.* **1998**, *63*, 5228. (b) Schleyer, P.v. R.; Freeman, P.K.; Jiao, H.; Goldfuβ, B. *Angew. Chem. Int. Ed. Engl.* **1995**, *34*, 337.
8. Krygowski, T. M.; Cyrañski, M. K.; Czarnocki, Z.; Häfelinger, G.; Katritzky, A. R. *Tetrahedron* **2000**, *56*, 1783.
9. (a) Gutman, I., Cyvin, S. J., Eds. *Topics in Current Chemsitry: Advances in the Theory of Benzenoid Hydrocarbons*, Vol. 3 (Springer-Verlag, New York) 1990. (b) Harvey, R. G., *Polycyclic Aromatic Hydrocarbons* (Wiley-VCH, New York) 1997. (c) Rienstra-Kiracofe, J. C.; Barden, C. J.; Brown, S. T.; Schaefer, H. F. *J. Phys. Chem.* A **2001**, *105*, 524. (d) Aihara, J.-I. *J. Phys. Chem.* A, **1999**, *103*, 7487.
10. Paine, R. T; Narula, C. J. *Chem. Rev.* **1990**, *90*, 73.
11. Durant, J. L.; Busby, W. F.; Lafleur, A. L.; Penman, B. W.; Crespi, C. L.; *Mutat. Res.* **1996**, *371*, 123.
12. Szczepanski, J.; Vala, M. *Nature* **1993**, *363*, 699.
13. Laubengayer, A. W.; Moews, P. C; Porter, R. F. *J. Am. Chem. Soc.* **1961,** *83*, 1337.
14. Manatov, G.; Margrave, J. L. *J. Inorg. Nucl. Chem.* **1961**, *20*, 348.
15. Faven, P. J.; Remsen, E. E.; Beck, J. S.; Carrol, P. J.; McGhie, A. R.; Sneddon, L. G. *Chem. Mater.* **1995**, *7*, 1942.
16. Kar, T.; Elmore, D. E.; Scheiner, S. *J. Mol. Str. (Theochem)* **1997**, *392*, 65.

17. B3LYP is Becke's three parameter hybrid method using the LYP correlation functional. (a) Becke, A. D. *J. Chem. Phys.* **1993**, *98*, 5648. (b) Lee, C.; Yang, W.; Parr, R. G. *Phys. Rev. B* **1988**, *37*, 785. (c) Vosoko, S. H.; Wilk, L.; Nusair, M. *Can. J. Phys.* **1980**, *58*, 1200.

18. Frisch, M. J.; Trucks, G. W.; Schlegel, H. B.; Gill, P. M. W.; Johnson, B.G.; Robb, M. A.; Cheeseman, J. R.; Keith, T.; Petersson, G. A.; Montgomery, J. A.; Raghavachari, K.; Al-Laham, M. A.; Zakrzewski, V. G.; Ortiz, J. V.; Foresman,J. B.; Cioslowski, J.; Stefanov, B. B.; Nanayakkara, A.; Challacombe, M.; Peng, C. Y.; Ayala, P. Y.; Chen, W.; Wong, M. W.; Andres, J. L.; Replogle, E. S.; Gomperts, R.; Martin, R. L.; Fox, D. J.; Binkley, J. S.; Defrees, D. J.; Baker, J.; Stewart, J. J. P.; Head-Gordon, M.; Gonzalez, C.; J. A. Pople, J. A. GAUSSIAN 94, Gaussian, Inc., Pittsburgh, PA, **1995**.

19. Schleyer, P. v. R.; Maerker, C.; Dransfeld, A.; Jiao, H.; Hommes, N. J. R. v. E. *J. Am. Chem. Soc.* **1996**, *118*, 6317.

20. Cunje,A.; Rodriquez, C. F.; Lien, M. H.; Hopkinson, A. C. *J. Org. Chem.* **1996**, *61*, 5212.

21. (a) Shurki, A.; Shaik, S. *Angew. Chem. Int. Ed. Engl.* **1997**, *36*, 2205. (b) Shaik, S.; Shurki, A.; Danovich, D.; Hiberty, P. C. *J. Am. Chem. Soc.* **1996**, *118,* 666. (c) Shaik, S.; Zilberg, S.; Haas, Y. *Acc. Chem. Res.* **1996**, *29*, 211.

22. Wiberg, K. E. *J. Org. Chem.* **1997**, *62*, 5720.

23. Schleyer, P. v. R.; Manoharan, M.; Jiao, H.; Stahl, F., *Org. Lett.* **2001**, *3*, 3643.

CHAPTER 4

ELECTRONIC STRUCTURE AND STABILITY OF TRICOORDINATE PYRAMIDAL BORON

[4.0] ABSTRACT:

Theoretical studies characterize $CBSiH_5$, $CBGeH_5$, and $CBSnH_5$, all with a tricoordinate pyramidal boron atom as minima on their respective potential energy surfaces. The extent of pyramidalization as well as the energy for inversion through the planar structure depend on the substituents on boron.

[4.1] Introduction :

The last two decades have witnessed a significant improvement in the theoretical understanding and experimental realization of novel molecules having unusual structures. The search for such molecules is spearheaded by that of planar tetracoordinate carbon atom.[1] The latest to join the club of molecules having such unusual structural features is the silicon analogue of allene.[2] Recently, Erker and coworkers have reviewed the existence of various compounds having planar tetracoordinate carbon atoms.[3] On the other hand, the question of planar tetracoordinate boron atoms is addressed only computationally.[4] The reports of such molecules having unusual geometries have set the stage for other rule breaking structures. Preference of trigonal planar arrangement in carbenium ions and in tricoordinate boron is one of the tenets of main group chemistry that remains unchallenged. An unconstrained pyramidal carbenium ion or its boron equivalent has remained elusive so far. In this chapter, we discuss the first computational[5] discovery of a neutral ground state molecule silaborirane ($CSiBH_5$) **1**, which contains a tricoordinate pyramidal boron. The conventional planar geometry **2** is a transition state with the imaginary frequency corresponding to pyramidalization around the boron atom. Similar results are obtained even when Si in **1** is replaced by Ge and Sn.

[4.2] Results and Discussion :

Structure **1** is derived from the cyclopropyl cation, **3** (C_{2v}), which is calculated to be a transition state.[6a,b] Replacement of $\{CH\}^+$ by $\{BH\}$ leads to borirane **4**, which is a minimum with a trigonal planar boron center.[6c] Replacement of one CH_2 group by an SiH_2 group yields a three membered ring comprised of three different atoms. Its conventional structure **2**, with a planar tricoordinate boron atom, is calculated to be a transition state with an imaginary frequency (331.4cm^{-1}at B3LYP/6-311+G**).[7] This leads to the minimum energy structure **1** with a pyramidal arrangement at the boron center, which is lower in energy by 2.4 kcal mol^{-1}. This energy difference increases to 4.1 kcal mol^{-1} at the CCSD(T)/ 6-311+G**level.[8-10]

Pyramidalization at the boron center causes substantial changes in the structure (Figure 5.1). In order to understand these changes, the structures **1** and **2** are visualized from different perspectives. While there is very little change in the H-Si-H and H-C-H angles of **1** and **2**, the H-Si-C and H-C-Si angles change on the transition from **2** to **1**, which is indicative of an unusual twisting of the CH_2 and SiH_2 groups with respect to each other (Table 4.1).

By symmetry, the pairs of angles H-Si-C (116.8°), H-C-Si (119.7°) and H-Si-B (122.2°) are the same in **2**. However in **1**, one of the H atoms attached to the silicon center moves closer to the CH_2 group and the other H atom moves away from it (H1-Si-C = 99.5°; H2-Si-C = 125.2°). A similar change is noticed at the CH_2 moiety. In addition, the SiH_2 group rotates by a few degrees around a hypothetical axis perpendicular to the SiH_2 plane and passing through the Si atom, so that the two H-Si-B angles are 125.9 and 123.2°. In this process the nature of C-Si bonding changes

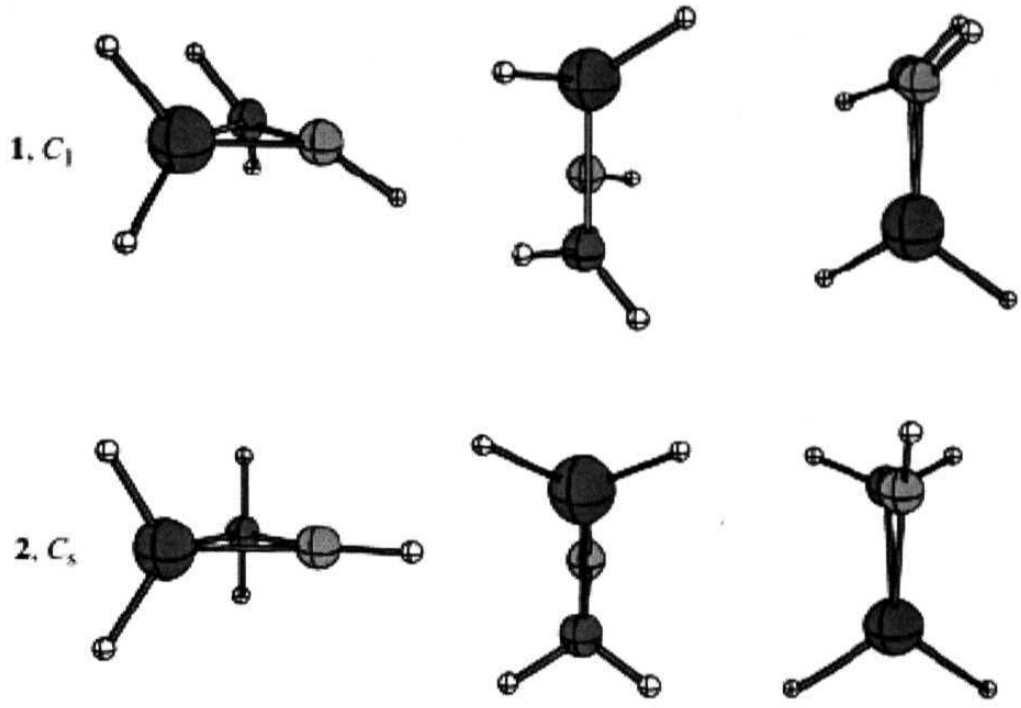

Figure 4.1. Structure of 1 and 2 viewed from different angles. The top row represents structure **1** with a pyramidal boron atom. The corresponding view of **2** with a trigonal planar boron atom is given below for comparison.

Table 4.1. Geometric Parameters of [Cy(CH_2)(SiH_2)(B-H)] Calculated at the CCSD(T)/6-311+G Level of Theory. Bond Lengths are in Å and Angles are in Degrees. The Numbers in Italics Indicate Wiberg Bond Index (WBI).**

Molecule	B–C	B–Si	C–Si	H-Si-H	H-C-H	H1-Si-C	H2-Si-C	H3-C-Si	H4-C-Si
$CBSiH_5$ (1, C_1)	1.498 *1.303*	1.912 *1.115*	2.107 *0.601*	110.2	111.8	99.5	125.2	86.7	137.9
$CBSiH_5$ (2, C_s)	1.573 *0.946*	1.971 *0.986*	1.903 *0.828*	113.5	110.4	116.8		119.7	

considerably. What was nearly an sp^3-sp^3 bond in $CSiBH_5$ now becomes an almost pure p-p bond (Table 4.2), which leads to an elongation of the C-Si bond to 2.109Å. Correspondingly there is an increase in the s character of the C-B and Si-B bonds, which corresponds to a reduction in their bond lengths.

Table 4.2. Hybridization of the B-C, B-Si and C-Si Bonds in 1 and 2 at the B3LYP/6-311+G Level of Theory using the NBO method.**[12]

Molecule	Bond X–Y	Occupancy	% X	%s (X)	%p (X)	% Y	%s (Y)	%p (Y)
$CBSiH_5$ (**1**, C_1)	B – C	1.98	33.2	31.7	67.9	66.8	39.2	60.6
	B – Si	1.96	48.5	27.6	71.9	51.5	34.2	65.3
	C – Si	1.68	70.8	8.6	91.1	29.2	8.6	90.0
$CBSiH_5$ (**2**, C_s)	B – C	1.98	32.2	28.5	71.2	67.8	28.7	71.1
	B – Si	1.97	51.6	28.6	71.1	48.4	24.4	75.0
	C – Si	1.97	70.1	21.3	78.5	29.9	17.9	81.0

A bonding description of structures **1** and **2** can be obtained in terms of Walsh orbitals.[11] The planar C_s structure **2** has two Walsh orbitals along the periphery of the ring (HOMO and HOMO-1, Figure 4.2). The LUMO is a p orbital on the boron center, which is perpendicular to the C-Si-B plane. There is a hyperconjugative stabilization of the π-type CH_2 and SiH_2 orbitals by the boron p orbital (not indicated in the Figure). One of the Walsh orbitals of structure **1** is stabilized by bringing the vacant p orbital (the LUMO of **2**) into a bonding form. This is achieved by reorienting the SiH_2 group as a whole, so that the *sp* hybrid on SiH_2 can interact with the new *sp* hybrid on the boron atom, which is pyramidalized (HOMO of **1**, Figure 4.2). Pyramidalization, therefore, is an attempt to involve the vacant p orbital on the boron atom in bonding to the Si atom. This behavior leads to the structural reorganizations that are shown in Figure 4.1. Such a process is not attractive in borirane (C_2BH_5) as the strong C-C bond determines the structure. An equivalent description of the bonding in **1** can be constructed by dividing **1** into SiH_2 and H_2C=BH fragments (Scheme 4.1a and b). The empty p_π orbital on SiH_2 receives electrons from the π MO of H_2C=BH which are concentrated on the carbon atom (Scheme 4.1c). The second interaction involves the donation of the lone pair on SiH_2 to the vacant hybridized orbital on the boron atom (Scheme 4d).

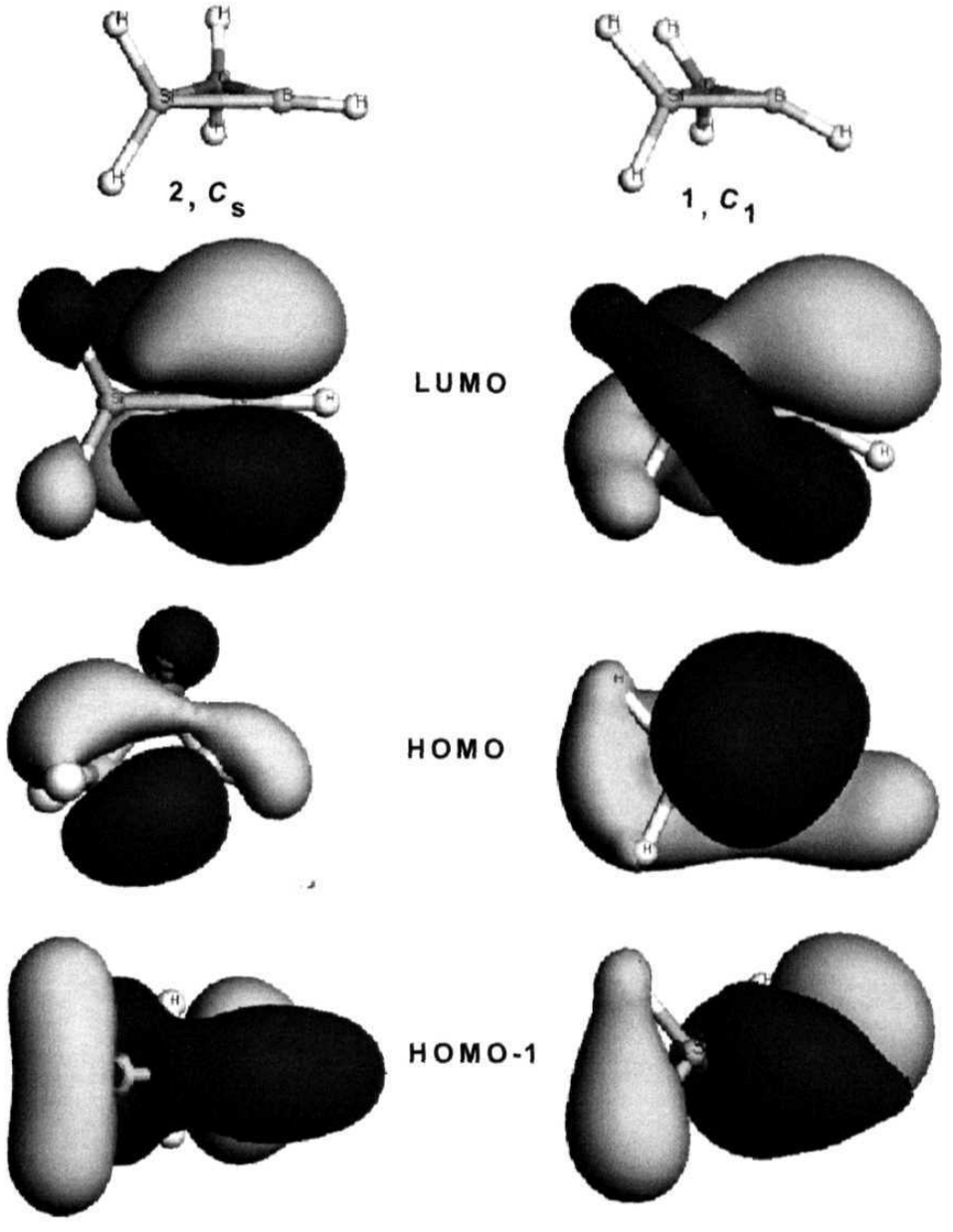

Figure 4.2. Frontier MOs corresponding to the planar (**2**) and pyramidal (**1**) structure: B (pink); Si (yellow); C (gray); H (white).

Scheme 4.1

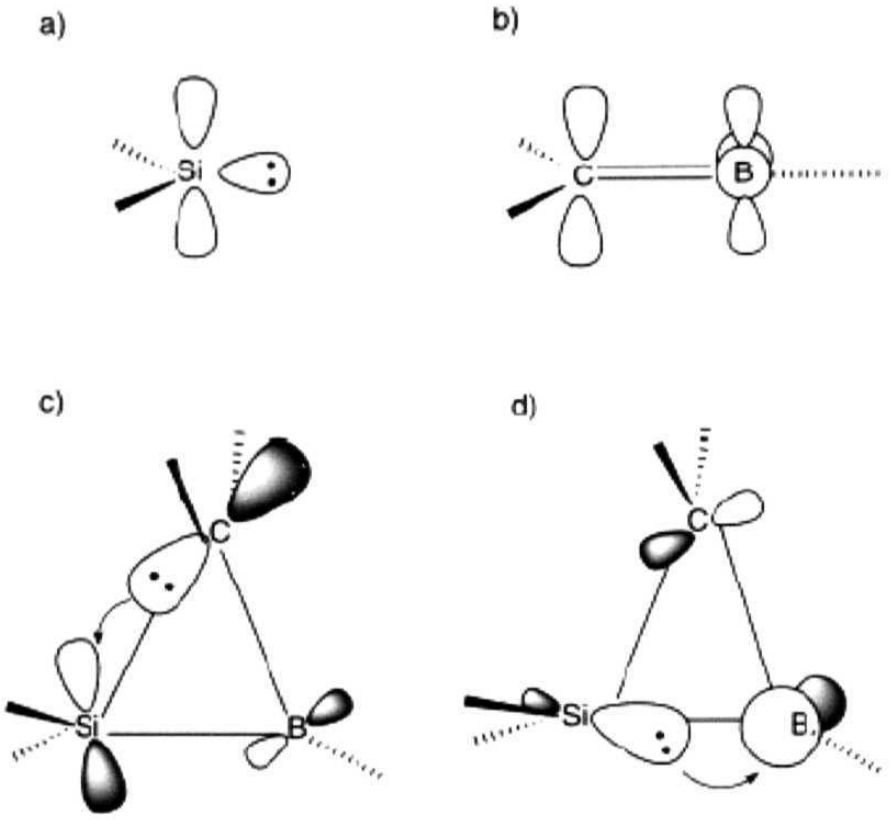

In view of the novelty of these results, we have carried out the optimization of **1** and **2** at the following levels of theory: HF/6-31G*, HF/6-311+G**, MP2/6-31G*[6b], B3LYP/6-31G*, B3LYP/6-311+G**, B3LYP/LANL2DZ[7] and CCSD(T)/6-311+G**[8-10]. At all these levels the C_1 structure with a pyramidal geometry is found to be a minimum (Table 4.3). At HF/6-31G* and HF/6-311+G** levels, the pyramidalization angle θ (calculated as 360° minus the sum of the three angles around boron) is 0.5° and 1.5° respectively, which makes the energy difference between **1** and **2** negligible. An allyl-type structure **5** is also calculated because the allyl cation **6** is more stable than the cyclopropyl cation **3**. At all levels, **5** is calculated to be higher in energy than either **1** or **2**.

Table 4.3. Total Energies (Including Zero Point Vibrational Energy (ZPVE) correction) of the Planar (2), Allyl (5) and Pyramidal (1) Isomers of [Cy(CH_2)(SiH_2)-(B-H)] Calculated at Various Level of Theory. Values in Parentheses Indicate the Number of Imaginary Frequencies. E_{rel} (kcal mol^{-1}) is the Energy Difference Between the Planar and Pyramidal Isomers. θ is the Pyramidalization Angle at Boron given in Degrees.

	Planar (2)	Allyl (5)	Pyramidal (1)	E_{rel}	θ
HF/6-31G*	-354.23407 (1)	-354.21118 (1)	-354.23387 (0)	-0.1	0.5
HF/6-311+G**	-354.27551 (1)	-354.25660 (1)	-354.27518 (0)	-0.2	1.5
MP2/6-31G*	-354.51730 (1)	-354.50932 (1)	-354.52106 (0)	2.4	19.0
B3LYP/6-31G*	-355.32435 (1)	-355.31846 (1)	-355.32781 (0)	2.2	17.3
B3LYP/LANL2DZ	-69.69861 (1)	-69.69574 (1)	-69.69843 (0)	-0.1	14.1
B3LYP/6-311+G**	-355.37132 (1)	-355.36744 (1)	-355.37513 (0)	2.4	16.5
CCSD(T)/6-311+G**	-354.71997	-354.71749	-354.72653	4.1	18.2

If the incentive for pyramidalization at the boron center is to involve the p orbital of B into Si-B bonding, substituents on boron that donates electrons to the vacant p orbital and thus make it less available for bonding, must reduce pyramidalization. We have calculated (B3LYP/6-311+G**)[7] the geometries of the derivatives of **1** and **2** where the hydrogen atom attached to boron is replaced by SiH_3, CH_3 and F (Table 4.4). The pyramidalization angle at the boron center decreases in going from H to F (H (16.5°) > SiH_3 (14.7°) > CH_3 (11.1°) > F (8.8°)). Thus, electron donation through π or pseudo πorbitals decreases the tendency to pyramidalize.

If one Si atom causes the pyramidalization, two of them should enhance the effect. We have calculated Si_2BH_5 structure at various levels and found it to have a C_s structure (**7**) with a pyramidal boron atom. The corresponding C_{2v} structure (**8**) with a

Table 4.4. Geometric Parameters and Relative Energies (Including ZPVE Correction) of [Cy(CH_2)(SiH_2)(B-R)], (R = H, SiH_3, CH_3, and F) Calculated at the B3LYP/6-311+G Level of Theory. Bond lengths are in Å and Angles are in Degrees; Wiberg Bond Index (WBI) Values are in Parentheses.**

Bond		R = H	SiH_3	CH_3	F
B–C	C_1	1.481 (1.331)	1.482 (1.369)	1.502 (1.20)	1.515 (1.082)
	C_s	1.551 (1.0)	1.557 (0.985)	1.553 (0.976)	1.539 (0.988)
B–Si	C_1	1.911 (1.117)	1.916 (1.114)	1.943 (1.043)	1.947 (1.0)
	C_s	1.966 (0.980)	1.982 (0.959)	1.977 (0.964)	1.955 (0.983)
C–Si	C_1	2.109 (0.617)	2.103 (0.573)	2.023 (0.680)	1.988 (0.749)
	C_s	1.904 (0.856)	1.894 (0.848)	1.912 (0.837)	1.943 (0.816)
θ	C_1	16.5	14.7	11.1	8.8
	C_s	0.0	0.0	0.0	0.0
E_{rel}	C_1	0.0	0.0	0.0	0.0
	C_s	2.4	2.2	0.5	-0.1

planar boron center is found to be higher in energy. The calculated value of θ is larger than that of **1**. The energy differences are also found to be considerably higher (Table 4.5).

The heavier group 14 elements, Ge and Sn, must also influence the pyramidalization of boron. Calculations at the B3LYP/LANL2DZ level find that θ decreases as Si (14.1°) is replaced by Ge (7.7°) or Sn (6.5°; Table 4.6). However, the inversion barrier increases in going from Si (0.7) to Ge (7.5) to Sn (12.7 kcal mol^{-1}). The unexpected nonplanar arrangement of tricoordinate boron center in **1** provides another demonstration of the many novel structural patterns that the heavier elements of the main group can contribute to the first-row elements.

Table 4.5. **Total Energies (Including ZPVE correction) of [Cy(SiH_2)(SiH_2)(B-H)] Isomers Calculated at Various Levels of Theory. Values in the Parentheses Indicate the Number of Imaginary Frequencies. E_{rel} (kcal mol^{-1}) is the Energy Difference Between Planar and Pyramidal Isomers. θ is the Pyramidalization Angle at Boron in Degrees.**

	Planar	Allyl	Pyramidal	E_{rel}	θ
HF/6-31G*	-605.27179 (0)	-605.27199 (1)	-605.27310 (0)	0.8	22.8
HF/6-311+G**	-605.32475 (0)	-605.32671 (1)	-605.32765 (0)	1.8	21.4
MP2/6-31G*	-605.50241 (1)	-605.52265 (1)	-605.52333 (0)	13.1	17.0
B3LYP/6-31G*	-606.70217 (2)	-606.71952 (1)	-606.71932 (0)	10.8	8.1
B3LYP/LANL2DZ	-35.46612 (1)	-35.48618 (0)	----	[a]	
B3LYP/6-311+G**	-606.76040 (1)	-606.77952 (0)	----	[a]	
CCSD(T)/6-311+G**	-605.71564	-605.73714	-605.73842	14.3	14.4

[a] leads to the allyl structure.

Table 4.6. **Relative Energies (in kcal mol^{-1}) of [Cy(CH_2)(B-H)(YH_2)], (Y= Si, Ge, Sn) with Pyramidal (C_1) and Planar (C_s) Boron Atoms, Calculated at the B3LYP/LANL2DZ Level of Theory. θ is the Pyramidalization Angle at Boron given in Degrees.**

		Si	Ge	Sn
E_{rel}+ZPVE ($kcalmol^{-1}$)	C_1	0.0	0.0	0.0
	C_s	-0.11	6.5	11.2
θ	C_1	14.1	7.7	6.5

[4.3] Conclusions

The electronic structure and bonding of molecules having a tricoordinated pyramidal boron atom were discussed using both *ab initio* and density functional theory. The extent of pyramidalization, and the difference in energy between the planar geometry (which is a transition state) and the pyramidal geometry, are found to be affected by the substituents on boron as well as by the nature of the heavy atom. The results were verified by performing calculations at different levels of theory.

[4.4] References

1. a) R. Hoffmann, R. W. Alder, C. F. Wilcox, Jr., *J. Am. Chem. Soc.* **1970**, *92*, 4992; b) J. B. Collins, J. D. Dill, E. D. Jemmis, Y. Apeloig, P. v. R. Schleyer, R. Seeger, J. A. Pople, *J. Am. Chem. Soc.* **1976**, *98*, 5419; c) D. R. Rasmussen, L. Radom, *Angew. Chem. Int. Ed. Engl.* **1999**, *38*, 2875; *Angew. Chem.* **1999**, *111*, 3051; d) Z. -X. Wang, P. v. R. Schleyer, *J. Am. Chem. Soc.* **2001**, *123*, 994.
2. S. Ischida, T. Iwamoto, C. Kabuto and M. Kira, *Nature*, **2003**, *421*, 725
3. a) D. Röttger, G. Erker, *Angew. Chem.* **1997**, *109*, 840; *Angew. Chem. Int. Ed. Engl.* **1997**, *36*, 812; b) W. Siebert, A. Gunale, *Chem. Soc. Rev.* **1999**, *28*, 367; c) X. Li, L. S. Wang, A. I. Boldyrev, J. Simons, *J. Am. Chem. Soc.* **1999**, *121*, 6033; d) L. S. Wang, A. I. Boldyrev, X. Li, J. Simons, *J. Am. Chem. Soc.* **2000**, *122*, 7681; e) *Chem. Eng. News* **2000**, *78* (34), 8.
4. a) C. Präsang, A. Mlodzianowska, Y. Sahin, M. Hofmann, G. Geiseler, W. Massa, A. Berndt, *Angew. Chem.* **2002**, *114*, 3529; *Angew. Chem. Int. Ed. Engl.* **2002**, *41*, 3380; b) C. Präsang, M. Hofmann, G. Geiseler, W. Massa, A. Berndt, *Angew. Chem.* **2002**, *114*, 1597; *Angew. Chem. Int. Ed. Engl.* **2002**, *41*, 1526; c) A. Maier, M. Hofmann, H. Pritzkow, W. Siebert, *Angew. Chem.* **2002**, *114*, 1600; *Angew. Chem. Int. Ed. Engl.* **2002**, *41*, 1529.
5. Gaussian 94, M. J. Frisch, G. W. Trucks, H. B. Schlegel, P. M. W. Gill, B. G. Johnson, M. A. Robb, J. R. Cheeseman, T. Keith, G. A. Petersson, J. A. Montgomery, K. Raghavachari, M. A. Al-Laham, V. G. Zakrzewski, J. V. Ortiz, J. B. Foresman, J. Cioslowski, B. B. Stefanov, A. Nanayakkara, M. Challacombe, C. Y. Peng, P. Y. Ayala, W. Chen, M. W. Wong, J. L. Andres, E. S. Replogle, R. Gomperts, R. L. Martin, D. J. Fox, J. S. Binkley, D. J. Defrees, J. Baker, J. P.

Stewart, M. Head-Gordon, C. Gonzalez, J. A. Pople, *Gaussian 94*, Gaussian, Inc., Pittsburgh, PA, **1995**.

6. a) L. Radom, P. C. Hariharan, J. A. Pople, P. v. R. Schleyer, *J. Am. Chem. Soc.* **1973**, *95*, 6531; b) W. A. Hehre, L. Radom, P. v. R. Schleyer, J. A. Pople, *Ab Initio Molecular Orbital Theory*, Wiley, New York, **1986**; c) M. Bühl, P. v. R. Schleyer, M. A. Ibrahim, T. Clark, *J. Am. Chem. Soc.* **1991**, *113*, 2466.
7. a) A. D. Becke, *J. Chem. Phys.* **1993**, *98*, 5648; b) A. D. Becke, *Phys. Rev. A* **1988**, *38*, 3098; c) C. Lee, W. Yang, R. G. Parr, *Phys. Rev. B* **1988**, *37*, 785. d) P. J. Hay. W. R. Wadt, *J. Chem. Phys.* **1985**, *82*, 299.
8. G. D. Purvis, R. J. Bartlett, *J. Chem. Phys.* **1982**, *76*, 1910.
9. K. Raghavachari, G. W. Trucks, J. A. Pople, M. Head-Gordon, *Chem. Phys. Lett.* **1989**, *157*, 479.
10. R. J. Bartlett, J. D. Watts, S. A. Kucharski, J. Noga, *Chem. Phys. Lett.* **1990**, *165*, 513.
11. a) A. D. Walsh, *Nature* **1947**, *159*, 712; b) A. D. Walsh, *Trans. Far. Soc.* **1949**, *45*, 179.
12. a) A. E. Reed, R. B. Weinstock, F. Weinhold, *J. Chem. Phys.* **1985**, *83*, 735; b) A. E. Reed, F. Weinhold, *J. Chem. Phys.* **1983**, *83*, 1736; c) A. E. Reed, F. Weinhold, L. A. Curtiss, *Chem. Rev.* **1988**, *88*, 899.

List of Publications

1. "Is Borazine Aromatic? Unusual Parallel Behavior between Hydrocarbons and Corresponding B-N Analogues" B. Kiran, **A. K. Phukan** and E. D. Jemmis *Inorg. Chem.* **2001,** *40,* 3615-3618.

2. "Structure and bonding of metallacyclocumulenes, radialenes, butadiyne complexes and their possible interconversion: a theoretical study" E. D. Jemmis, **A. K. Phukan** and U. Rosenthal *J. Organomet. Chem.* **2001**, *635*, 204–211.

3. "Dependence of the Structure and Stability of Cyclocumulenes and Cyclopropenes on the Replacement of the CH_2 Group by Titanocene and Zirconocene: A Density Functional Theory Study" E. D. Jemmis, **A. K. Phukan** and K. T. Giju *Organometallics* **2002,** *21,* 2254-2261.

4. "Stabilization of Tricoordinate Pyramidal Boron: Theoretical Studies on $CBSiH_5$, BSi_2H_5, $CBGeH_5$, and $CBSnH_5$" K. T. Giju, **A. K. Phukan** and E. D. Jemmis *Angew. Chem. Int. Ed.* **2003**, *42*, 539-542.

5. "Structure and Neutral Homoaromaticity of Metallacyclopentene, pentadiene, penyne and pentratriene: A Density Functional Study" E.D. Jemmis, **A.K. Phukan**, H. Jiao and U. Rosenthal *Organometallics* **2003,** *22,* 4958-4965

6. "Structure, Reactivity and Aromaticity of Acenes and Their BN Analogues : A Density Functional and Electrostatic Investigation" Rashmi P. Kalagi, Shridhar R. Gadre, **A. K. Phukan** and E. D. Jemmis (Submitted to *Inorg. Chem.* for publication)